



# TRADITIONAL KNOWLEDGE, TECHNOLOGIES AND PRACTICE FOR CLIMATE CHANGE MITIGATION: A CASE STUDY OF COMMUNITY COMPOSTING IN CAMEROON

Lawrence Oben Mbeng<sup>[a]</sup>

**Keywords:** composting; traditional technologies, practices and knowledge; climate change mitigation

Using participant observation and appraisal methods, the present study shows that with traditional knowledge, technologies and practices, a significant quantity of household waste was diverted away from the landfill and transformed into organic compost for use by farmers with the possibility of improving existing carbon sinks and reducing net CO<sub>2</sub> emissions.

Corresponding Author

Tel: (+237) 70 03 62 24)

E-Mail: obenmbeng@yahoo.co.uk

[a] The University of Douala, Institute of Fisheries and Aquatic Sciences at Yabassi, P.O. Box 7236, Bassa Douala, Cameroon

## Introduction

Traditional knowledge, technologies and practices as highlighted in the UN processes such as the United Nations Framework Convention on Climate Change and the UN Intergovernmental Panel on Climate Change have been documented as cost-effective terrestrial mitigation solutions that have the potential to improve existing carbon sinks and reduce net CO<sub>2</sub> emissions<sup>1,2</sup>. It is on this basis that the contributions of the waste sector to emissions of climate change gases are becoming better understood. At the same time, the important role of the waste management sector as a means through which to mitigate climate change, commonly abandoned in the past, is becoming more recognized. For example, in developing countries, the low cost and simplicity of composting, together with the high organic content of waste make small-scale composting a promising solution. Furthermore, increased composting of municipal waste could reduce waste management costs and emissions, and create both employment and public health benefits. Composting also decreases environmental problems related to the management of wastes by decreasing the volumes of waste sent to landfill and by killing possibly dangerous organisms. A target for European Union countries is to decrease the quantity of organic waste going to landfill sites by 20% by 2010 and by 50% by 2050 (Council Directive 1999/31/EC). The follow-up of this directive could result in a large increase in the composting of organic wastes<sup>3</sup>.

In the Industrialized countries, increased composting of household food waste would reduce greenhouse emissions, but would require additional separation of household waste, which may limit the penetration of composting<sup>2</sup>. Notwithstanding, emissions reported to the UNFCCC have shown a stabilizing or even declining trend in recent years for many countries of the developed world<sup>1</sup>. However, the

estimation of the past, current and future emissions as well as the mitigation potential in the waste sector has many uncertainties as shown in Fig. 1. According to<sup>4,5</sup> the most important uncertainties relates to:

- the poor quality of activity data needed for estimation of emissions;
- the data on emissions from the waste sector only extending out to 2020; and
- waste statistics lacking in many countries due to the differences in waste-related definitions and coverage of waste collection.

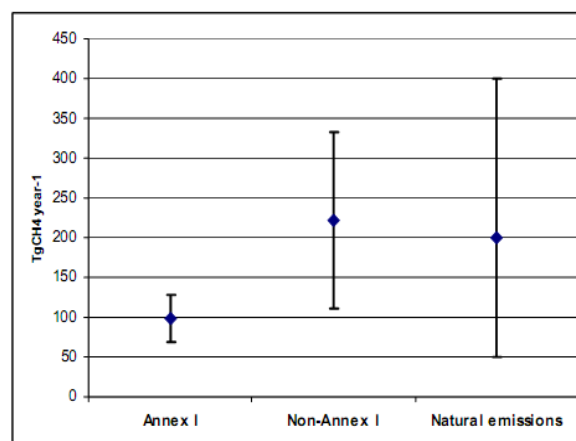


**Figure 1.** Estimates of total anthropogenic methane emissions from Annex I countries (developed countries) and Non-Annex I countries (developing countries) in 2000 and natural emissions with related indicative approximate levels of uncertainties.<sup>1,8</sup>

It is therefore an undeniable fact that the waste sector is an important contributor to climate change because according to<sup>6</sup>, CH<sub>4</sub> produced at solid waste disposal sites contributes approximately 3-4 percent to the annual global anthropogenic greenhouse gas emissions (See Figure 1), and is expected to increase with increasing global population and GDP. Notwithstanding, the use of traditional knowledge, technologies and practices in the production of compost from organic waste for use in agriculture and horticulture

could contribute significantly in reducing greenhouse gas emissions; improve soil quality, replacement of chemical fertilizers, reduced use of pesticides, enhanced tillage and less consumption of fuels<sup>7</sup>. This research study makes an evaluation of a community composting in Cameroon from a participatory and rapid appraisal method. In this study, GICABIO was chosen because it is a local community initiative based on sustainable waste management practices with the possibility to generate knowledge that can contribute to policy formulation for climate change mitigation in Cameroon.

### History of composting in Cameroon

In response to an increase in the biodegradable fraction of the household waste in Yaounde, Cameroon, youths in the Messa neighborhood and a Non Governmental Organization (PSU), French acronym for Programme Sociale d'Urgence used traditional knowledge, technologies and practices to transform the organic fraction of household waste into organic compost. The composting process lasted about a month with the heap being turned 4 times, after which a ten-week maturation period is recommended. A study done in a ward of the city of Yaounde found out that there were 16 valid market gardening sites which could absorb 8,000 tonnes of garbage per year, i.e. 5 % of all solid waste produced in the city<sup>9</sup>. This traditional initiative was later followed by research at the Higher Polytechnique College of Yaounde in 1992 to forge out a scientific method for composting<sup>10</sup>. With the support of PNUD and French Cooperation Agency<sup>11</sup>, 15 composting sites based on traditional knowledge and practice became operational in Yaounde. Other towns like Bafoussam, Bafang, Nkongsamba, Garoua<sup>11-13</sup> also got involved in composting but not without numerous setbacks such as short period of funding by donors, low selling price, little or no financial compensation from the citizens<sup>14</sup>.

### The relevance of the composting

Composting is a range of processes involving thermophilic aerobic micro-organisms to convert organic waste materials into stable humic substances and inorganic plant nutrients (compost). Composting involves a multiplicity of physical parameters and feedstock varying simultaneously. Therefore, an efficient compost production requires a thorough understanding of the process dynamics in terms of the feedstock materials used and the interactions of the physical parameters (Table 1) such as temperature, moisture content, bulk density, porosity and oxygen availability.<sup>15-17</sup>

The micro-organisms involved in the composting process include bacteria of the species Actinomycetes and fungi (moulds and yeast) while the by products are carbon dioxide, water and heat energy<sup>15</sup>. However, applying compost to soil not only increases the total organic carbon (TOC) but plays an important role in microbial proliferation and activity<sup>18</sup>. Although the application of compost is considered a suitable tool for mitigating climate change and improving soil fertility, very few studies have been conducted in semi-arid climates to evaluate the joint effect of such practice on the structure and function of the soil's microbial community.

**Table 1.** Characteristic of compost for use in agriculture<sup>15</sup>.

Agricultural Parameters	Reported as (units of measure)	Recommended Range
pH	pH units (1:5 water extract)	7.0 - 8.7
Moisture Content	% m/m of fresh weight	35 - 55
Organic Matter Content	% dry weight	>25
Screen aperture size	mm	40 maximum for soil improvement 25 maximum for top dressing grassland
C:N Ratio		20:1 maximum

Despite the lack of sufficient knowledge, compost use (see Table 2) has an important task to play in making both the developed and the developing countries more environmentally sustainable. This can be made possible given the fact that composting is higher in the waste management hierarchy than landfill, hence an environmentally friendly and economical alternative method for treating solid organic waste, thus reducing the amount of waste to be transported and discarded in landfills and built environments. It can also be a valuable source of raw material (fertilizer) for agriculture and as an income generator.<sup>15,19-22</sup>

Compost also has the potential of replacing about a million cubic metres of peat per annum, to meet its obligations under the Biodiversity Directive, and to support sustainable agricultural practices by returning nutrients to the soil and averting the decline in soil quality. Composts help to increase soil functionality and elasticity, and maintain biologically diverse habitats. This will help protect soils against powerful rainfall events and extended summer droughts, a very common scenario in Sub-Saharan African countries<sup>24</sup>.

According to<sup>25</sup>, agricultural production in Sub-Saharan African Countries has indeed been sensitive to climatic changes. Figures 2 and 3 provide graphical illustration of trends in rising temperature and declining precipitation and climatic changes for Sub-Saharan African (SSA) and Non Sub-Saharan African (NSSA). Therefore, compost use can supply some nutrients which can effectively replace artificial fertilizers and improve soil buffering capacity and reduce nitrogen leaching. Notably, composts derived from biodegradable wastes have the potential to off-set carbon dioxide emissions equivalent to over a million cars a year through carbon sequestration.<sup>24</sup>

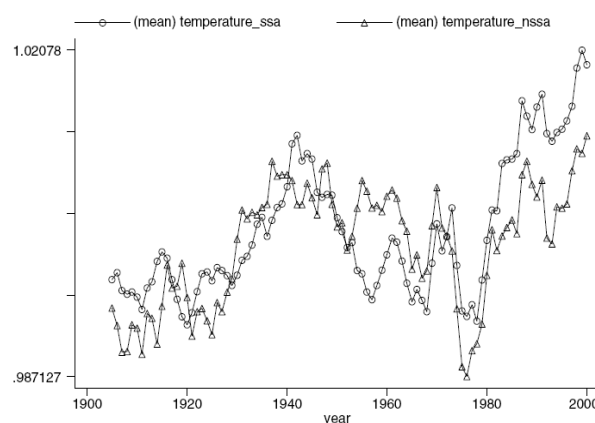


**Figure 2.** Normalized mean temperature for Sub-Saharan African (SSA) and Non Sub-Saharan African (NSSA) countries<sup>25</sup>.

Table 2. The use of different types of compost<sup>23</sup>.

Type of compost	Properties/parameter	Mode of use	Amounts of compost
1. Green compost	Organic matter	Mulching or soil amendment <sup>a</sup>	3–10 cm layer or 10–600 ton ha <sup>-1a</sup>
2. Compost from household waste	N-content, stability and phytotoxicology	Mulching or soil amendment	33–6 cm layer or 100–150 kg N ha <sup>-1b</sup>
3. Compost with municipal sludge	Ca and pH, N, organic matter	Soil amendment	100–150 kg N ha <sup>-1</sup> , or according to the liming effects
4. Soil mixes	Variable	Growing medium	Depending on the conditions

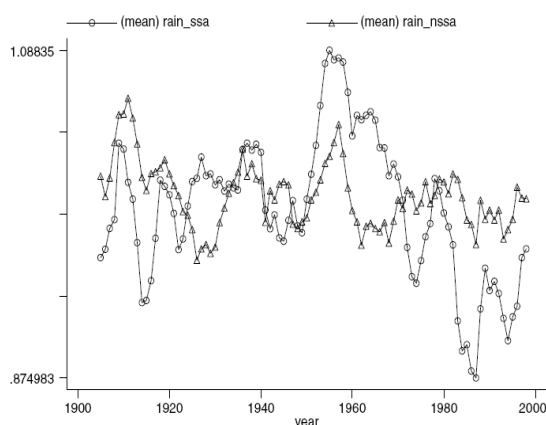


**Figure 3.** Normalized mean rainfall for Sub-Sahara Africa (SSA) and Non Sub-Sahara African (NSSA) countries<sup>25</sup>.

## Materials and methods

### Site description and field study

Cameroon is located in Central Africa and bordered on the west by the Gulf of Guinea, north west by Nigeria, north east by Chad with Lake Chad on its northern tip, east by Central African Republic and to the south by Congo and Gabon<sup>26</sup>. A socio-economic survey was conducted on four neighbourhoods (Banengo 1, Bamendzi, Ndiandam, Kouogou) in Bafoussam, the capital town of the West Region in Cameroon. The aim was to determine local community / voluntary group activity, availability of kerbside recycling and regularity of collection services by a local waste collection company, HYSACAM. Added to this was to provide a clue on household waste arisings and the way it was being perceived and managed.

Participant observation and appraisal methods were used to evaluate the composting process (Fig. 4). Participant observation is a method in which the observer participates in the daily life of the people under study either openly in the role of researcher while participatory appraisals is an approach of learning about communities that places equal value on the knowledge and experience of local people with different background and experience and their capacity to come up with solutions to problems affecting them<sup>27</sup>.

## Results and Discussion

Since its inception in 1995, the GICABIO project has had a positive socio-economic and environmental impact in Bafoussam, the regional capital of the West Region of Cameroon. Environmentally, of the 80 tonnes of household waste produced daily and destined for the landfill, approximately 10 tonnes were collected and transformed into compost<sup>28</sup>. Socio-economically, it has improved the livelihood of 200 unemployed youths who earned some money from the collection and transportation of household waste to composting sites as well as enabled Cameroonian farmers to have access to a cheap compost to fertilize their farmlands. Between January and June 27, 8 tonnes of compost was produced<sup>28</sup>. Despite this success, numerous constraints were identified. The fact that the composting activity was done manually puts plenty of strain on the workers. Transportation cost was observed as a major barrier to willingness-to-pay (WTP) for compost in the study area. In line with<sup>29</sup>, the effective demand for compost for agricultural purposes in Cameroon is marginal and restricted by farmers transport costs. In a study to estimate the demand for municipal waste compost via farmer's willingness-to-pay (WTP) in Ghana,<sup>29</sup> it was reported that, the majority of respondents were positive in their responses and perceptions in the demand for compost. The WTP analysis (profit analysis) was important in highlighting variables, which explain variations in the WTP and in due course allows the quantification of the compost demand under different scenarios of subsidized and non-subsidized compost. Irrespective of the inconsistencies observed in the farmer's WTP, the low market price (1.5 US Dollars) compared to 5 US Dollars for mineral fertilizer was responsible for the increase use of organic compost in agriculture (Fig. 4) e.g. (demonstration farms, tomato, beet root, cabbage, lettuce and green vegetables) and horticulture (flower nurseries and gardens).

The absence of complementary standards governing application to land however raises questions on the effectiveness of traditional knowledge, technologies and practices in improving existing carbon sinks and to reduce net CO<sub>2</sub> emissions. Despite these uncertainties, decomposition at the piling and maturation phases of the composting process (Fig. 4) depended on the climatic condition (Fig. 2 and 3) and the type of waste (Table 2).

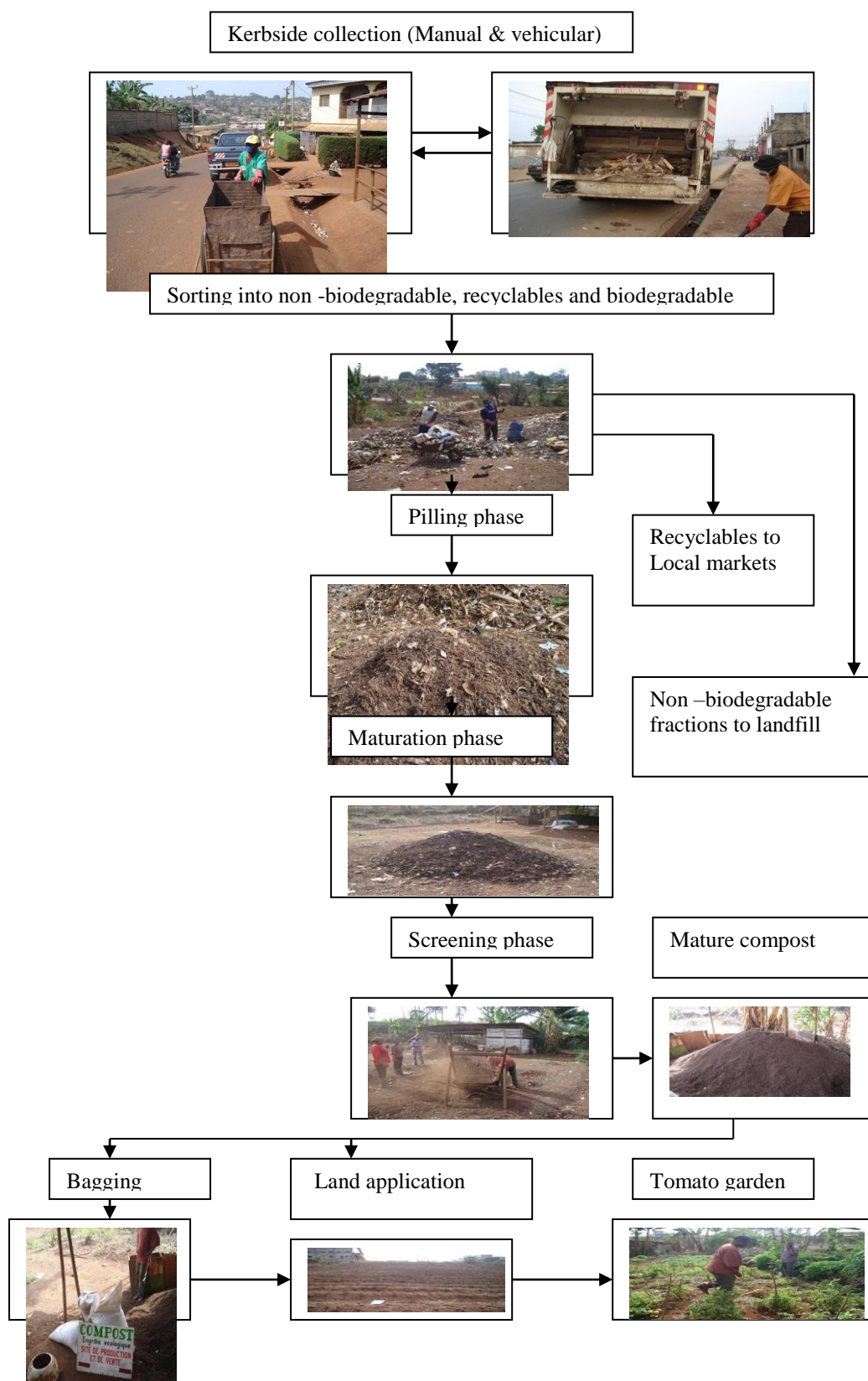


Figure 4: Flow Chart of the composting process and application

Cameroon, like in other Sub-Sahara African countries with rising temperatures and declining precipitation<sup>25</sup>, the decomposition process is slow and takes several months, 3 to 4 months during the raining season and 4 to 5 months in the dry season.<sup>30</sup> Under such conditions, to estimate emissions during the composting process requires data on the type and composition of the waste to be composted. However, in the absence of such data it becomes impossible to calculate the mitigation potential of composting to climate change. Although not within the scope of this work, the results indicate that a significant quantity of household waste was being diverted away from the landfill which is in line with the European Union directives (Council Directive 1999/31/EC).

## Conclusions

The GICABIO study highlights the importance of using traditional knowledge, technologies and practices in compost production and indicated that a significant quantity of household waste was being diverted away from the landfill and transformed into organic compost for use by farmers, with the possibility of improving existing carbon sinks and reducing net CO<sub>2</sub> emissions. Climatic conditions and the waste types were determining factors for the quality of the compost that was produced. However, in the absence of compost specification, and data on waste characterization, uncertainties reigns as to the effectiveness of traditional knowledge, technologies and practices in improving existing carbon sinks and to reduce net CO<sub>2</sub> emissions. It is for the reason that this work recommends that, traditional knowledge, technologies and practices should be integrated with modern composting technologies to better understand the mitigation potentials to climate change.

## References

- <sup>1</sup>UNFCCC, *Greenhouse Gas Emissions Data for 1990 –2003 submitted to the United Nations Framework Convention on Climate Change*, UNFCCC Secretariat, Bonn, Germany, **2005**.
- <sup>2</sup>IPCC, *Climate Change Mitigation Contribution of Working Group III to the Third Assessment Report of the Intergovernmental Panel on Climate Change (IPCC)*, Metz, B., Davidson, O., Swart, R. & Pan, J. (eds.) Cambridge University Press, Cambridge, UK, **2001**.
- <sup>3</sup>Crowe, M., Nolan, K., Collins, C., Carty, G., Donlon, B., Kristoffersen, M., *Biodegradable Municipal Waste Management in Europe*. European Environment Agency. Available from: <http://www.eea.eu.int/S>, **2002**.
- <sup>4</sup>USEPA, *Global anthropogenic Non-CO<sub>2</sub> greenhouse gas emissions: 1990-2020*. Office of Atmospheric Programs Climate Change Division, U.S. Environmental Protection Agency, Washington D.C., USA. (Draft December **2005**).
- <sup>5</sup>ADB, *Asia Least-cost Greenhouse Gas Abatement Strategy ALGAS. Summary Report*. Asian Development Bank, Global Environment Facility, United Nations Development Programme. Manila, Philippines, **1998**. <http://www.vtt.fi/inf/pdf/workingpapers/2004/W5.pdf>
- <sup>6</sup>Monni, Suvi, Pipatti, Riitta, Lehtil, Antti, Savolainen, Ilkka & Syri, Sanna., *Global climate change mitigation scenarios for solid waste management*, Espoo., **2006**. VTT Publications 603, 51 .
- <sup>7</sup>Eunomia, *SEA Scoping report for Northamptonshire*, Waste Management Partnership, Bristol, UK. **2006**.
- <sup>8</sup>IEA, *CO<sub>2</sub> emissions from fuel combustion 1971-2003*, IEA, Paris, France, **2005**
- <sup>9</sup>*Municipal Africa*, April **1994**. I, 2.
- <sup>10</sup>Ngnikam, E., Vermande, P. & Rousseaux, P., *Cahiers Agricult.*, **1993**, 2, 264.
- <sup>11</sup>Ndoumbe N. H., Ngnikam, E. & Wethe, J., *Bull. Afr. Bioresour. Éner. Dev. Environ. (Dakar)*, **1995**, 4, 4.
- <sup>12</sup>CIPCRE, *Projet pilote de compostage décentralisé des ordures ménagères dans la ville de Bafoussam*, Rapport d'exécution de projet (non publié), **1997**, 70.
- <sup>13</sup>CPSS et AFVP, *Rapport de clôture du projet de compostage des ordures ménagères et maraîchage périurbain à Garoua*. Garoua : AFVP, Mission Française de Coopération, **1997**, 36.
- <sup>14</sup>Ngnikam, E., *Evaluation environnementale et économique de systèmes de gestion des déchets solides municipaux : analyse du cas de Yaoundé au Cameroun*. Thèse de doctorat, STD, INSA de Lyon, **2000**, 363.
- <sup>15</sup>WRAP, *Specification for the use of compost in horticulture*, Banbury, UK, **2005**.
- <sup>16</sup>Mohee, R., & Mudhoo, A., *Powder Technol.*, **2005**, 155, 92.
- <sup>17</sup>Iyengar, S. R., & Bhavne, P. P., *Waste Manag.*, **2006**, 26, 1070.
- <sup>18</sup>Tejada, M., & Gonzalez, J. L., *Eur. J. Agron.*, **2005**, 23, 336.
- <sup>19</sup>Huang, G. F., Wu, Q. T., Wong, J. W. C., & Nagar, B. B., *Bioresource Technol.*, **2006**, 97, 1834.
- <sup>20</sup>Zurbrugg, C., Drescher, S., Rytz, I., Sinh. A. H. M., and Enaytullah, I., *Resources, Conserv. Recycling*, **2005**, 43, 281.
- <sup>21</sup>Probert, E. J., Watts, B. M., & Bentley, S. P., *Int. J. Environ. Sustainable Dev.*, **2003**, 2(4), 437.
- <sup>22</sup>TCA, *The state of composting and biological waste treatment 2004/05 in the UK*, **2006**.
- <sup>23</sup>Sæbø, A., & Ferrini, F., *Urban Forestry & Urban Greening.*, **2006**, 4, 159.
- <sup>24</sup>Lal, R., *Soil surface management in the tropics for intensive land use and high and sustained productivity*. In: Steward B. A., (Ed.), *Improving Agriculture Production in the Tropics. Advances in Soil Science*, Springer, New York., **1986**, 5, 245.
- <sup>25</sup>Barrios, S., Ouattara, B., & Strobl, E., *Food Policy*, **2008**, 33(4), 287.
- <sup>26</sup>Human Development Report, "Human and income poverty: Developing countries", **2005**. [Online]. Available: [http://hdr.undp.org/hdr2006/statistics/documents/hpi\\_1.pdf](http://hdr.undp.org/hdr2006/statistics/documents/hpi_1.pdf). [Accessed] **05 /5/ 2008**.
- <sup>27</sup>Denscombe, M., *The good research guide for small –scale social research projects*, Maidenhead Philadelphia Open University Press, **2003**.
- <sup>28</sup>CIPCRE, *Rapport d'Activités et financier*, **2006**
- <sup>29</sup>Danso, G., Drechsel, P., & Gyiele, L., *Urban household perception of urine-excreta and solid waste source separation in urban areas of Ghana*. In: Werner, C., et al. (Eds.), *Ecosan – Closing the Loop*. GTZ and IWA, Lubeck, Germany., **2004**, 191–196.
- <sup>30</sup>Mbeng, L. O., *The impact of public attitudes and behaviour on the effective valorisation of household organic waste into agricultural compost: Case study Limbe and Douala, Cameroon*. Ph.D. dissertation; School of Applied Sciences, The University of Northampton: Northampton, UK, **2009**.

Received: 26.09.2012.  
Accepted: 03.10.2012.



# CORROSION BEHAVIOUR OF MILD STEEL IN SIMULATED CONCRETE PORE SOLUTION PREPARED IN RAIN WATER, WELL WATER AND SEA WATER

M. Pandiarajan<sup>[a]\*</sup>, P. Prabhakar<sup>[b]</sup> and S. Rajendran<sup>[a,c]</sup>

**Keywords:** simulated concrete pore solution, mild steel, rain water, well water, sea water, polarization study.

Concrete admixtures can be prepared in various water samples such as rain water, well water, and sea water. These waters contain various types of ions. So corrosion behaviour of mild steel immersed in simulated concrete pore solution prepared with the above water samples will vary. Corrosion resistance of mild steel in simulated concrete pore solution prepared with above water samples has been evaluated by polarization study. The corrosion resistance of mild steel in various samples of water is as follows: Rain water>Well water>Sea water. The corrosion resistance of mild steel in simulated concrete pore solution prepared in various water samples are in the decreasing order: Rain water>Well water> Sea water. This is revealed by the linear polarization resistance values and corrosion current values.

\* Corresponding Authors

E-Mail: pandiarajan777@gmail.com

[a] Corrosion Research Centre, PG and research Department of Chemistry, G.T.N Arts College, Dindigul- 624 005. E.mail: pandiarajan777@gmail.com

[b] PG and research Department of Chemistry, APA College of Arts and Culture, Palani, Dindigul

[c] Corrosion Research Centre, R.V.S. School of Engineering and Technology, Dindigul- 624 005. E.mail:srmjoany@sify.com

## INTRODUCTION

Reinforced concrete is widely used for building materials and plays a significant role in economic development. However, the premature degradation of reinforced concrete structures due to the reinforcing steel corrosion has become a serious problem in modern society, which results in a huge economic loss<sup>1-3</sup>.

Under normal conditions, reinforcing steel in concrete can be protected from corrosion by forming a compact passive film on its surface in concrete pore solution with high alkalinity (pH 12.5-13.5). However, the passive film can be locally damaged and the localized corrosion of reinforcing steel takes place when pH and/or the chloride concentration at the steel/concrete interface reach the critical values for corrosion.<sup>4-9</sup> The pH of concrete pore solution decreased during concrete carbonation due to the neutralization of Ca(OH)<sub>2</sub> in the interstitial solution with the acidic gases (CO<sub>2</sub>, SO<sub>2</sub>, etc.) which diffuse into the steel/concrete interface from the air<sup>8</sup>. The pH value of concrete pore solution is one of the most important parameters affecting the corrosion behaviour of reinforcing steel in concrete.

In spite of the extensive studies of corrosion behaviours of reinforcing steel<sup>4-10</sup>, the exact mechanism of its depassivation is still unclear. Even though the effect of pH on the corrosion of reinforcing steel was discovered decades ago, there were only a few studies focusing on the depassivation of the steel caused by decreasing pH of concrete pore solution during the carbonation process.<sup>8,11-13</sup> In the urban and industrial areas, the acidic gases (CO<sub>2</sub>, SO<sub>2</sub>, NO<sub>2</sub>, etc.) can make the local atmosphere acidic, and attack

the hydrated concrete. The reactions of neutralization in concrete may decrease the pH value of concrete pore solution, induce the steel surface depassivation, and consequently cause the steel corrosion.

Several research papers have investigated the corrosion behaviour of metals in presence of simulated concrete pore (SCP) solutions<sup>14-25</sup>. Usually steel rebars have been used in such studies. The Present Study is undertaken to investigate the corrosion of mild steel in SCPS prepared in rain water, well water and sea water. A saturated solution of calcium hydroxide is used as SCP solution<sup>26-30</sup>. Polarization study has been used to evaluate the corrosion resistance of mild steel.

## MATERIALS AND METHODS

### Metal specimens

Mild steel specimen was used in the present study. (Composition (wt %): 0.026 S, 0.06 P, 0.4 Mn, 0.1 C and balance iron<sup>31</sup>).

The composition of rainwater (collected from roof top and stored in concrete tank), well water and sea water used in the present study is given the Table 1.

Table 1.

Parameters	Rainwater	Well water	Sea water
pH	8.15	8.38	7.18
Total Dissolved Solids	273 ppm	2013ppm	39392 ppm
Electrical Conductivity	390 1/cmΩ	3110 1/cmΩ	57929 1/cmΩ
Nitrate	9 ppm	0	0
Chloride	72 ppm	665ppm	16850
Sulphate	14 ppm	14ppm	6010
Fluoride	0.2 ppm	0	0
Total Hardness as CaCO <sub>3</sub>	88 ppm	1100ppm	112 ppm

Table 2. Corrosion parameters of mild steel immersed in simulated concrete pore solution (saturated calcium hydroxide solution), obtained by potentiodynamic polarization study.

System	$E_{\text{corr}}$ , mV vs SCE	$b_c$ mV/decade	$b_a$ , mV/decade	LPR, $\Omega \text{ cm}^2$	$I_{\text{corr}}$ , $\text{A cm}^{-2}$
Rain water	-822	156	287	15273	$2.887 \times 10^{-6}$
SCPS prepared in rain water	-470	212	196	94806	$4.68 \times 10^{-7}$
Well water	-833	153	302	13264	$3.329 \times 10^{-6}$
SCPS prepared in well water	-631	194	187	35638	$1.162 \times 10^{-6}$
Sea water	-846	150	264	5548	$7.506 \times 10^{-6}$
SCPS prepared in sea water	-800	159	234	6281	$6.568 \times 10^{-6}$

### Simulated Concrete Pore (SCP) Solution

A saturated calcium hydroxide solution is used in the present study, as SCP solution. The electrodes made of mild steel wire were immersed in the SCP solution and polarization study was carried out.

### Potentiodynamic polarization

Polarization studies were carried out in a CHI – Electrochemical workstation with impedance, Model 660A. A three-electrode cell assembly was used. The working electrode was mild steel. A saturated calomel electrode (SCE) was the reference electrode and platinum was the counter electrode. From the polarization study, corrosion parameters such as corrosion potential ( $E_{\text{corr}}$ ), corrosion current ( $I_{\text{corr}}$ ) and Tafel slopes (anodic =  $b_a$  and cathodic =  $b_c$ ) were calculated.

## RESULTS AND DISCUSSIONS

Corrosion behaviour of mild steel in simulated concrete pore solution (SCP), saturated calcium hydroxide solution) have been investigated by polarization study.

### Polarization Study

The polarization curves of mild steel prepared in simulated concrete pore solution are shown in Figs. 1 to 3. The corrosion parameters such as corrosion potential ( $E_{\text{corr}}$ ), Tafel slopes ( $b_c$  = cathodic;  $b_a$  = anodic), Linear polarization resistance (LPR), and corrosion current ( $I_{\text{corr}}$ ) are given in Table 2

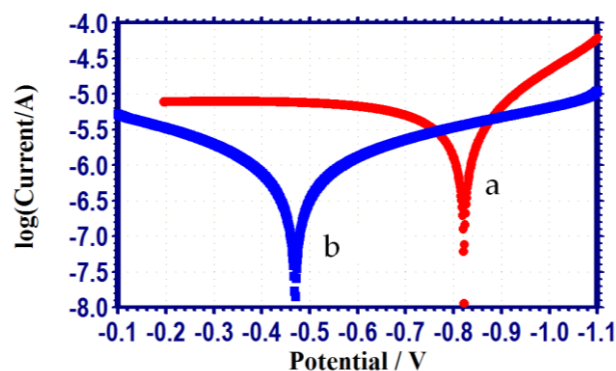


Figure 1. Polarization curves of mild steel immersed in various test solution a) Rain water; b) SCPS prepared in rain water

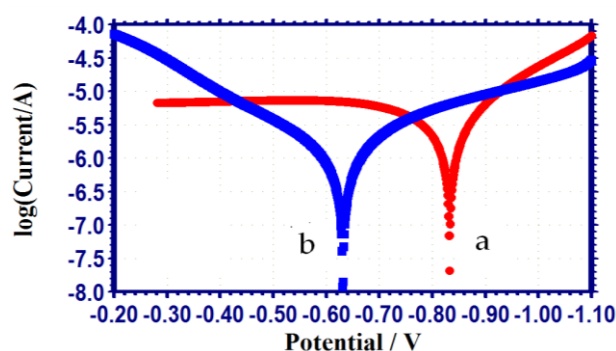


Figure 2. Polarization curves of mild steel immersed in various test solution. a) Well water. b) SCPS prepared in well water.

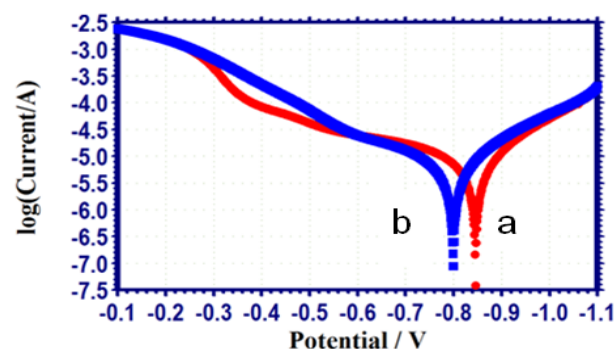


Figure 3. Polarization curves of mild steel immersed in various test solution. a) Sea water; b) SCPS prepared in sea water

It is observed from Table 2 that the decreasing order of corrosion resistance of mild steel immersed in simulated concrete pore solution prepared in rainwater, well water and sea water is as follows rain water > well water > sea water.

This is revealed by the fact that the LPR values are in the decreasing order namely 15273, 13264 and 5548  $\text{ohm cm}^2$ , further the corrosion current values increase from rainwater [ $2.887 \times 10^{-6} \text{ A/cm}^2$ ] to well water [ $3.329 \times 10^{-6} \text{ A/cm}^2$ ] and then to sea water [ $7.506 \times 10^{-6} \text{ A/cm}^2$ ]<sup>32-41</sup>.

It is also observed that the corrosion resistance of mild steel immersed in simulated concrete pore solution prepared in rainwater is greater than the corrosion resistance of mild steel in rainwater alone. Similarly the corrosion resistance of mild steel immersed in simulated concrete pore solution prepared in well water is greater than the corrosion resistance of mild steel in well water, the corrosion

resistance of mild steel immersed in simulated concrete pore solution prepared in sea water is greater than the corrosion resistance of mild steel in sea water.

The corrosion resistance of mild steel in simulated concrete pore solution prepared in various water samples are in the decreasing order: Rain water>Well water>Seawater.

## CONCLUSION

Corrosion resistance of mild steel in simulated concrete pore solution prepared with rain water, well water and sea water samples has been evaluated by polarization study.

The corrosion resistance of mild steel in various samples of water is as follows: Rain water> Well water> Sea water.

The corrosion resistance of mild steel in simulated concrete pore solution prepared in various water samples are in the decreasing order: Rain water>Well water>Seawater.

This is revealed by the linear polarization resistance values and corrosion current values. So it is concluded from these study that it is better to use rainwater to prepare concrete admixtures.

## ACKNOWLEDGEMENT

The authors are thankful to their management and St.Joseph's Research and Educational Trust, Dindigul for their help and encouragement.

## REFERENCES

- <sup>1</sup>Ahmad S, *Cement Concrete Comp.*,**2003**, 25, 459.
- <sup>2</sup>Biezma M. V and San, J. R. C. *Corros. Eng. Sci. Techn.*, **2005**, 40, 344.
- <sup>3</sup>Thangavel, K., *Corros. Rev.* **2004**, 22, 55
- <sup>4</sup>Moreno, M., Morris, W., Alvarez, M. G. and Duffo, G. S., *Corros. Sci.*, **2004**, 46, 2681.
- <sup>5</sup>Kumar, V., *Corros. Rev.*, **1998**, 16, 317.
- <sup>6</sup>Maslehuddin, M., Al-Zahrani, M. M., Ibrahim, M., Al-Mehthel, M. H. and Al-Idi, S. H., *Constr. Build. Mater.*, **2007**, 21, 1825.
- <sup>7</sup>Du, R. G, Hu, R. G., Huang, R. S and Lin, C. J., *Anal. Chem.*, **2006**, 78, 3179.
- <sup>8</sup>Huet, B., L'Hostis, V., Miserque, F. and Idrissi, H., *Electrochim. Acta.*, **2005**, 51, 172.
- <sup>9</sup>Alonso, C., Castellote, M. and Andrade, C., *Electrochim. Acta* **2002**, 47, 3469.
- <sup>10</sup>Poupard, O., Ait-Mokhtar, A. and Dumargue, P., *Cement Concrete Res.*, **2004**, 34, 991.
- <sup>11</sup>Duffo, G. S., Morris, W., Raspini, I. and Saragovi, C., *Corros. Sci.*, **2004**, 46, 2143.
- <sup>12</sup>Yeih, W. C and Chang, J. J., *Constr. Build. Mater.*, **2005**, 19, 516.
- <sup>13</sup>Garces, P., Andrade, M. C., Saez, A. and Alonso, M. C., *Corros. Sci.*, **2005**, 47, 289.
- <sup>14</sup>Zhou X ,Yang H. Y, Wang F. H, *Corros. Sci. Protec. Technol.*, **2010**, 22(4), 343.
- <sup>15</sup>Fajardo, S, Bastidas, D. M , Ryan, M. P, Criado, M., McPhail, D. S., Bastidas, J. M., *Appl. Surf. Sci.*, **2010**, 256(21), 6139.
- <sup>16</sup>Chen, W., Du, R. G., Ye, C.-Q., Zhu, Y.-F., Lin, C.-J., *Electrochim. Acta.*, **2010**, 55(20), 5677.
- <sup>17</sup>Wang, L., Zhao, Y.-L., Tiedao Xuebao (*J. China Railway Soc.*), **2010**, 32(4) 96.
- <sup>18</sup>Chastre, C., Silva, M. A. G., *Eng. Struct.*, **2010**, 32(8), 2268.
- <sup>19</sup>Suh, K., Mullins, G., Sen, R., Winters, D., *J. Composit. Construct.*, **2010**, 14(4) 388.
- <sup>20</sup>Zhang, J. X., Sun, H. H., Sun, Y. M., Zhang, N., *J. Zhejiang Univ. Sci. A.*, **2010**, 11(5), 382.
- <sup>21</sup>Dao, V. T. N., Dux, P. F., Morris, P. H., Carse, A. H., *ACI Mater. J.*, **2010**, 107(3), 291.
- <sup>22</sup>Ghods, P., Isgor, O. B., McRae, G. A., Gu, G. P., *Corros. Sci.*, **2010**, 52(5), 1649.
- <sup>23</sup>Fan, Y. F., Hu, Z. Q., Zhang, Y. Z., Liu, J. L., *Construct. Build. Mater.*, **2010**, 24(10), 1975.
- <sup>24</sup>Kenny, A., Katz, A., *Adv. Mater. Res.*, **2010**, 95, 69.
- <sup>25</sup>Huet, B., L'Hostis, V., Tricheux, L., Idrissi, H., *Mater. Corros.*, **2010**, 61(2), 111.
- <sup>26</sup>Allahkaram S.R, Khodayari, *Anti-Corros. Methods Mater.*, **2008**, 55, 250.
- <sup>27</sup>Mennucci, M. M., Banczek, E. P., Rodrigues, P. R. P., Costa, I., *Cement Concrete Compost.* **2009**, 31, 418.
- <sup>28</sup>Kitowski, C. J., Wheat, H. G, *Corrosion*, **1997**, 53 ,216.
- <sup>29</sup>Hurley, M. F, Scully, J. R., *Corrosion*, **2006**, 62, 892.
- <sup>30</sup>Li, L., Sagues, A. A., *Corrosion* , **2004**, 60, 195.
- <sup>31</sup>Arockia, S. J., Rajendran, S., Garga Sri, V., Amalraj, J., A. and Narayanasamy, B., *Portugaliae Electrochim. Acta*, **2009**, 27, 1.
- <sup>32</sup>Kavipriya, K., Sathiyabama, J., Rajendran, S., Krishnaveni, A. *Int. J. Adv. Eng. Sci. Technol.*, **2012**, 2(2), 106.
- <sup>33</sup>Manimaran, N., Rajendran, S., Manivannan, M., Saranya, R. *J. Chem. Biol. Phys. Sci. Sect A.*, **2012**, 2(2), 568.
- <sup>34</sup>Sahayaraja, A., Rajendran, S. *J. Electrochem. Sci. Eng.* **2012**, 2, 91.
- <sup>35</sup>Manimaran, N., Rajendran, S., Manivannan, M., Johnmary, S. *Res. J. Chem. Sci.* **2012**, 2(3), 52.
- <sup>36</sup>Sribharathy, V., Rajendran, S. *Int. J. Adv. Eng. Sci. Technol.* **2011**, 1(1), 77.
- <sup>37</sup>Anbarasi, M. C., Rajendran, S., Vijaya, N., Manivannan, M., Shanthi, T. *The Open Corros. J.*, **2011**, 4, 40.
- <sup>38</sup>Johnsirani, V., Rajendran, S., Sathiyabama, J., Muthumegala, T. S., Krishnaveni, A., Hajarabeevi, N. *Bulg. Chem. Commun.* **2012**, 44(1), 41.
- <sup>39</sup>Sangeetha, M., Rajendran, S., Sathiyabama, J., Krishnaveni, A., Shanthi, P., Manimaran, N., Shyamaladevi, B. *Portugaliae Electrochim. Acta*, **2011**, 29(6), 429.
- <sup>40</sup>Manivannan, M., *Int. J. Adv. Eng. Sci. Technol.*, **2011**, 3, 8048.
- <sup>41</sup>Noreen, A., Benita, S. H., Rajendran, S., *Portugaliae Electrochim. Acta .*, **2010**, 28(1), 1.

Received: 22.09.2012.  
Accepted: 02. 10.2012.



# STRUCTURAL AND THERMAL INVESTIGATIONS OF NOVEL CHARGE-TRANSFER COMPLEXES OF THYMOL AND THE ACCEPTORS PICRIC ACID, CHLORANILIC ACID, 1,3-DINITROBENZENE AND *p*-CHLORANIL

Abdel Majid A. Adam<sup>[a]</sup>, Moamen S. Refat<sup>[a,b]\*</sup>, Hosam A. Saad<sup>[a,c]</sup> and Hala H. Eldaroti<sup>[d]</sup>

**Keywords:** Thymol, Charge-transfer, Benesi–Hildebrand method, Thermal analysis

Thymol (Thy) is a widely known anti-microbial agent and can be found as one of the components of many essential oils. Intermolecular charge-transfer complexes between the Thy as a donor and picric acid (PA), chloranilic acid (CLA), 1,3-dinitrobenzene (DNB) or *p*-chloranil (*p*-CHL) as a  $\pi$ -acceptor have been structurally and thermally studied in methanol at room temperature. Based on elemental analyses (CHN) and photometric titrations, the stoichiometry of the complexes (Thy: acceptor molar ratios) was determined to be 1:1 for all four complexes. The formation constant ( $K_{CT}$ ), molar extinction coefficient ( $\epsilon_{CT}$ ) and other spectroscopic data have been determined using the Benesi–Hildebrand method and its modifications. The newly synthesized CT complexes have been characterized via elemental analyses (CHN), IR, <sup>1</sup>H-NMR, and electronic absorption spectroscopy. Thermogravimetric analyses (TG) were also used to investigate the thermal stability of the synthesized solid CT complexes.

\* Corresponding Authors

E-Mail: msrefat@yahoo.com

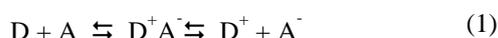
- [a] Department of Chemistry, Faculty of Science, Taif University, Al-Hawiah, Taif, P.O. Box 888 Zip Code 21974, Saudi Arabia  
 [b] Department of Chemistry, Faculty of Science, Port Said University, Port Said, Egypt  
 [c] Department of Chemistry, Faculty of Science, Zagazig University, Zagazig, Egypt  
 [d] Department of Chemistry, Faculty of Education, Alzaeim Alazhari University, Khartoum, Sudan

species are intensively studied because of their special type of interaction, which is accompanied by the transfer of an electron from the donor to the acceptor<sup>29,30</sup>. In addition, the protonation of the donor from acidic acceptors is a route for the formation of ion-pair adducts<sup>31-33</sup>.

Considerable attention has recently been devoted to the formation of stable charge-transfer complexes that result from the reaction between acceptors and drugs or biological compounds. This interest stems from the significant physical and chemical properties of these complexes. For example, the complexation of charge-transfer complexes with drugs has been recognized as an important phenomenon in the drug-receptor binding mechanism and in many other biological processes. Herein, the CT interaction between the anti-microbial agent thymol and four acceptors are investigated. Thymol (Thy, C<sub>10</sub>H<sub>14</sub>O), a phenol derivative, is the main constituent in natural essential oils from many herbs, such as Thyme, Oregano and winter savory<sup>34-36</sup>. Thymol has an antimicrobial effect on bacteria, fungi, and yeasts. It is able to inhibit both Gram-positive and Gram-negative bacteria, including the potential pathogenic strains of *Bacillus subtilis*, *Escherichia coli*, *Klebsiella pneumoniae* and *Staphylococcus aureus* also. Amongst the identified natural anti-microbial agents (thymol, carvacrol, citronella, eugenol and terpinen-4-ol), thymol showed the highest antibacterial activity against *Staphylococcus aureus*, *Escherichia coli* and *Pseudomonas aeruginosa*<sup>37</sup>. Due to its bactericidal action against oral bacteria, it is commonly incorporated in mouthwashers. Thymol and essential oils rich in thymol, have proved beneficial in medical<sup>38,39</sup>, food<sup>40</sup>, agricultural<sup>41</sup>, veterinarian and pest control applications<sup>42</sup>.

## Introduction

The term charge-transfer complex (CTC) was first introduced by Mulliken<sup>1,2</sup> and has been widely discussed by Foster<sup>3</sup>. Mulliken<sup>4,5</sup> demonstrated that the charge-transfer interactions within a molecular complex that consists of an electron donor, D, and an electron acceptor, A, involve a resonance with a transfer of charge from D to A:



Charge-transfer complexation is of great importance in chemical reactions, including addition, substitution, condensation<sup>6,7</sup>, biochemical and bioelectrochemical energy-transfer processes<sup>8</sup>, biological systems<sup>9</sup>, and drug-receptor binding mechanisms. For example, drug action, enzyme catalysis, ion transfers through lipophilic membranes<sup>10</sup>, and certain  $\pi$ -acceptors have successfully been used in the pharmaceutical analysis of some drugs in pure form or in pharmaceutical preparations<sup>11-17</sup>. Furthermore, charge-transfer complexation is also of great importance in many applications and fields, such as in non-linear optical materials, electrically conductive materials<sup>18-21</sup>, second-order non-linear optical activity<sup>22</sup>, microemulsions<sup>23</sup>, surface chemistry<sup>23</sup>, photocatalysts<sup>24</sup>, dendrimers<sup>25</sup>, solar energy storage<sup>26</sup>, organic semiconductors<sup>27</sup>, and the investigation of redox processes<sup>28</sup>. Charge-transfer complexes that use organic

The purpose of the work reported here was to study the structural and thermal stability of charge-transfer complexes formed between thymol with picric acid (PA), chloranilic acid (CLA), 1,3-dinitrobenzene (DNB) and *p*-chloranil (*p*-CHL). The elemental analysis, infrared (IR),

$^1\text{H-NMR}$  and electronic absorption spectroscopy were used to interpret the behavior of the interactions. The spectroscopic physical data were analyzed in terms of the formation constant ( $K_{CT}$ ), the molar extinction coefficient ( $\epsilon_{CT}$ ), the standard free energy ( $\Delta G^\circ$ ), the oscillator strength ( $f$ ), the transition dipole moment ( $\mu$ ), the resonance energy ( $R_N$ ) and the ionization potential ( $I_D$ ). The thermal behaviors of the obtained complexes have also been investigated.

## Experimental

### Chemicals

All chemical used were of high grade of purity. Thymol (Thy) ( $\text{MF}=\text{C}_{10}\text{H}_{14}\text{O}$ ) was obtained from Sigma-Aldrich Chemical Company, USA with a stated purity of more than 99.6% and was used without further purification. Picric acid (2,4,6-trinitrophenol, PA), 1,3-dinitrobenzene (DNB), chloranilic acid (CLA) and *p*-chloranil (*p*-CHL) were purchased from Merck Chemical Company and were also used as received.

### Synthesis

The solid CT products of Thy with PA, CLA, DNB and *p*-CHL were synthesized by mixing equimolar amounts of Thy donor with each acceptor in methanol. The mixtures were stirred for 20 min, and allowed to evaporate slowly at room temperature, which resulted in the precipitation of the solid CT complexes. The separated complexes were filtered off, washed well with little amounts of methanol, and then collected and dried under vacuum over anhydrous calcium chloride for 24 h.

### Photometric titration

Photometric titration measurements were carried out for the reactions of Thy with PA, CLA, DNB and *p*-CHL against methanol as a blank at wavelengths of 354, 285, 300 and 284 nm, respectively. A 0.25, 0.50, 0.75, 1.00, 1.50, 2.0, 2.50, 3.00, 3.50 or 4.00 mL aliquot of a standard solution ( $5.0 \times 10^{-4}$  M) of the appropriate acceptor in MeOH was added to 1.00 ml of  $5.0 \times 10^{-4}$  M Thy, which was also dissolved in MeOH. The total volume of the mixture was 5 mL. The concentration of EC ( $C_d$ ) in the reaction mixture was maintained at  $5.0 \times 10^{-4}$  M, whereas the concentration of the acceptors ( $C_a$ ) changed over a wide range of concentrations ( $0.25 \times 10^{-4}$  M to  $4.00 \times 10^{-4}$  M) to produce solutions with an acceptor molar ratio that varied from 4:1 to 1:4. The stoichiometry of the molecular CT complexes was obtained from the determination of the conventional spectrophotometric molar ratio according to known methods<sup>43</sup> using a plot of the absorbance of each CT complex as a function of the  $C_d:C_a$  ratio. Modified Benesi-Hildebrand plots<sup>44,45</sup> were constructed to allow the calculation of the formation constant,  $K_{CT}$ , and the absorptivity,  $\epsilon_{CT}$ , values for each CT complex in this study.

### Instrumentation

The elemental analyses of the carbon, hydrogen and nitrogen contents were performed by the microanalysis facility at Cairo University, Egypt, using a Perkin-Elmer CHN 2400 (USA). The electronic absorption spectra of methanolic solutions of the donor, acceptors and resulting CT complexes were recorded over a wavelength range of 200-800 nm using a Perkin-Elmer Lambda 25 UV/Vis double-beam spectrophotometer at Taif University, Saudi Arabia. The instrument was equipped with a quartz cell with a 1.0 cm path length. The mid-infrared (IR) spectra (KBr discs) within the range of  $4000\text{--}400\text{ cm}^{-1}$  for the solid CT complexes were recorded on a Shimadzu FT-IR spectrophotometer with 30 scans at  $2\text{ cm}^{-1}$  resolution. The Raman laser spectra of the samples were measured on a Bruker FT-Raman spectrophotometer equipped with a 50 mW laser at Taif University, Saudi Arabia.  $^1\text{H-NMR}$  spectra were collected by the Analytical Center at King Abdul Aziz University, Saudi Arabia, on a Bruker DRX-250 spectrometer operating at 250.13 MHz with a dual 5 mm probe head. The measurements were performed at ambient temperature using DMSO- $d_6$  (dimethylsulfoxide,  $d_6$ ) as a solvent and TMS (tetramethylsilane) as an internal reference. The  $^1\text{H-NMR}$  data are expressed in parts per million (ppm) and are internally referenced to the residual proton impurity in the DMSO as solvent. Thermogravimetric analysis (TGA) was performed under an air atmosphere between room temperature and  $800\text{ }^\circ\text{C}$  at a heating rate of  $10\text{ }^\circ\text{C}/\text{min}$  using a Shimadzu TGA-50H thermal analyzer at the Central Lab at Ain Shams University, Egypt.

## Results and discussion

### Elemental analyses results

Elemental analyses (C, H, and N) of the Thy CT complexes were performed, and the obtained analytical data are as follows:

1 [(Thy)(PA)];  $\text{C}_{16}\text{H}_{17}\text{N}_3\text{O}_8$ ; Mol. wt.=379.32; Orange; Anal. Calcd.: C, 50.62; H, 4.48; N, 11.07. Found: C, 51.01; H, 4.37; N, 10.73.

2 [(Thy)(CLA)];  $\text{C}_{16}\text{H}_{16}\text{Cl}_2\text{O}_5$ ; Mol. wt.=359.20; Dark red; Anal. Calcd.: C, 53.45; H, 4.45. Found: C, 53.61; H, 4.54.

3 [(Thy)(DNB)];  $\text{C}_{16}\text{H}_{18}\text{N}_2\text{O}_5$ ; Mol. wt.=318.32; Pale brown; Anal. Calcd.: C, 60.32; H, 5.65; N, 8.80. Found: C, 60.50; H, 5.37; N, 8.67

4 [(Thy)(*p*-CHL)];  $\text{C}_{16}\text{H}_{14}\text{Cl}_4\text{O}_3$ ; Mol. wt.=396.10; Orange yellow; Anal. Calcd.: %C, 48.47; %H, 3.53. Found: %C, 48.40; %H, 3.59.

The resulting values are in good agreement with the calculated values, and the suggested values are in agreement with the molar ratios determined from the photometric titration curves.

The stoichiometry of all complexes was found to be 1:1 ratios. Based on the obtained data, the formed charge-transfer complexes were formulated as [(Thy)(PA)], [(Thy)(CLA)], [(Thy)(DNB)] and [(Thy)(*p*-CHL)].

### Electronic absorption spectra

Figure 1 shows the electronic absorption spectra of the Thy donor, acceptors and the formed CT complexes. These spectra revealed new absorption bands that are attributed to the CT interactions. These bands are observed at 354, 285, 300 and 284 nm for the Thy/PA, Thy/CLA, Thy/DNB and Thy/*p*-CHL complexes, respectively. These peak absorbance values that appeared in the spectra assigned to the formed CT complexes were measured and plotted as function of the  $C_d$ :  $C_a$  ratio according to the known method. Photometric titration plots based on these measurements (Figure 2) confirmed the complex formation at a ratio (Thy: acceptor) of 1:1 in all cases. The formation constant ( $K_{CT}$ ) and the molar absorptivity ( $\epsilon$ ) of these complexes were calculated by applying the 1:1 modified Benesi–Hildebrand equation in Eqn. (2)<sup>44</sup>:

$$\frac{C_a C_d}{A} = \frac{1}{K\epsilon} + \frac{(C_a + C_d)}{\epsilon} \quad (2)$$

where  $C_a$  and  $C_d$  are the initial concentrations of the electron acceptor and the electron donor, respectively, and  $A$  is the absorbance of the strongly detected CT band. Plotting  $(C_a C_d)/A$  values versus the corresponding  $(C_a + C_d)$  values for the formed EC charge-transfer complexes, straight line are obtained supporting our finding of the formation of 1:1 complexes. In the plots, the slope and intercept equal  $1/\epsilon$  and  $1/K\epsilon$ , respectively. The modified Benesi–Hildebrand plots are shown in Figure 3 and the values of both  $K_{CT}$  and  $\epsilon$  associated with the complexes are given in Table 1. These complexes exhibit high values of both the formation constant ( $K_{CT}$ ) and the extinction coefficients ( $\epsilon$ ). These high values of  $K_{CT}$  reflect the high stabilities of the formed CT complexes. The equilibrium constants are strongly dependent on the nature of the used acceptor including the type of electron withdrawing substituents to it such as nitro and halo groups<sup>46</sup>. The data reveal that the [(Thy)(CLA)] complex shows a higher  $K_{CT}$  value compared with the other complexes, reflecting the relatively higher powerful electron acceptance ability for CLA.

### Calculation of the spectroscopic and physical data

The spectroscopic and physical data, such as the standard free energy ( $\Delta G^\circ$ ), the oscillator strength ( $f$ ), the transition dipole moment ( $\mu$ ), the resonance energy ( $R_N$ ), and the ionization potential ( $I_P$ ), were estimated for samples dissolved in methanol at 25 °C. The oscillator strength ( $f$ ) is a dimensionless quantity used to express the transition probability of the CT-band. From the CT absorption spectra<sup>47</sup>, and can be estimated using the approximate formula<sup>48</sup>:

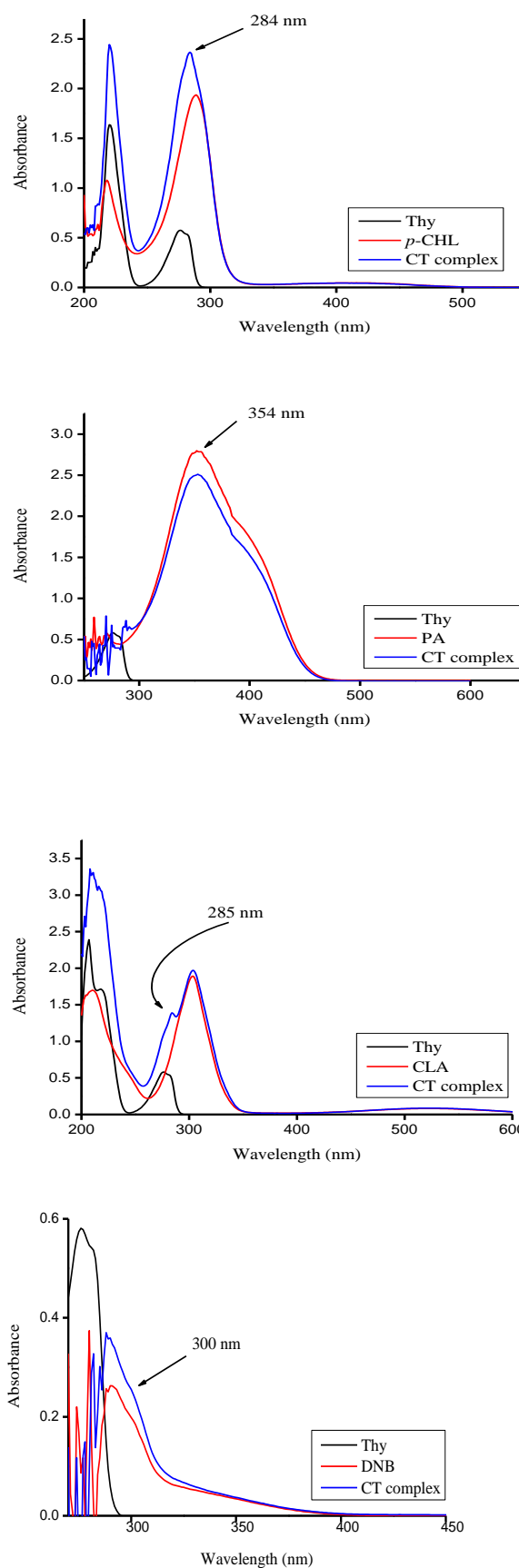


**Figure 1.** Electronic absorption spectra of Thy CT complexes at the detectable peak.

$$f = 4.319 \times 10^9 \int \varepsilon_{CT} d\nu \quad (3)$$

where  $\int \varepsilon_{CT} d\nu$  is the area under the curve of the extinction coefficient of the absorption band in question plotted as a function of frequency. To a first approximation,

$$f = 4.319 \times 10^9 \varepsilon_{CT} \nu^{1/2} \quad (4)$$

where  $\varepsilon_{CT}$  is the maximum extinction coefficient of the CT band, and  $\nu_{1/2}$  is the half-bandwidth in  $\text{cm}^{-1}$  (i.e., the width of the band at half the maximum extinction). The transition dipole moments ( $\mu$ ) of the Thy CT complexes have been calculated from Eq. 5<sup>49</sup>:

$$\mu = 0.0958 \left[ \varepsilon_{CT} \frac{\nu_{1/2}}{\nu_{\max}} \right]^{1/2} \quad (5)$$

The transition dipole moment can be used to determine if a particular transition is allowed; the transition from a bonding  $\pi$  orbital to an antibonding  $\pi^*$  orbital is allowed because the integral that defines the transition dipole moment is nonzero. The ionization potentials ( $I_p$ ) of the Thy donor in the charge-transfer complexes were calculated using the empirical equation derived by Aloisi and Pignataro represented in Eq. 6<sup>50</sup>:

$$I_p(\text{eV}) = 5.76 + 1.53 \times 10^{-4} \nu_{CT} \quad (6)$$

where  $\nu_{CT}$  is the wavenumber in  $\text{cm}^{-1}$  that corresponds to the CT band formed from the interaction between the donor and the acceptor. The electron-donating power of a donor molecule is measured by its ionization potential, which is the energy required to remove an electron from the highest occupied molecular orbital. Briegleb and Czekalla<sup>51</sup> theoretically derived the following relationship to obtain the resonance energy ( $R_N$ ):

$$\varepsilon_{CT} = \frac{7.7 \times 10^{-4}}{\frac{h\nu_{CT}}{R_N} - 3.5} \quad (7)$$

where  $\varepsilon_{CT}$  is the molar absorptivity coefficient of the CT complex at the maximum of the CT absorption,  $\nu_{CT}$  is the frequency of the CT peak, and  $R_N$  is the resonance energy of the complex in the ground state, which contributes to the stability constant of the complex (a ground-state property). The energy values ( $E_{CT}$ ) of the  $n \rightarrow \pi^*$  and  $\pi - \pi^*$  interactions between the donor (EC) and the acceptors were calculated using the equation derived by Briegleb<sup>52</sup>:

$$E_{CT} = h\nu_{CT} = \frac{1243.667}{\lambda_{CT}} \quad (8)$$

where  $\lambda_{CT}$  is the wavelength of the CT band of the formed complex. The standard free energy of complexation ( $\Delta G^\circ$ ) for each complex was calculated from the formation constants using the equation derived by Martin et al.<sup>53</sup>:

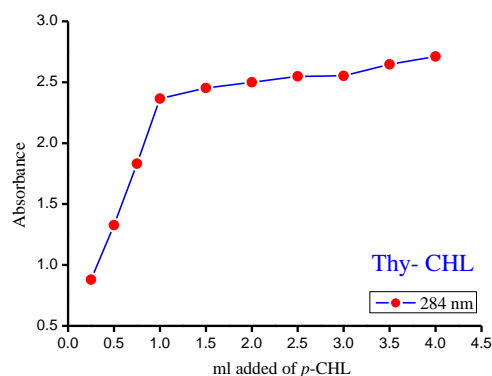
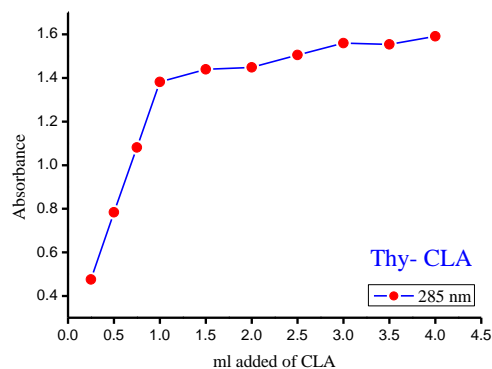
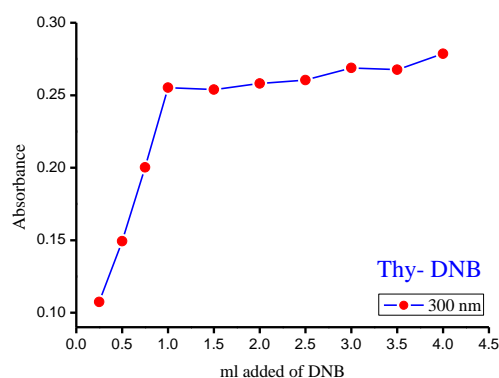
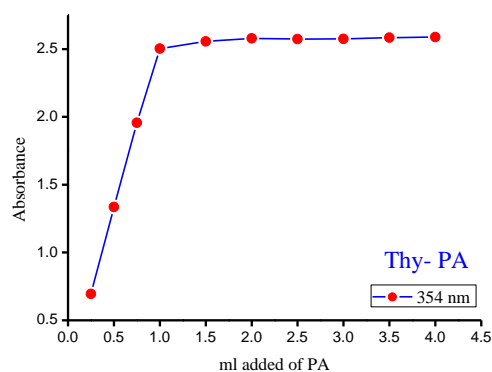


**Figure 2.** Photometric titration curves for Thy CT complexes at detectable peaks.

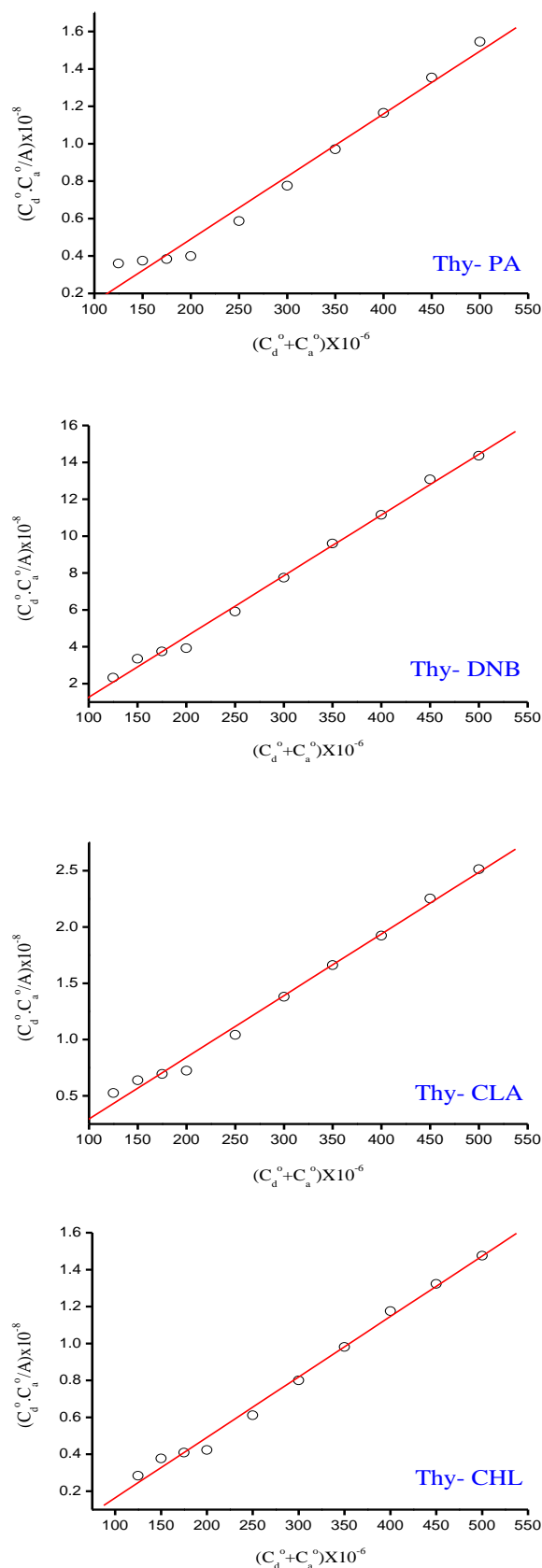
$$\Delta G = -2.303RT \lg K_{CT} \quad (9)$$

where  $\Delta G^\circ$  is the free energy change of the CT complex ( $\text{kJmol}^{-1}$ ),  $R$  is the gas constant ( $8.314 \text{ Jmol}^{-1}\text{K}$ ),  $T$  is the absolute temperature in K, and  $K_{CT}$  is the formation constant of the complex ( $\text{Lmol}^{-1}$ ) at room temperature.

The calculated spectroscopic and physical values ( $f$ ,  $\mu$ ,  $I_P$ ,  $R_N$  and  $\Delta G^\circ$ ) for the Thy CT complexes using these equations are presented in Table 1. [(Thy)(CLA)] complex exhibits considerably higher values of both the oscillator strength ( $f$ ) and the transition dipole moment ( $\mu$ ). CLA is a strong electron acceptor to form stable CT complexes with the donors. Beside this function, CLA is a strong acid ( $\text{pK}_1=1.07$  and  $\text{pK}_2=2.24$ )<sup>54</sup>, hence a proton transfer from CLA to the donors is expected. The observed high values of  $f$  indicate a strong interaction between the donor-acceptor pairs with relatively high probabilities of CT transitions<sup>55</sup>. Further evidence for the nature of CT interactions is the calculation of the standard free energy change ( $\Delta G^\circ$ ). The obtained values of  $\Delta G^\circ$  for the Thy/PA, Thy/CLA, Thy/DNB and Thy/*p*-CHL complexes are  $-35.8$ ,  $-36.1$ ,  $-35.4$  and  $-36 \text{ kJmol}^{-1}$ , respectively; these negative values indicate that the interaction between Thy and the acceptors is exothermic and spontaneous<sup>56, 57</sup>.

### IR spectra

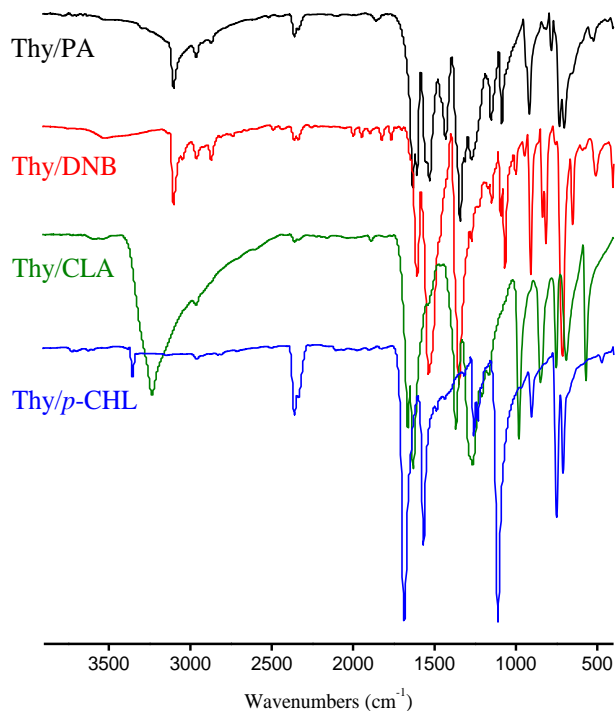
The IR absorption spectra of the Thy solid CT complexes were recorded in the frequency range  $4000\text{--}400 \text{ cm}^{-1}$  using KBr disc. These spectra are shown in Figure 4 while their band assignments are given in Table 2. In the IR spectra of the [(Thy)(PA)] and [(Thy)(CLA)] complexes, the characteristic bands of Thy observed at  $3613 \text{ cm}^{-1}$ , which is assigned to  $\nu(\text{O-H})$  stretching vibration, shifted to lower value and reduced in intensity after complexation. Also, the IR spectra of these complexes are characterized by weak bands that appear between  $2400\text{--}2800 \text{ cm}^{-1}$ , which does not appear in the spectra of the free Thy donor or those of the PA and CLA acceptors. These peaks are due to hydrogen bonding in the complex formed through the transfer of a proton from PA or CLA to the  $-\text{OH}$  group of the Thy donor. These observations clearly indicate that the complexation occurs through the protonation of the  $-\text{OH}$  group in the Thy donor via a proton-transfer phenomenon from the acidic center of each acceptor to the lone pair of electrons on the Thy oxygen atom based on acid-base theory<sup>59-63</sup>. Thus, one can say that the charge-transfer molecular complexes between Thy and PA or CLA acceptors are stabilized by hydrogen bonding. Because DNB and *p*-CHL acceptors lack acidic centres, the molecular complexes can be concluded to form through  $\pi \rightarrow \pi^*$  charge migration from the HOMO of the donor to the LUMO of the acceptor. The  $\pi \rightarrow \pi^*$  CT complex is formed via the benzene ring (electron-rich group) of the Thy and the DNB and *p*-CHL reagents (electron acceptor). The group of bands are exhibited at  $2920$  and  $2843 \text{ cm}^{-1}$  in [(Thy)(DNB)] complex, and at  $2890$  and  $2836 \text{ cm}^{-1}$  in [(Thy)(*p*-CHL)] complex were assigned to symmetric stretching vibrations of the  $\nu(\text{C-H})$  with different position wavenumbers compared with the free Thy.



**Figure 3.** The modified Benesi-Hildebrand plots of Thy CT complexes at detectable peaks.

**Table 1.** Spectrophotometric results of the Thy CT complexes

Complex	CT-absorption, nm	$E_{ct}$ , eV	$K$ (Lmol <sup>-1</sup> )	$\epsilon_{max}$ (L mol <sup>-1</sup> cm <sup>-1</sup> )	$f$	$\mu$	$I_p$	$R_N$	$\Delta G^\circ$ (25 °C) (kJ mol <sup>-1</sup> )
[(Thy)(PA)]	354	3.513	$1.86 \times 10^4$	$2.99 \times 10^4$	12.89	31.14	10.08	0.99	-35,771
[(Thy)(CLA)]	285	4.364	$2.16 \times 10^4$	$1.83 \times 10^4$	39.40	48.85	11.13	1.23	-36,146
[(Thy)(DNB)]	300	4.146	$1.62 \times 10^4$	$3.04 \times 10^4$	27.39	23.60	10.86	1.10	-35,426
[(Thy)( <i>p</i> -CHL)]	284	4.379	$2.00 \times 10^4$	$3.06 \times 10^4$	37.73	47.72	11.15	1.24	-35,949

**Figure 4.** Infrared spectra of Thy CT complexes.

The stretching vibration of  $\nu(\text{C}=\text{O})$  absorption band in free *p*-CHL appeared at  $1685 \text{ cm}^{-1}$ , but under complexation this band is still un-shifted. Also, the bands associated with  $\nu(\text{C}-\text{Cl})$  vibration that appeared at 903, 750 and  $709 \text{ cm}^{-1}$  in free *p*-CHL were shifted to lower wavenumbers and decreasing in the intensities of the characteristic peaks, these results due to the increasing in the electron density around *p*-CHL moiety. These observations proved that the complexation of Thy with DNB and *p*-CHL take place via the  $\pi \rightarrow \pi^*$  transition. Based on these data, the suggested complexation mechanism between Thy donor and acceptors is illustrated in Scheme 1.

### <sup>1</sup>H-NMR spectra

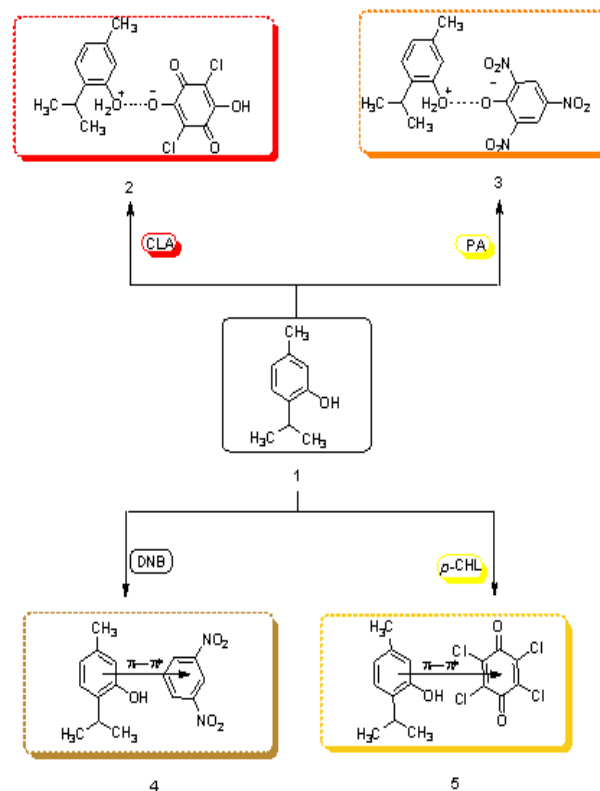
The 400 MHz nuclear magnetic resonance (<sup>1</sup>H-NMR) spectra of the Thy complexes were measured in DMSO-*d*<sub>6</sub> at room temperature. The chemical shifts ( $\delta$ ) of the different types of protons of the complexes are;

[(Thy)(PA)] complex; (2-isopropyl-5-methylphenyl)oxonium 2,4,6-trinitrobenzenolate; <sup>1</sup>H NMR (400 MHz, DMSO-*d*<sub>6</sub>): 1.59 (d, 6H, 2CH<sub>3</sub>), 2.59 (s,

3H, CH<sub>3</sub>), 3.21 (m, 1H, CH(CH<sub>3</sub>)<sub>2</sub>), 7.26 (d, 1H, Ar-H, C<sub>4</sub> thymol), 7.39 (d, 1H, Ar-H, C<sub>3</sub> thymol), 7.63 (s, 1H, Ar-H, C<sub>6</sub> thymol), 9.00 (s, 2H, Ar-H, picric acid ring), 12.2 (s, 2H, Ar-OH<sub>2</sub><sup>+</sup>, thymol).

[(Thy)(CLA)] complex; (2-isopropyl-5-methylphenyl)oxonium 2,5-dichloro-4-hydroxy-3,6-dioxocyclohexa-1,4-dien-1-olate; <sup>1</sup>H-NMR (400 MHz, DMSO-*d*<sub>6</sub>): 1.60 (d, 6H, 2CH<sub>3</sub>), 2.59 (s, 3H, CH<sub>3</sub>), 3.21 (m, 1H, CH(CH<sub>3</sub>)<sub>2</sub>), 7.25 (d, 1H, Ar-H, C<sub>4</sub> thymol), 7.40 (d, 1H, Ar-H, C<sub>3</sub> thymol), 7.63 (s, 1H, Ar-H, C<sub>6</sub> thymol), 11.9 (s, 1H, Ar-OH, CLA ring), 12.2 (s, 2H, Ar-OH<sub>2</sub><sup>+</sup>, thymol).

[(Thy)(DNB)] complex; 2-isopropyl-5-methylphenol compound with 1,3-dinitrobenzene (1:1); <sup>1</sup>H-NMR (400 MHz, DMSO-*d*<sub>6</sub>): 1.18 (d, 6H, 2CH<sub>3</sub>), 2.40 (s, 3H, CH<sub>3</sub>), 3.19 (m, 1H, CH(CH<sub>3</sub>)<sub>2</sub>), 4.27 (s, 1H, OH), 6.89 (d, 1H, Ar-H, C<sub>4</sub> thymol), 7.22 (s, 1H, Ar-H, C<sub>6</sub> thymol), 7.37 (d, 1H, Ar-H, C<sub>3</sub> thymol), 8.07 (d, 2H, Ar-H, C<sub>4</sub>, C<sub>6</sub> dinitrobenzene ring), 8.19 (t, 1H, Ar-H, C<sub>5</sub> dinitrobenzene ring), 8.47 (s, 1H, Ar-H, C<sub>2</sub> dinitrobenzene ring)

**Scheme 1.** Complexation mechanism between Thy donor and acceptors.

**Table 2.** Characteristic infrared frequencies ( $\text{cm}^{-1}$ ) and tentative assignments of Thy, PA, CLA, DNB, *p*-CHL and their CT complexes.

Thy	PA	CLA	DNB	<i>p</i> -CHL	[(Thy)(acceptor)] complex				Assignments <sup>(a)</sup>
					PA	CLA	DNB	<i>p</i> -CHL	
3613		3235	3110	3354	3103	3256	3103	3355	$\nu(\text{O-H})$
2963	2980				2965	2966	2920	2890	$\nu(\text{C-H})$
2872	2872				2760	2778	2843	2836	Hydrogen bond
	1861				1858		1824		
1626	1632	1664		1685	1633	1665		1685	$\nu(\text{C=O})$
	1608	1630	1608		1609	1631	1609		$\nu(\text{NO}_2)$
1516	1529		1538	1567	1530	1541	1537	1568	$\nu(\text{C=C})$
1460	1432			1487	1431	1462		1437	
1419	1343	1368	1364	1316	1342	1369	1349	1317	$\delta(\text{CH})$ deformation
1290	1312	1263			1313	1265	1271	1258	$\nu(\text{C-O})$
1216	1263	1207			1272	1209		1233	$\nu(\text{C-N})$
1160	1150	1168	1150		1152	1168	1148	1110	$\nu(\text{C-C})$
1087	1086		1069		1085		1068		
946	917	981	914	903	918	982	909	896	$\nu(\text{C-Cl})$
868	829	851	837		782	849	815		
	781	752	727	750	732	752	712	740	$\nu(\text{C-Cl}) + \delta(\text{NO}_2)$
593	652	690	663	709	703	691	651	701	
579	522	569			523	569	510	473	

<sup>a</sup>  $\nu$ , stretching;  $\nu_s$ , symmetrical stretching;  $\nu_{as}$ , asymmetrical stretching;  $\delta$ , bending.

[(Thy)(*p*-CHL)] complex; 2,3,5,6-tetrachlorocyclohexa-2,5-diene-1,4-dione compound with 2-isopropyl-5-methylphenol (1:1); <sup>1</sup>H-NMR (400 MHz, DMSO-*d*<sub>6</sub>): 1.62 (d, 6H, 2CH<sub>3</sub>), 2.59 (s, 3H, CH<sub>3</sub>), 3.30 (m, 1H, CH(CH<sub>3</sub>)<sub>2</sub>), 4.67 (s, H, Ar-OH, thymol), 7.12 (d, 1H, Ar-H, C<sub>4</sub> thymol), 7.40 (s, 1H, Ar-H, C<sub>6</sub> thymol), 7.77 (d, 1H, Ar-H, C<sub>3</sub> thymol).

The three aromatic protons of Thy appear at  $\delta$  7.37-7.77 (C<sub>3</sub>), 6.89-7.26 (C<sub>4</sub>) and 7.22-7.63 (C<sub>6</sub>) ppm. The aliphatic protons of Thy appear at  $\delta$  1.18-1.62 ppm (6H), 2.40-2.59 ppm (3H) and 3.19-3.30 (1H), corresponds to the protons of 2CH<sub>3</sub>, CH<sub>3</sub> and CH groups, respectively. The intensities and chemical shifts of the aromatic and aliphatic signals have been significantly affected by the complexation and the accompanying changes in the structural configuration. The new peak observed at 12.2 ppm in [(Thy)(PA)] complex, which is not detected in the spectrum of the free Thy donor, is attributed to the formation of a hydrogen bond between PA and Thy. The peak at  $\delta$  = 11.94 ppm, which is assigned to the -OH proton of free picric acid<sup>64</sup>, was absent in the spectrum of this complex. Together, these data indicate that the hydroxyl and phenolic groups are involved in the formation of the CT complex between Thy and PA.

In the [(Thy)CLA] complex, the phenolic proton (-OH) signal, which is observed at approximately  $\delta$ ~9.15 ppm in the spectrum of the free CLA acceptor<sup>57</sup>, decreased in intensity with an down-field shift for the non-hydrogen-bonded one ( $\delta$ ~11.9) in the spectrum of the CT complex. Instead, a new peak is observed at 12.2 ppm, attributing to two protons of OH<sub>2</sub><sup>+</sup>. This situation confirmed the transfer of the phenolic proton of CLA to the (-OH) group of Thy.

### Thermal analysis

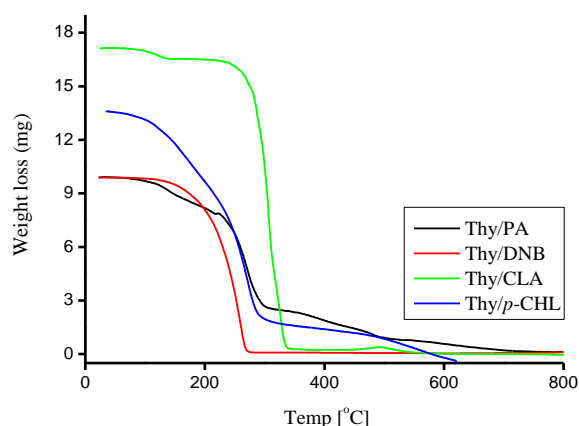
The thermogravimetric analysis (TG) provided information about the thermal stabilities of the prepared charge-transfer complexes and about the differences in the physical behavior of the starting and resulting compounds. In order to verify charge-transfer interaction between Thy donor and acceptors and thermal stability of the new CT complexes, the thermogravimetric analysis of Thy CT complexes were carried out over the temperature range of 25-800 °C under an air atmosphere using 9.9, 9.87, 17.12 and 13.60 mg samples for [(Thy)(PA)], [(Thy)(CLA)], [(Thy)(DNB)] and [(Thy)(*p*-CHL)] complexes, respectively. The TG curves were redrawn as mg mass loss versus temperature. Figure 5 shows the thermograms for Thy CT complexes and thermal analyses data are listed in Table 3. The obtained data indicate that the [(Thy)(PA)] complex decomposes in three clear decomposition steps within the 25-800 °C temperature range. The first decomposition step within the temperature range 25-152 °C has a weight loss about 12.20% and is attributed to the liberation of NO<sub>2</sub> molecule. The second decomposition step existed within the 152-300 °C temperature range and is reasonably explained by the loss of 5C<sub>2</sub>H<sub>2</sub>, 2NO<sub>2</sub> and CO<sub>2</sub> molecules.

The final decomposition step found within the temperature range 300-800 °C which corresponds to the liberation of 2C<sub>2</sub>H<sub>2</sub>, CO<sub>2</sub> and 3/2H<sub>2</sub> molecules. This step is associated with a total weight loss of 25.77%, which is in good agreement with the calculated value (26.10%). The [(Thy)(CLA)] complex is thermally stable in the 25-675 °C temperature range. The thermal decomposition of the complex is a two-steps process.

**Table 3.** Thermal decomposition data for the Thy CT complexes.

Complex	Stage	TG range, °C	Mass loss, %		Detected fragments
			Found	Calculated	
[Thy](PA) (C <sub>16</sub> H <sub>17</sub> N <sub>3</sub> O <sub>8</sub> )	I	25-152	12.20	12.13	NO <sub>2</sub>
	II	152-300	62.03	61.69	5C <sub>2</sub> H <sub>2</sub> + 2NO <sub>2</sub> + CO <sub>2</sub>
	III	300-800	25.77	26.10	2C <sub>2</sub> H <sub>2</sub> + CO <sub>2</sub> + 3/2H <sub>2</sub>
[Thy](CLA) (C <sub>16</sub> H <sub>16</sub> Cl <sub>2</sub> O <sub>5</sub> )	I	25-220	3.97	3.34	CO <sub>2</sub>
	II	220-675	96.03	96.60	6C <sub>2</sub> H <sub>2</sub> + Cl <sub>2</sub> + 3CO <sub>2</sub> + 2H <sub>2</sub>
[Thy](DNB) (C <sub>16</sub> H <sub>18</sub> N <sub>2</sub> O <sub>5</sub> )	I	25-800	100.00	99.90	7C <sub>2</sub> H <sub>2</sub> + 2NO <sub>2</sub> + 2CO <sub>2</sub> + 2H <sub>2</sub>
[Thy]( <i>p</i> -CHL) (C <sub>16</sub> H <sub>14</sub> Cl <sub>4</sub> O <sub>3</sub> )	I	25-345	86.16	86.34	6C <sub>2</sub> H <sub>2</sub> + 2Cl <sub>2</sub> + CO <sub>2</sub>
	II	345-600	13.84	13.63	C <sub>2</sub> H <sub>2</sub> + CO <sub>2</sub>

The first mass loss step occurs between 25-220 °C corresponds to the loss of CO<sub>2</sub> molecule with a weight loss of 3.97% close to the expected theoretical value of 3.34%. The second degradation step at 220-675 °C has an extremely large scale of weight loss for about 96.03%, and is attributed to the loss of 6C<sub>2</sub>H<sub>2</sub>, Cl<sub>2</sub>, 3CO<sub>2</sub> and 2H<sub>2</sub> molecules. The curve of [(Thy)(DNB)] complex was thermally decomposed in one decomposition step within temperature range 25-800 °C, and may be assigned to the liberation of 7C<sub>2</sub>H<sub>2</sub>, 2NO<sub>2</sub>, 2CO<sub>2</sub> and 2H<sub>2</sub>.

**Figure 5.** TG curves of Thy CT complexes.

The thermal analysis curve of the [(Thy)(*p*-CHL)] complex indicates that the decomposition occurs in two main stages in the temperature range of 25-600°C. The first decomposition step within the temperature range 25-345 °C corresponding to loss of 6C<sub>2</sub>H<sub>2</sub>, 2Cl<sub>2</sub> and CO<sub>2</sub> molecules representing a weight loss of 86.16% very close to the expected theoretical value of 86.34%. The second decomposition step found within the temperature range 345-600 °C which corresponds to the liberation of C<sub>2</sub>H<sub>2</sub> and CO<sub>2</sub> molecules representing a weight loss of 13.84% very close to the expected theoretical value of 13.63%.

## Conclusion

Recently, considerable attention has been devoted to the formation of stable charge-transfer complexes that result from the reaction between acceptors and drugs or biological compounds. This interest stems from the significant physical and chemical properties of these complexes. The results reported in this paper are concerned with the preparation, characterization, structural and thermal studies of novel charge-transfer complexes formed between the anti-microbial agent; thymol (Thy) and the acceptors picric acid (PA), chloranilic acid (CLA, 1,3-dinitrobenzene (DNB) and *p*-chloranil (*p*-CHL). It is observed that the reaction stoichiometry is 1:1, and the resulting CT complexes were shown to have the general formula: [(Thy)(acceptor)]. The interaction between the Thy and PA or CLA acceptors was stabilized by hydrogen bonding. The obtained complexes were thermally stable. Physical parameters such as formation constant ( $K_{CT}$ ), molar extinction coefficient ( $\epsilon_{CT}$ ) and other spectroscopic data have also been determined.

## References

- <sup>1</sup>Mulliken, R. S. *J. Am. Chem. Soc.*, **1950**, 72, 4493.
- <sup>2</sup>Mulliken, R. S., Pearson, W. B. *Molecular Complexes*, Wiley Publishers, New York, **1969**.
- <sup>3</sup>Foster, R. *Charge Transfer Complexes*, Academic press, London, **1969**.
- <sup>4</sup>Mulliken, R. S. *J. Am. Chem. Soc.*, **1952**, 74, 811.
- <sup>5</sup>Mulliken, R. S. *J. Phys. Chem.*, **1952**, 56, 801.
- <sup>6</sup>Roy, T., Dutta, K., Nayek, M. K., Mukherjee, A. K., Banerjee, M., Seal, B. K. *J. Chem. Soc., Perkin Trans.*, **1999**, 2, 2219.
- <sup>7</sup>Fla, F. P., Palou, J., Valero, R., Hall, C. D.; Speers, P., *J. Chem. Soc., Perkin Trans.*, **1991**, 2, 1925.
- <sup>8</sup>Roy, D. K., Saha, A., Mukherjee, A. K. *Spectrochim. Acta A*, **2005**, 61, 2017.

- <sup>9</sup>Slifkin, A. M. *Charge-transfer Interaction of Biomolecules*, Academic Press, New York, **1971**.
- <sup>10</sup>Dozal, A., Keyzer, H., Kim, H.K., Wang, W. W. *Int. J. Antimicrob. Agent*, **2000**, *14*, 261.
- <sup>11</sup>Korolkovas, A. *Essentials of Medical Chemistry*, 2<sup>nd</sup> ed., (Chapter 3). Wiley, New York, **1998**
- <sup>12</sup>Abou Attia, F. M. *Farmaco*, **2000**, *55*, 659.
- <sup>13</sup>Basavaiah, K. *Farmaco*, **2004**, *59*, 315.
- <sup>14</sup>Saleh, G. A., Askal, H. F., Radwan, M. F., Omar, M. A. *Talanta*, **2001**, *54*(6), 1205.
- <sup>15</sup>Salem, H. J. *Pharm. Biomed. Anal.*, **2002**, *29*(3), 527.
- <sup>16</sup>Pandeewaran, M., El-Mossalamy, E. H., Elango, E. H. *Int. J. Chem. Kinet.*, **2009**, *41*, 787.
- <sup>17</sup>Pandeewaran, M., Elango, K. P. *Spectrochim. Acta A*, **2010**, *75*, 1462.
- <sup>18</sup>Yakuphanoglu, F., Arslan, M. *Solid State Commun.*, **2004**, *132*, 229.
- <sup>19</sup>Yakuphanoglu, F., Arslan, M. *Opt. Mater.*, **2004**, *27*, 29.
- <sup>20</sup>Yakuphanoglu, F., Arslan, M., Kucukislamoglu, M.; Zengin, M. *Sol. Energy*, **2005**, *79*, 96.
- <sup>21</sup>Chakraborty, B.; Mukherjee, A. S.; Seal, B. K. *Spectrochim. Acta A*, **2001**, *57*, 223.
- <sup>22</sup>Krishnamurthy, M.; Surendrababu, K.; Muralikrishna, U. *Indian J. Chem. A*, **1988**, *27*, 669.
- <sup>23</sup>Andrade, S. M., Costa, S. M. B., Pansu, R. *J. Colloid Interface Sci.*, **2000**, *226*, 260.
- <sup>24</sup>Dabestani, R.; Reszka, K. J.; Sigman, M. E. *J. Photochem. Photobiol. A*, **1998**, *117*, 223.
- <sup>25</sup>Jakubiak, R., Bao, Z., Rothberg, L. *Synth. Met.*, **2000**, *114*, 61.
- <sup>26</sup>Takahasi, K., Horino, K., Komura, T., Murata, K. *Bull. Chem. Soc. Jpn.*, **1993**, *66*, 733.
- <sup>27</sup>Eychmuller, A.; Rogach, A. L.; *Pure Appl. Chem.*, **2000**, *72*, 179.
- <sup>28</sup>Brueggermann, K., Czernuszewicz, R. S., Kochi, J. K. *J. Phys. Chem.*, **1992**, *96*, 4405.
- <sup>29</sup>Das, S. K., Krishnamoorthy, G., Dofra, S. K. *Can. J. Chem.*, **2000**, *78*, 191.
- <sup>30</sup>Jones, G., Jimenez, J. A. C. *Tetrahedron Lett.*, **1999**, *40*, 8551.
- <sup>31</sup>Smith, G., Lynch, D. E., Byriel, K. A., Kennard, C. H. L. *J. Chem. Crystallogr.*, **1997**, *27*, 307.
- <sup>32</sup>Smith, G., Lynch, D. E.; Bott, R. C., *Aust. J. Chem.*, **1998**, *51*, 159.
- <sup>33</sup>Smith, G., Bott, R. C., Rae, A. D., Willis, A. C. *Aust. J. Chem.*, **2000**, *53*, 531.
- <sup>34</sup>Hsu, S., Lin, K., Chou, C., Chiang, A., Liang, W., Chang, H., Tsai, J., Liao, W., Huang, F., Huang, J. K., Chen, I., Liu, S., Kuo, C.; Jan, C. *Eur. J. Pharmacol.*, **2011**, *670*, 85.
- <sup>35</sup>Nerio, L. S., Olivero-Verbel, J., Stashenko, E. *Bioresour. Technol.*, **2010**, *101*, 372.
- <sup>36</sup>Gujar, J. G., Wagh, S. J., Gaikar, V. G. *Sep. Purif. Technol.*, **2010**, *70*, 257.
- <sup>37</sup>Wattanasatcha, A., Rengpipat, S., Wanichwecharungruang, S. *Int. J. Pharm.*, **2012**, *434*, 360.
- <sup>38</sup>Silva, M. A, da Daemona, E., Monterio, C. M. O., Maturanoa, R., Britoa, F. C., Massoni, T. *Vet. Parasitol.*, **2011**, *183*, 136.
- <sup>39</sup>Buyukleyla, M., Rencuzogullari, E. *Ecotoxicol. Environ. Saf.*, **2009**, *72*, 943.
- <sup>40</sup>Shapira, R., Mimran, E. *Microb. Drug Resist.*, **2007**, *13*, 157.
- <sup>41</sup>Lazar-Baker, E. E., Hetherington, S. D., Ku, V. V., Newman, S. M. *Lett. Appl. Microbiol.*, **2010**, *52*, 227.
- <sup>42</sup>Glenn, G. M., Klamczynski, A. P., Imam, S. H., Chiou, B., Orts, W. J., Woods, D. F. *J. Agric. Food Chem.*, **2010**, *58*, 4180.
- <sup>43</sup>Skoog, D. A. *Principle of Instrumental Analysis*, 3rd ed., (Chapter 7), Saunders, New York, USA, **1985**.
- <sup>44</sup>Benesi, H. A., Hildebrand, J. H. *J. Am. Chem. Soc.*, **1949**, *71*, 2703.
- <sup>45</sup>Abu-Eittah, R., Al-Sugeir, F., *Can. J. Chem.*, **1976**, *54*, 3705.
- <sup>46</sup>Hossan, A. S. M.; Abou-Melha, H. M.; Refat, M. S. *Spectrochim. Acta A*, **2011**, *79*, 583.
- <sup>47</sup>Lever, A. B. P. *Inorganic Electronic Spectroscopy*, 2<sup>nd</sup> ed., Elsevier, Amsterdam, **1985**, p. 161.
- <sup>48</sup>Tsubomura, H., Lang, R. P. *J. Am. Chem. Soc.*, **1961**, *83*, 2085.
- <sup>49</sup>Rathone, R., Lindeman, S. V., Kochi, J. K. *J. Am. Chem. Soc.*, **1997**, *119*,
- <sup>50</sup>Aloisi, G., Pignataro, S., *J. Chem. Soc., Faraday Trans.* **1972**, *69*, 534.
- <sup>51</sup>Briegleb, G., Czekalla, J., *Z. Phys. Chem. (Frankfurt)*, **1960**, *24*, 237.
- <sup>52</sup>Briegleb, G. *Z. Angew. Chem.* **1960**, *72*, 401, *Z. Angew. Chem.* **1964**, *76*, 326.
- <sup>53</sup>Martin, A. N., Swarbrick, J., Cammarata, A., *Physical Pharmacy*, 3<sup>rd</sup> ed., Lee and Febiger, Philadelphia, PA, **1969**, p. 344.
- <sup>54</sup>El-Sayed, M., Agrawl, S. *Talanta*, **1982**, *29*, 535.
- <sup>55</sup>Refat, M.S.; Elfalaky, A.; Elesh, E. *J. Mol. Struct.*, **2011**, *990*, 217.
- <sup>56</sup>Al-Ahmary, K. M., Habeeb, M. M., Al-Solmy, E. A; *J. Mol. Liq.*, **2011**, *162*, 129.
- <sup>57</sup>Al-Attas, A. S., Habeeb, M. M., Al-Raimi, D. S. *J. Mol. Struct.*, **2009**, *928*, 158.
- <sup>58</sup>Refat, M. S., El-Zayat, L. A., Yesilel, O. Z., *Spectrochim. Acta A*, **2010**, *75*, 745.
- <sup>59</sup>Refat, M. S., Saad, H. A., Adam, A. A. *J. Mol. Struct.*, **2011**, *995*, 116.
- <sup>60</sup>Bellamy, L. J. *The infrared Spectra of Complex Molecules*, Chapman & Hall, London, 1975.
- <sup>61</sup>Bharathikannan, R., Chandramohan, A., Kandhaswamy, M. A., Chandrasekaran, J., Renganathan, R., Kandavelu, V. *Cryst. Res. Technol.*, **2008**, *43*(6), 683.
- <sup>62</sup>Gaballa, A. S., Teleb, S. M., Nour, E., *J. Mol. Struct.*, **2012**, *1024*, 32.
- <sup>63</sup>Adam, A. A., *J. Mol. Struct.*, **2012**, *1030*, 26.
- <sup>64</sup>Kross, R. D., Fassel, V. A., *J. Am. Chem. Soc.*, **1957**, *79*, 38.

Received: 29.09.2012.

Accepted: 05.10.2012.



# GREEN SYNTHESIS OF NANO-Fe-BIOTITE FOR REMOVAL OF HAZARDOUS METALS IONS FROM AQUEOUS SOLUTIONS

Khaled M. Elsabawy<sup>1,2,\*</sup>, Morsy M.A.Sekkina<sup>1</sup> and Ahmed T.Tawfik<sup>1,3</sup>

**Keywords:** biotite, heavy metals, uranium, thorium, removal, fluoride-free, wastewater

This paper represents synthesis of a new family of a fluoride-free Fe-Biotite type compound having the general formula  $\text{NaFe}_{2.5}(\text{Al,Si})_4\text{O}_{10}(\text{OH})_2$ . It was prepared carefully by using solid-state reaction technique with nominal compositions of individual oxides in the main formula for the potential remediation of heavy metals and some radioactive elements from applying solution. The structural and micro-structural properties were determined using both XRD, SEM and IR techniques. The particle size estimated was 56 nm. Further electron spin resonance (ESR) proved that Fe-biotite is paramagnetic in nature, electrical conductivity was measured as a function of absolute temperature, while the thermal stability of the samples were studied using thermogravimetry (TG). Analytical applications were done by using (AAS). Investigations proved that synthetic fluoride-free Fe-biotite has medium of strong efficiency as cation selective clay towards metals under test.

## Corresponding Authors

Tel: +9660503252190

E-Mail: [ksabawy@yahoo.com](mailto:ksabawy@yahoo.com)

- [a] Materials Science Unit, Chemistry Department, Faculty of Science, Tanta University, 31725-Tanta-Egypt
- [b] Faculty of Science-Chemistry Department-Taif University-Taif-Alhawayah-888-Saudi Arabia
- [c] Egyptian Environmental Affairs Agency-Egypt

## Introduction

The extensive use of metals in industries such as mining, electroplating, battery, alloys processing, and other human activities (agricultural practices, transport, and waste disposal) have introduced substantial amounts of toxic heavy metals into the aquatic and terrestrial environment<sup>1</sup>. The removal of metal ions from industrial wastewaters using different adsorbents is always a subject of great interest,<sup>2,3</sup> because industrial wastewaters often contain considerable amounts of metal ions that would be dangerous to public health and the environment if discharged without adequate treatment.

Industrial activities generate a wide diversity of wastewaters, often containing agents that cause pollution, which can cause dangerous consequences for human beings by affecting the ecosystems. To minimize these unfavorable conditions, adsorption methodologies have been proposed as an alternative process for resolving such problems.<sup>4-9</sup>

Composite adsorbents/ion exchangers have been widely studied for treatment of liquid radioactive wastes. The composite ion exchangers present improved qualities with respect to those of pure inorganic exchangers or resins, such as; better selectivity for the capture of some ions, increased mechanical and chemical resistance, more regular form of the grains, smaller solubility in water than the respective inorganic compound, and better kinetics of exchange relatively to the pure inorganic exchangers. The composite

ion exchangers are generally obtained by implantation of inorganic (e.g. clay minerals, cement, silica-gel or alumina)

into the wide range organic materials during the polymerisation process.<sup>10,11</sup>

The composite ion exchangers have been used in several studies for the treatment of low and medium level liquid radioactive wastes<sup>10-12</sup> and to investigate of sorption behavior of I-V group.<sup>13</sup>

Biotite is a member of the trioctahedral micas. It is commonly found in almost all types of granitic rocks and Some metamorphic rocks. Such a silicate mineral commonly coexists with quartz and feldspar, which are widely used as natural dosimeters for retrospective dosimetry and dating.<sup>14</sup>

Fe(II) is an important inorganic reductant that is abundant in soils and sediments. Fe(II) is found in many silicates, and oxidation-reduction reactions between aqueous species and structurally bound Fe on or beneath the surface of both silicates and oxides can control the redox state of associated solutes.<sup>15-17</sup>

Naturally occurring micas must be modified for use as commercial and cost-effective ion exchangers suitable to separate radionuclides from groundwater or aqueous nuclear wastes because micas have low cation exchange capacity (CEC). The low CEC of micas is due to interlayer potassium ions which are fixed. A few attempts have been made to improve CEC of the micas. Interlayer potassium ions can be replaced by sodium.

Green chemistry is a design, development, implementation of chemical products and processes to reduce or eliminate the use and generation of substances hazardous to human health and environment, the present study aims to: (1) synthesis the Fe-Biotite adsorbent from eco-friendly and low cost raw materials:

(i)- an attempt to synthesize the mica without using fluorine to prevent release of fluorides into the environment during synthesis process.

(ii) by using  $\text{Na}^+$  as interlayer ion to increase cation exchange of the mica for remediation;

(2) In order to characterize the adsorbent with a variety of techniques; and finally (3) to evaluate the performance of Fe-Biotite for effective Ag(I), Hg(II), As(V), Cr(III), Pb(II), Th (IV), U(VI), removal from aqueous solution.

## Experimental and Methods

### Materials

All reagents used were of analytical grade, Aluminum silicate  $\text{Al}_2\text{SiO}_5$  (BHD), anhydrous sodium carbonate  $\text{Na}_2\text{CO}_3$  (GPR), Ferric oxide  $\text{Fe}_2\text{O}_3$  were mixed in the chemical compositions corresponding to synthesizing  $\{\text{NaFe}_{2.5}(\text{Al},\text{Si})_4\text{O}_{10}(\text{OH})_2\}$ , which have chemical formula of Fe-Biotite.

### Clay's synthesis

The sample of synthetic free-fluoride Fe-biotite was prepared carefully by using solid-state reaction technique with nominal compositions of individual oxides in the main formula, aluminum silicate  $\text{Al}_2\text{O}_3 \cdot \text{SiO}_2$  (10.7 g), sodium carbonate (anhydrous)  $\text{Na}_2\text{CO}_3$  (0.8g), ferric oxide  $\text{Fe}_2\text{O}_3$  (3.5 g). The powder mixtures were mixed in a ball mill and then blending to make a homogeneous mass with uniform distribution of particle size and composition. The green compacted metals powder were heated in a controlled atmosphere furnace to a temperature below its melting point in sealed platinum container at 900-950 °C for 9 h, followed by sintering step at 880 °C to allow packed metal powders to bond together and finally, annealing step that the temperature have gradual decrease till reach room temperature.

### Adsorbent characterization techniques

#### X-ray diffraction

The X-ray diffraction pattern was obtained using an X'Pert SW. X-ray diffractometer with filtered  $\text{CuK}\alpha$  radiation ( $\lambda=1.54 \text{ \AA}$ ), at 40 Kv and 30 mA. The scanning speed was in the range of  $2\theta=5-70$  (298 K). To determine the crystal size, Debye-Scherrer equation was used.<sup>18</sup>

$$D = \frac{0.9\lambda}{\beta \cos \theta} \quad (1)$$

where  $\lambda$  is the wavelength,  $\beta$  is the FWHM (full half width maximum) of Bragg's peak corrected using the

corresponding peak in micron-sized powder and  $\theta$  is the Bragg's angle.

#### Infrared spectrum

The IR spectra were scanned on NICOLET 6700 FTIR Thermoscientific spectrophotometer using the KBr disc technique between (4000 and 400  $\text{cm}^{-1}$ ). The method includes mixing few mgs of a fine powder of the sample with KBr powder in agate mortar. The mixture was then pressed by means of a hydraulic press. The transmittance was automatically registered against wave-number ( $\text{cm}^{-1}$ ).

#### Scanning electron-microscope

A Philips model XL 30 CP scanning electron microscope (SEM) was used to take micrographs of the clay samples.

#### Electron spin resonance spectra

The (ESR) spectra were taken using (Bruker Elexys.500) operated at X-band frequency for investigation with fixed parameters and were at microwave frequency: 9.71 GHz, receiver gain: 30, sweep width: 6000 center at 3480 Gs, and microwave power: 0.002026W.

#### Thermal studies

Thermo-gravimetric analysis (TGA) and differential thermal analysis (DTA) were carried out on using a Shimadzu DTA-50H thermal analyzer. The sample was placed in platinum crucible ( $0.1 \text{ cm}^3$ ) the system were studied under nitrogen atmosphere with a heating rate  $10 \text{ }^\circ\text{C min}^{-1}$  and following rate at  $20 \text{ ml min}^{-1}$ , constant weight of sample, 4.7 mg was used.

#### Conductance measurements

The dc conductance was measured over the temperature range 10-500 °C using A KEITHLEY 175 multi-meter (ASA). The pellet of synthetic Fe-biotite was sandwiched between spring loaded copper electrodes mounted into a specially designed temperature-controlled chromel-alumel thermocouple. Measurements were conducted in such a way that at each temperature, sufficient time was allowed to attain thermal equilibrium.

The number of conduction electron  $n$  is given by:

$$n = n_0 e^{-E_g/kT} \quad (2)$$

where  $n_0$  is the concentration of atoms at the lattice site,  $E_g$  is the band gap, and  $k$  is the Boltzman constant (assuming  $E_g \approx kT$ ), the conductivity relationship becomes

$$\sigma = (n_0 e^{-E_g/kT}) e \mu \quad (3)$$

where

$$A = n_0 \epsilon \mu. \quad (4)$$

$$\lg \sigma = \lg A - \frac{E_g}{2.303kT} \quad (5)$$

The plot of  $\lg \sigma$  against  $1/T$  should give a straight line with a slope of  $-E/2.303k$ . The measurements of  $\sigma$  as a function of temperature will permit calculation of the band gap energy  $E_g$  of materials behavior.

### Adsorption experiments

Determination of distribution coefficient values of Fe-biotite was performed by using a series of metal ions. The selected metal ions were Ag(I), Hg(II), As(V), Cr(III), Pb(II). The concentration of each metal ion solution was adjusted as (10 mg L<sup>-1</sup> of each). In a 50 ml measuring flask, for each experiment, (2 g) of sorbent material was suspended in 50 mL of metal ion solution<sup>19</sup> the flask was shaken and kept the solution for 24 h at room temperature. The pH was adjusted as previous studies. The specific adsorption of Pb<sup>2+</sup> ion was examined at the pH about 4 to avoid the hydrolysis, at higher PH values, and the dissolution of biotite, at lower pH values.<sup>20</sup> The optimum pH for adsorption silver ions from aqueous solution was found to be 4.0.<sup>21</sup> Arsenate sorption onto biotite shows a broader maximum in the pH range 4.6–5.6.<sup>23</sup> The optimum pH value appeared to be about 5.0, at lower pH (<5), Hg(II) was in the free ionic form of Hg<sup>2+</sup><sup>23</sup> and Cr(III) sorption was found to be at pH 5.0.<sup>24</sup> The pH adjusted by additions of non-complexing substances such as HNO<sub>3</sub> or NaOH. And did not observe desorption to the solution directly in contact with biotite. This mixture was filtered using whatman filter paper 40 ashless/circles 125 mm diameter. The concentration of metal ion in the sample, standard and blank solutions were determined by atomic absorption analysis (AAS) and the amount of each metal sorbed by sorbent was calculated by difference.

The adsorption removal efficiency ( $\varphi$ ) of heavy metals from aqueous solution was calculated as follows:

$$\varphi (\%) = 100 \frac{C_0 - C_f}{C_0} \quad (6)$$

where  $C_0$  and  $C_f$  are the liquid-phase concentrations of heavy metal before and after adsorption, respectively.

Evaluation of the metal binding properties is considered more convenient by the distribution coefficient ( $K_d$ ) when possible concentrations of the tested metal ions are at very low concentration levels, especially in the range of ppm or ppb. The  $K_d$  value is determined from Eq. (7) (in ml/g)

$$K_d = \frac{m_{\text{adsorbent}}}{m_{\text{solution}}} \frac{v}{m} \quad (7)$$

where  $v$  is the volume of the solution (mL) and  $m$  is the weight of adsorbent (g).

The uranyl nitrate (UO<sub>2</sub>(NO<sub>3</sub>)<sub>2</sub>) and thorium dioxide (ThO<sub>2</sub>) solutions of given concentration, volume was added to a conical flask containing the synthetic Fe-biotite. The mixture was shaken and left at room temperature and pH 4.0 for 24h. The uranium (VI) and thorium (IV) in solution was determined by using CARY 400 scan UV-VIS spectrophotometer at 652 and 660nm respectively. The amount of adsorption at equilibrium time  $t, q_e$  (mg/g), was calculated by:

$$q_e = \frac{C_0 - C_e}{W} v \quad (8)$$

where  $C_0$  and  $C_e$  are the liquid-phase concentrations of uranium(VI) and thorium(IV) at the initial concentration and equilibrium time, respectively;  $v$  the volume of the solution (mL);  $W$  is the mass of dry adsorbent used (g). The adsorption removal efficiency of uranium (VI) and thorium (IV) from aqueous solution was calculated as described above.

## Results and Discussion

### Characterization of synthetic Fe-biotite

Biotite (ideal formula [NaFe<sub>2.5</sub>(Si,Al)<sub>4</sub>O<sub>10</sub>(OH)<sub>2</sub>] is a 2:1 phyllosilicate mineral with tightly held, non-hydrated interlayer cations. The 2:1 layer has octahedrally coordinated cations sandwiched between two sheets of Si, Al tetrahedra. The main cations in the octahedral layer are divalent iron Fe(II), and the interlayer ion is mainly Na. that cause expansion of the interlayer regions due to an exchange of non hydrated K with Na.

The analysis of the corresponding  $2\theta$  values and the inter-planer spacing  $d(\text{\AA})$  were carried out using computerized program indicating that, the X-ray crystalline structure mainly belongs to a monoclinic phase in major beside few peaks of silicate(Fig.1).

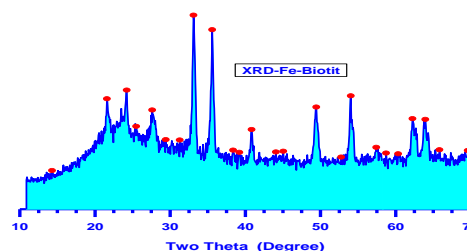


**Figure 1.** XRD pattern of fluoride-free Fe-biotite .

The crystal size of detected phase was calculated using Scherer's equation and found to be 56 nm. This indicates

that, the actual grain size in the material bulk is smaller than that detected on the surface morphology.

The FTIR spectra of Fe-biotite, was reported in Fig. 2. The spectrum of Fe-biotite shows infrared bands of OH stretching at  $3420\text{ cm}^{-1}$  and Si-O-Si bending at  $1030\text{ cm}^{-1}$ .<sup>25</sup> Fe-biotite also shows a wide and intense band at  $1490\text{ cm}^{-1}$  and two weaker bands at  $829$  and  $529\text{ cm}^{-1}$ . The last band is due to OH bending Fe<sup>3+</sup> hydration water.

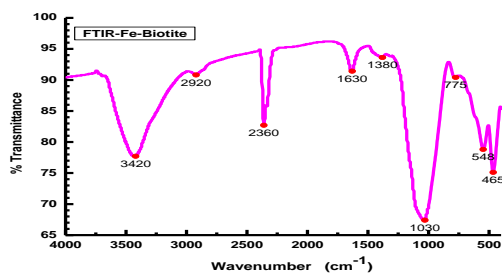


**Figure 2.** FTIR spectra of fluoride-free Fe-biotite

TGA and DTA thermographs (Supplementary material and Fig.3) represent the synthetic (Fe-biotite) clay. TGA curve exhibit three main steps of weight loss. Initial step ( $T < 400\text{ }^{\circ}\text{C}$ ) a weight loss (about 5%) corresponding to both adsorbed and interlayer water loss takes place. Second step, the TGA curve shows a gradual decrease (about 2.3%) in the range  $450\text{--}500\text{ }^{\circ}\text{C}$  which is attributed to water loss. Finally, a third main loss occurs at temperatures in the range  $630\text{--}830\text{ }^{\circ}\text{C}$ , where the TG curve displays a step weight loss (about 3.4 %) related to release of structural OH of Fe-biotite.

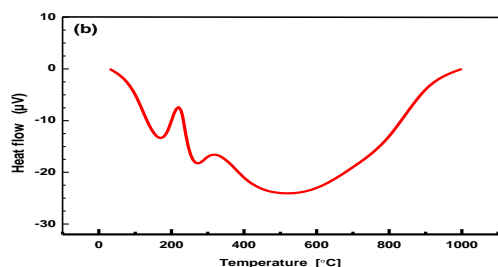


**Figure 3.** DTA curve of fluoride-free Fe-Biotite sample .

DTA curve of Fe-biotite, shown in (Fig. 3), illustrate endothermic peak at  $187\text{ }^{\circ}\text{C}$  due to dehydration effect, followed by exothermic peak at  $220\text{ }^{\circ}\text{C}$  is associated with the formation of structure.<sup>26</sup>

The ESR spectra of Fe-biotite were shown (Fig. 4). The spectrum recorded one intense absorption band at high field, which is isotropic due to the tumbling motion of the molecules. The magnetic susceptibility of 1.81 BM for Fe(II) indicates the presence of one unpaired electron, showing the structure is mononuclear in nature. This fact is also evident from g signal which appear at a lower magnetic field  $3800\text{ G}$ . The observed g-value suggests that one ESR signals originates from Fe ion situated on an interstitial site.<sup>27</sup>

The SEM micrograph of the synthetic Fe-biotite sample was shown in (Fig. 5). It is seen from figure that Fe-biotite shows irregular platelets-like structure which have ragged edges and form sub-rounded flakes. SEM of Fe-biotite indicates that the well crystallized clay sample contains stacked flasks of large particles which give low specific area

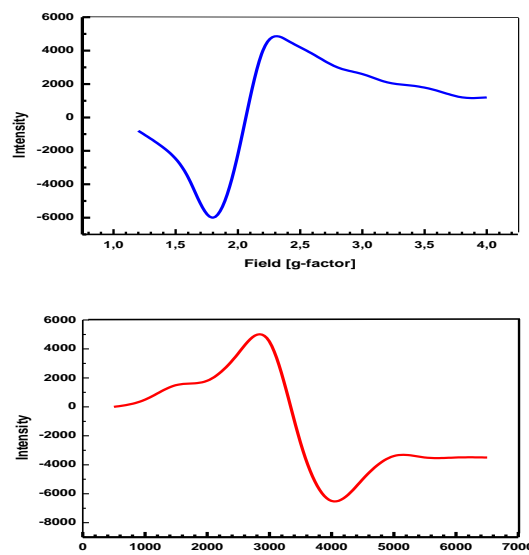


**Figure 4.** ESR spectra of free-fluoride Fe-Biotite sample

The temperature dependence of the electrical conductivity of synthetic Fe-biotite shows remarkable hysteresis Fig.(6). The electrical conductivity at a given temperature is significantly lower after heating than before. In order to investigate the hysteresis of conductivity, we conducted stepwise heating experiments of biotite. With increasing the temperature the conductivity decreases and gradually reaches a stationary value. Then the temperature was increased to the next value. The conductivity increase at a fixed temperature is not significant below  $450\text{ }^{\circ}\text{C}$ .

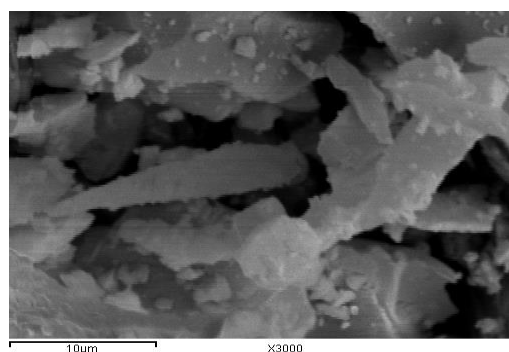


**Figure 5.** SEM of free-fluoride Fe-Biotite sample

Remarkable increase is observed at the temperature of  $450\text{--}500\text{ }^{\circ}\text{C}$ . The conductivity increase is not significant above  $500\text{ }^{\circ}\text{C}$ . The conductivity at a fixed temperature does not change during cooling.<sup>28</sup> The band gap energy was calculated from fig.6 found be  $-140\text{ JK}^{-1}$ . Mica has a possibility as ionic conductors because they are a layered compound having interlayer cations.<sup>29</sup>

Micas with smaller interlayer cations, e.g. Na-type have a higher possibility as the ionic conductors. Removal of heavy metals from aqueous solution by using synthetic Fe-biotite. Sorption is a transfer of ions from liquid phase to the solid phase. Recently, adsorption has become one of the alternative treatment techniques for wastewater laden with heavy metals. Basically, adsorption is a mass transfer process by which a substance is transferred from the liquid phase to the surface of a solid, and becomes bound by physical and/ or chemical interactions.<sup>30</sup>

In general, there are three main steps involved in pollutant sorption onto solid sorbent:

- (i) the transport of the pollutant from the bulk solution to the sorbent surface;
- (ii) adsorption on the particle surface; and
- (iii) transport within the sorbent particle.

Technical applicability and cost-effectiveness are the key factors that play major roles in the selection of the most suitable adsorbent to treat inorganic effluent.

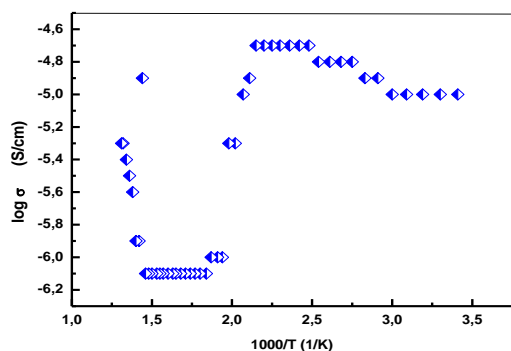


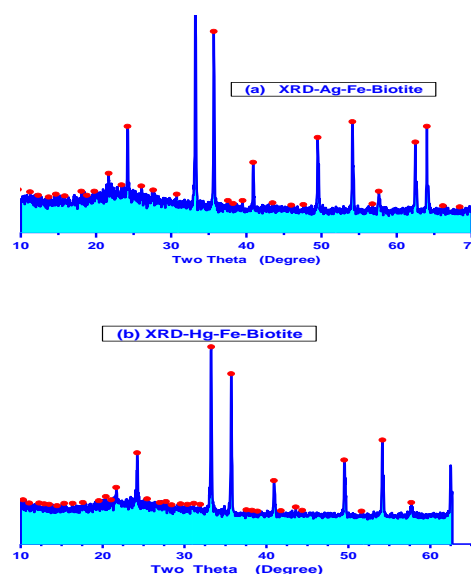
**Figure 6.** Temperature dependence of the electrical conductivity of free-fluoride Fe-Biotite

The Atomic absorption spectrophotometric analysis of heavy metals after adsorbed on synthetic Fe-biotite revealed that a high level of adsorption was that the percentage removal of Ag(I), As(V), Pb(II), Cr(III) and Hg(II) ion by the adsorbent in solution would interact with the binding sites and thus facilitated reached to 99.8%, 69.3%, 33%, 28%, 11% and adsorption and  $K_d$  values were  $14681 \text{ mg L}^{-1}$ ,  $56.4 \text{ mg L}^{-1}$ ,  $12.3 \text{ mg L}^{-1}$ ,  $9.72 \text{ mg L}^{-1}$ ,  $3.1 \text{ mg L}^{-1}$ , and respectively.

The synthetic mica gave high removal efficiency (% E) and good distribution ratio ( $K_d$ ) value for uptake of investigated heavy metals from  $10 \text{ ml g}^{-1}$  background solution and thus proving that synthetic free-fluoride Fe-biotite is capable of removing these cations from contaminated water or soil because better access of the interlayer space due to reduced charge.<sup>31</sup>

As a general rule, the relative adsorbent affinity for a metallic cation increases with the cation ability to form inner cation sphere coordination complexes. For a same valence cation series, this tendency is positively related to metallic ionic radius.<sup>32</sup>

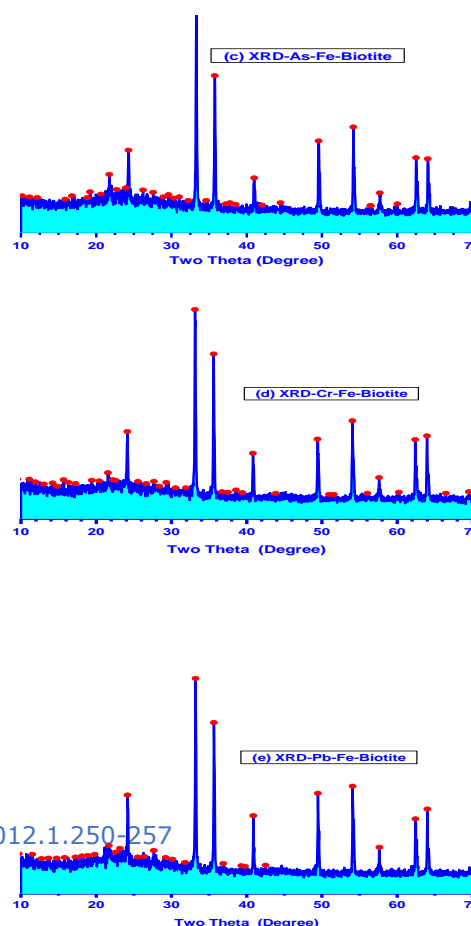
For each sorbent element, Figs. (7a-f) and Figs. (8a-e) plots the XRD and FTIR respectively, of each element sorbed and retained on the sorbent in the sorption experiments against its initial concentration in the sorption



solution (ICSS).

**Figure 7.a-e.** XRD of Fe-biotite after Ag, Hg, As, Cr and Pb-adsorption

Diffractograms of the samples and FTIR Figs. (7a-f) and Figs. (8a-e) respectively showed that structures after adsorption of heavy metals almost changed than the original before treatment. The peaks centered between  $2930 \text{ cm}^{-1}$  and  $2360 \text{ cm}^{-1}$  are due to the presence of KBr disc used as a “matrix” and therefore are not diagnostic of any mineral.<sup>33</sup>



The characteristic of synthetic Fe-biotite peak at 36 (2 $\theta$ ) was reduced to about 33(2 $\theta$ ). One would expect that it should be due to the heavy metal removal process.<sup>34</sup> The metal uptake is attributed to different mechanisms of ion-exchange and adsorption processes.<sup>35</sup> During the ion-exchange process, metal ions move through the pores of the biotite and channels of the lattice, and they replace exchangeable cations (mainly sodium) and additionally exchange with protons of surface hydroxyl groups.

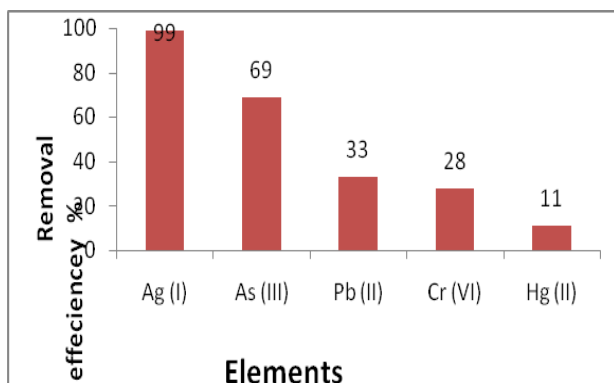


**Figure 7f.** Removal efficiency values of Fe-biotite towards different heavy metals cations solutions.

In the case of exchange with sodium,  $\text{Na}^+(\text{biotite}) + \text{M}^+(\text{solution}) \rightarrow \text{M}^+(\text{biotite}) + \text{Na}^+(\text{solution})$  reaction, in which sodium ions placed on the biotite surface exchange with the metal ions ( $\text{M}^+$ ) in the solution, occurs. When the exchange site is a hydroxyl group,  $\text{biotite-OH}(\text{biotite}) + \text{M}^+(\text{solution}) \rightarrow \text{biotite-O-M}(\text{biotite}) + \text{H}^+(\text{solution})$  exchange reaction occurs and in this case, metal ions ( $\text{M}^+$ ) exchange with the  $\text{H}^+$  ions.

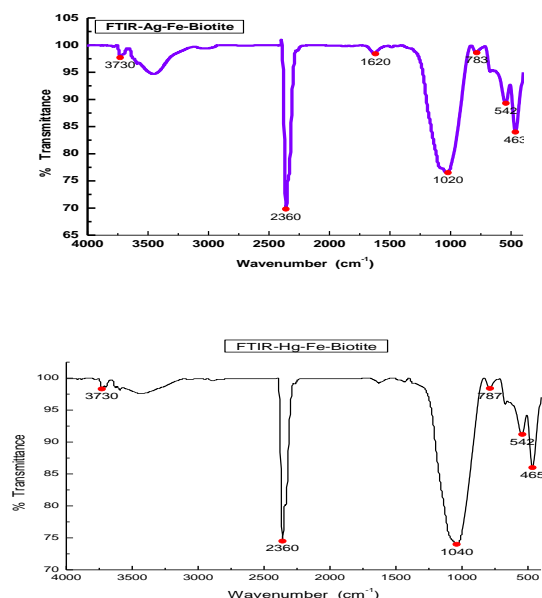


**Figure 8a and b.** FTIR spectra for Fe-biotite after (a) Ag-adsorption, (b) after Hg-Adsorption

Diffusion was faster through the pores and retarded when the ions moved through the smaller diameter channels. The ion-exchange processes in biotite are affected by several factors such as concentration and nature of cations, pH and crystal structure of the biotite. The effect of these parameters has been investigated in several studies due to

the importance of biotite's mineral stability in the applications of biotite as an ion exchanger.<sup>36,37</sup> These data confirm that, the cation selectivity of Fe-biotite towards the investigated metals that captured through silicate layers.

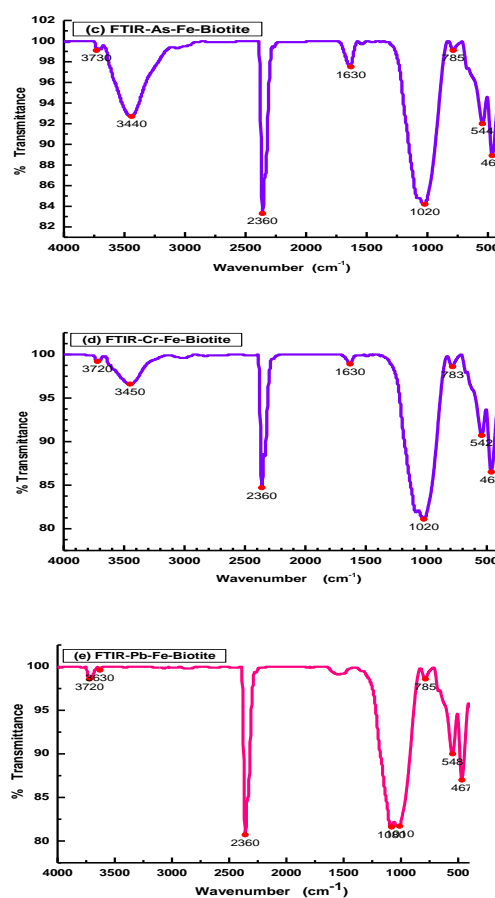


**Figure 8c-e.** FT-IR spectra of Fe-biotite (c) after As adsorption; (d) after Cr adsorption; (e) after Pb adsorption

#### Uptake of thorium and uranium cations by newly synthetic Fe-biotite

Depending on the structure of the adsorbent, several diffusion mechanisms become dominant and sometimes only two or three of them compete or cooperate. The dominant mechanism also depends on a combination of adsorbate, adsorbent and adsorption conditions, such as temperature and concentration range.<sup>38</sup>

The adsorption of thorium ion onto the biotite is mainly affected by the surface hydroxyl groups of the adsorbent. The silicon atoms at the surface tend to maintain their tetrahedral coordination with oxygen. They complete their coordination at room temperature by attachment to monovalent hydroxyl groups, forming silanol groups. Theoretically, a pattern in which one silicon atom bears two or three hydroxyl groups, yielding silanediol and silanetriol groups respectively is possible. It has already been reported as improbable that silanetriol groups exist at the silica surface.<sup>39,40</sup> The types of silanol groups and hydrous oxide surface groups in alumina are given in Fig. 11.<sup>39</sup> These groups give the adsorption property to perlite, similar like biotite.

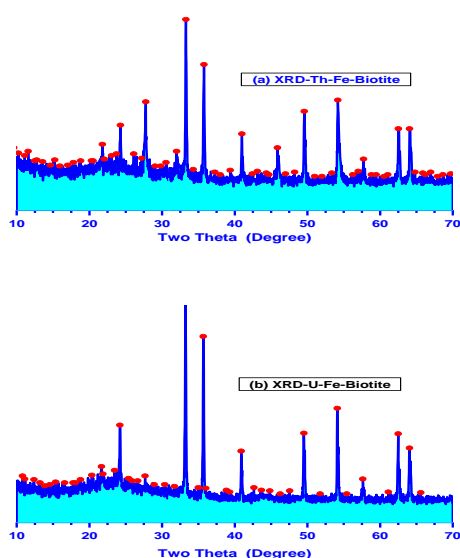


**Figure 9a and b.** X-ray diffraction patterns of Fe-biotite after (a) Th- adsorption, (b) U-Adsorption .

It seems that once U(VI) ions are adsorbed and have penetrated into the interlayer region, they become immobile.<sup>41</sup> This statement is partly supported by the observation that U(VI) was partially reduced to U(IV) on ferrous mica.<sup>42</sup>

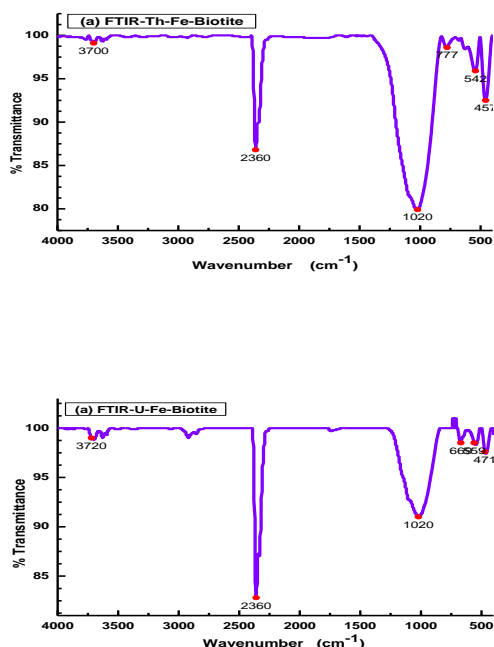


**Figure 10a and b.** Infrared absorption spectra recorded after U and Th capture on the Fe-biotite .

The result showed higher efficiency removal for uranium than the previous studied which reported that the maximum amount of uranium sorbed onto each individual mineral was different and ranged from 48% of the initially added uranium for quartz, 58% for albite, 70% for muscovite and chlorite, to 97% for phyllite

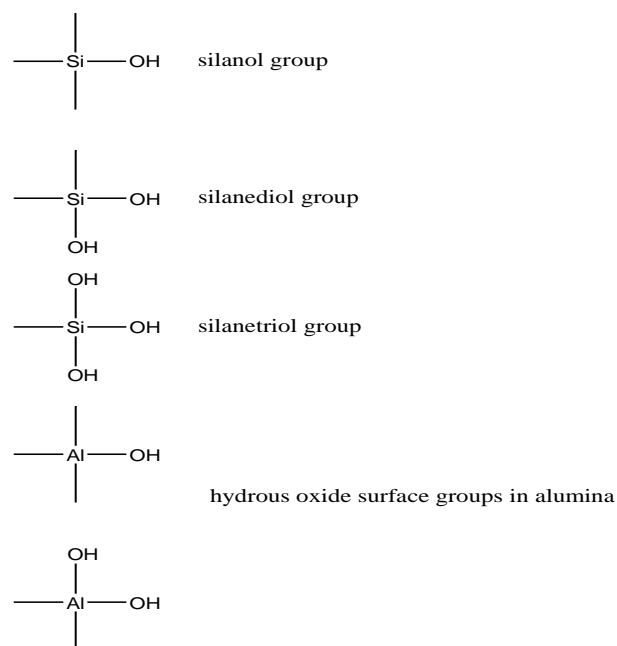


**Figure 11.** The types of silanol groups and the hydrous oxide surface groups in alumina by Dogan et al.<sup>29</sup>

## Conclusions

The conclusive remarks inside this paper can be briefed as follows:

1. Green synthesis of fluoride-free  $\text{NaFe}_{2.5}(\text{Al,Si})_4\text{O}_{10}(\text{OH})_2$  for remediation of contaminated effluents has been developed.
2. Fe-biotite shows moderate to strong strength as cation selective ion exchanger for the tested toxic metals
3. Sorption of heavy metal ions by Fe-biotite was established according to the aforementioned group of BATNEEC (best available technology not entailing excessive costs) treatment technologies as a standard process has been developed.

## Acknowledgments

The authors are thankful to the Department of Chemistry, faculty of Science, University of Tanta, Egypt for providing laboratory facilities.

## References

- <sup>1</sup>O'Connell, D. W., Birkinshaw, C., & O'Dwyer, T. F., *Bioresour. Technol.*, **2008**, *99*, 6709.
- <sup>2</sup>Abollino, O. Aceto, M. Sarzanini, C. Mentasti, E., *Anal. Chim. Acta.*, **2000**, *411*, 223.
- <sup>3</sup>Huang, C. P., Tsong, M. W., Hsieh, Y. S. in: K. Peters, D. Bhattacharya (Eds.), *AIChE Symp. Ser., Heavy Metal Separation Processes*, American Institute of Chemical Engineers, New York, **1985**.

- <sup>4</sup>Bhattacharyya, K. G. Gupta, S. S., *Colloids Surf.* **2006**, *277*, 191.
- <sup>5</sup>Sharma, P., Tomar, R., *Micropor. Mesopor. Mater.*, **2008**, *116*, 641.
- <sup>6</sup>Babel, S., Kurniawan, T. A., *J. Hazard. Mater.*, **2003**, *97*, 219.
- <sup>7</sup>Naseem, R., Tahir, S. S., *Water Res.* **2001**, *35*, 3982.
- <sup>8</sup>Tsoufifis, T., Xidas, P., Jankovic, L., Gournis, D., Saranti, A., Bakas, T., Karakassides, M.A., *Diamond Relat. Mater.* **2007**, *16*, 155.
- <sup>9</sup>Karadag, D., Koc, Y., Turan, M., Ozturk, M., *J. Hazard. Mater.* **2007**, *144*, 432.
- <sup>10</sup>Sebesta, F. Motl, A. John, J. Proc. Int. Conf. Nuclear Waste Manag. Environ. Remediation, **1993**, *3*, 871., Prague, Czech Republic
- <sup>11</sup>Sebesta, F. John, J. *An Overview of the Development, Testing, and Application of Composite Absorbers*, Los Alamos National Laboratory, Report No: LA-12875-MS, **1995**, p. 30.
- <sup>12</sup>Tranter, T. J., Herbst, R. S., Todd, T. A., Olson, A. L., Eldredge, H. B., *Adv. Environ. Res.*, **2002**, *6*, 107.
- <sup>13</sup>Szeglovski, Z., Constantinescu, O., Hussonnois, H., *Radiochem. Acta.*, **1994**, *64*, 127.
- <sup>14</sup>Aitken, M. J. *Thermoluminescence Dating*, Academic Press, London, **1985**.
- <sup>15</sup>Ilton, E. S. and Veblen, D. R., *Geochim. Cosmochim. Acta* **1994**, *58*, 2777.
- <sup>16</sup>Gan, H., Bailey, G. W., and Yu, Y. S., *Clays Clay Miner.*, **1996**, *44*, 734.
- <sup>17</sup>Peterson, M. L. Brown, G. E. Jr., Parks, G. A. and Stein, C. L., *Geochim. Cosmochim. Acta* **1997**, *61*, 3399.
- <sup>18</sup>Profi, S., Sideris, C. and Filippakis, S. E., *N. Jb. Miner. Mh.*, **1973**, *H1*, 8.
- <sup>19</sup>Covelo, E. F. Vega, F. A. Andrade, M. L., *J. Hazard. Mater.* **2007**, *140*, 308.
- <sup>20</sup>Lazarevic, S., Jankovic-Castvan, I., Jovanovic, D., Milonjic, S., Janackovic, D., Petrovic, R., *App. Clay Sci.*, **2007**, *37*, 47.
- <sup>21</sup>Akgul, M., Karabakan, A., Acar, O., Yurum, Y., *Micropor. Mesopor. Mater.*, **2006**, *94*, 99.
- <sup>22</sup>Frost, R. R., Griffin, R. A., *Soil Sci. Soc. Am. J.*, **1977**, *41*, 53.
- <sup>23</sup>Gonc, C., Rocha, A., Zaia, D. A. M., da Silva Alfaya, R. V., da Silva Alfaya, A. A., *J. Hazard. Mater.* **2009**, *166*, 383.
- <sup>24</sup>Zhou, Y.-F., Haynes, R. J., *Water, Air, & Soil Pollut.*, **2011**, *215*(1-4), 631.
- <sup>25</sup>Farmer, V. C., *The Infrared Spectra of Minerals*. Mineralogical Society, London (1974).
- <sup>26</sup>Mohsen, Q., El-Maghraby, A., *Arabian J. Chem.*, **2010**, *3*, 271.
- <sup>27</sup>Josephyus, R. S., Nair, M. S., *Arabian J. Chem.*, **2010**, *3*, 195.
- <sup>28</sup>Tate, I., Kitajima K. and Daimon, N., *Kogyou Kagaku (J. Chem. Soc. Japan)*, **1968**, *71*, 976.
- <sup>29</sup>Mahmoud, M. E., Osman, M. M., Hafez, O. F., Elmelegy, E., *J. Hazard Mater.*, **2010**, *173*, 349.
- <sup>30</sup>Kurniawan, T. A., Babel, S., *2<sup>nd</sup> Int. Conf. Energy Technol. Clean Environ. (RCETE)*, **2003**, *2*, 1110. Phuket, Thailand, 12–14 February
- <sup>31</sup>Komarneni, S., Pidugu, R., Amonette, J.E., *J. Mater. Chem.*, **1998**, *8*, 205.
- <sup>32</sup>Sposito, G., *The Chemistry of Soils*. Oxford University Press, New York, USA, **1989**.
- <sup>33</sup>Lugwisha, E. H.J., *Tanz. J. Sci.*, **2011**, *37*, 167.
- <sup>34</sup>Vengris, T., Binkiene, R., Sveikauskaite, A., *J. Appl. Clay Sci.*, **2001**, *18*, 183.
- <sup>35</sup>Erdem, E., Karapinar, N., Donat, R., *J. Colloid. Interface. Sci.*, **2004**, *280*(2), 309.
- <sup>36</sup>Chakraborty, S., Wolthers, M., Chatterjee, D., Charlet, L., *J. Colloid Interface Sci.*, **2007**, *309*, 392.
- <sup>37</sup>Cho Y. C., Komarneni, S., *App. Clay Sci.*, **2009**, *44*, 15.
- <sup>38</sup>Suzuki, M., *Adsorption Engineering*. Kodansha, Tokyo, **1990**.
- <sup>39</sup>Dogan, M., Alkan, M., Onganer, Y., *Water Air Soil Pollut.*, **2000**, *120*, 229.
- <sup>40</sup>Talip, Z., Eral, M., Hiçsönmez, U., *J. Environ. Radioact.* **2009**, *100*, 139.
- <sup>41</sup>Lee, S. Y., Baik, M. H., Lee, Y. J., Lee, Y. B., *App. Clay Sci.*, **2009**, *46*(3), 255.
- <sup>42</sup>Ilton, E. S., Haiduc, A., Moses, C. O., Heald, S. M., Elbert, D. C., Veblen, D. R., *Geochim. Cosmochim. Acta* **2004**, *68*, 2417.

Received: 29.Sept. 2012.

Accepted: 07. Oct. 2012.



# INVESTIGATION ON THE EFFECT OF PARTICLE SIZE AND ADSORPTION KINETICS FOR THE REMOVAL OF Cr(VI) FROM THE AQUEOUS SOLUTIONS USING LOW COST SORBENT.

R. Hema Krishna<sup>[a]\*</sup> and A. V. V. S. Swamy<sup>[b]</sup>

**Keywords:** Adsorption, Cr (VI) ions, powder of calcined brick, Particle size, Adsorption Kinetics, Langmuir Lagergren rate constant.

The potential to remove Chromium (VI) from aqueous solutions through sorption using powder of calcined brick (PCB) was investigated using batch tests. The influence of physico-chemical key parameters such as the initial metal ion concentration, agitation time and the particle size of adsorbent have been considered in batch tests. The optimum results were determined at an initial metal ion concentration was 10 mg L<sup>-1</sup>, agitation time – 60 min, and the particle size (0.6 mm). The % adsorption, Lagergren rate constant ( $K_{ad} \text{ (min}^{-1}) = 6.60 \times 10^{-2}$  for Cr(VI) 10 mg L<sup>-1</sup>) were determined for the adsorption system as a function of sorbate concentration. The kinetic data obtained were fitted to pseudo first order model.

\* Corresponding Authors

Tel; 001-6475026323

E-Mail: [hkravuri32@gmail.com](mailto:hkravuri32@gmail.com); [arzavvsswamy1962@gmail.com](mailto:arzavvsswamy1962@gmail.com)

[a] Department of chemistry, University of Toronto, Ontario, Canada. M3J 1P3

[b] Department of Environmental Sciences, Acharya Nagarjuna University, India-522510.

## Introduction

Heavy metal pollution has been increasing with the diversifying industrial activity. Industries such as textiles, dye industry, drugs and pharmaceutical industries, tanning, electroplating, etc., use heavy metals in considerable quantities. The heavy metals are used as catalysts and are recovered as far as possible and ultimately discharged along with the wastewater generated in the industry. Their abuse harms the living systems. For that matter any 'matter' in a wrong concentration, in a wrong place and in a wrong time is named as a 'pollutant'. The modern technology developed by the man, not only depleted the wealth of nature but also created environmental degradation. The problem of water pollution due to heavy metals and their impact on environment is presently the focus of international attention. The removal of heavy metals was also tried with zeolite and crystal gravel in combination with porous iron. The removal was tried not only from aqueous solutions but also from the urban storm water. The presence of heavy metals in the sewage water had been the main problem in the sewage treatment plants of the urban areas. Hence there have been efforts to remove the heavy metals from the sewage before they are let out in to the natural systems<sup>1</sup> have studied the efficiency of the porous iron individually and in combination with zeolite and crystal gravel, in the removal of coexistent heavy metals from simulated urban storm water. The equilibrium data of their study demonstrated a good fit with the Freundlich model and showed affinity in the order: Cd > Zn > Ni > Cu > As > Cr studied<sup>2</sup> the removal of Cr(VI) using hydrous concrete particles which had Si, Al, Fe, Ca and Mg as Major components. They compared the adsorption free energy of  $\text{HCrO}_4^-$  and  $\text{CrO}_4^{2-}$

and reported hydrous concrete particles good adsorbent. Low cost materials like linseed straw, pressed sludge cake, coal dust, pyrolysed tyre, and sugar beet pulp and leather hide powder had been used. Modified cellulose was also reported in literature by Navarro<sup>3</sup> and Bandyopadhyay<sup>4</sup> studied removal of Cr(VI) on sand as well as in combination with activated carbon too. They came out with some interesting facts that mixed adsorbent becomes effective at high dosage ( $\geq 2.5$  g/100 ml) and also in good agreement with Langmuir adsorption isotherm. They concluded that adsorption is more favorable for mixed adsorbent as compared to activated carbon alone. In choosing a waste water treatment technology, factors like nature of pollutants, permissible limits and economy of the treatment method have to be considered. Recent research of selective and sensitive methods for the determination of metals in water at trace levels. Among available methods, adsorption appears to have least adverse effects. The use of waste material from industries and agriculture for the removal of metal ions which reduces the treatment cost, and also provides a solution for the solid waste management of the industries. Most of the industries cannot afford to use conventional wastewater treatment methods due to their high cost. It is expected that the present work in this publication may fulfill the aforesaid requirement partially. The present study includes the studies on the effect of particle size and adsorption kinetics on removal of chromium(VI) ions using powder of calcined brick. The efficiency of this adsorbent was studied and maximum adsorption and lowest equilibrium time for this adsorbent was recorded. The present work helps the individual organizations to remove the excess concentrations of the chromium(VI) from their effluents within their premises without much effort and time.

## Experimental

*Adsorbent:* Easy availability, economical to use and proven potential for other metals, have been the reasons for selection of this adsorbent Powder of calcined brick (PCB) was used to adsorb chromium (VI).

**Powder of calcined brick (PCB):** The calcined bricks were collected from the kiln and powdered. The powder was soaked for 24 hours in distilled water and then thoroughly washed for 4 to 5 times. The powder was in air and sieved to select 0.6 mm sized particles.

**Measurement of moisture content:** Ten grams of the adsorbent powder was taken into a Petri dish and overheated for two hours. After heating the plates were instantaneously placed in a desiccator. The powder thus cooled and weighed. The difference between initial and final weights was taken as the moisture content.

**Preparation of metal-ion solution:** The chromium(VI) was estimated using standard methods. AR grade chemicals and double distilled water were used for all the analyses. The concentrations of the metal ions were estimated using UV-visible spectrophotometer (ELICO SL 150)

**Standard chromium Solution:** Potassium dichromate AR grade was used to prepared standard chromium(VI) solution. 2.830 g of potassium dichromate was weighed and taken into 1000 ml volumetric flask.

**Analysis of chromium(VI):** The metal ion concentrations were estimated by adoption the procedures described in the methods. Chromium(VI) was estimated using UV-VIS spectrophotometer (ELICO-SL 150) by diphenyl carbazide (DPC) method. Different dilutions of Cr(VI) solutions containing less than 30 mg L<sup>-1</sup> of chromium concentrations were added with 2.5 ml of diphenyl carbazide solution. The diphenyl carbazide solution was prepared by dissolving 200 mg of diphenyl carbazide in 100 ml of 95% alcohol. The contents were mixed with an acid solution of 40 ml of concentrated H<sub>2</sub>SO<sub>4</sub> and 360 ml of distilled water. The contents were refrigerated for not less than 24 hrs, and to a maximum of one month. The absorbance was measured in the UV-visible spectrophotometer at 540 nm. The reagent blank was also measured following the same procedure. A calibration curve was prepared for Cr(VI) standard solutions and absorbance. The concentration in the sample was established by reading from the calibration curve. The results for a heavy metal concentrations were expressed in mg L<sup>-1</sup> while those of the concentration equilibrium, equilibrium time, and adsorption capacity etc., were compared with the Langmuir and Freundlich isotherms

**Batch equilibrium method:** All experiments were carried out at room temperature (27 °C) in batch mode. Batch mode was selected because of its simplicity and reliability. The experiments were carried out by taking 50 ml metal ion sample (AR grade) in a 100 ml Erlenmeyer flask and after pH adjustments; a known quantity of dried adsorbent was added. The flasks were agitated at 165 rpm for predetermined time intervals using a mechanical shaker until equilibrium conditions were reached. After shaking, the suspension was allowed to settle. The residual mass adsorbed with metal ion was filtered using whatman 42 filter paper (Whatman International Ltd., Maid Stone, England), filtrate was collected and subjected for metal ion estimation using UV-visible spectrophotometer (ELICO SL 150). The values of percent metal uptake by the sorbent (sorption

efficiency,  $\zeta$ ) and the amount of metal ion adsorbed ( $q_e$ ) has been calculated using the following relationships

$$\zeta = 100 \frac{C_i - C_f}{C_i} \quad (1)$$

$$q_e = \frac{C_i - C_f}{m} v \quad (2)$$

where,

$C_i$ - initial concentration of metal ion in the solution, mg L<sup>-1</sup>

$C_f$ - final concentration of metal ion in the solution, mg L<sup>-1</sup>

$m$  - mass of adsorbent, g L<sup>-1</sup>

$v$  - volume of solution (lit)

$q_e$  - amount of metal ion adsorbed per gram of adsorbent.

Control experiments were carried out and the average values of duplicate runs were obtained and analyzed (error:  $\pm 1-2\%$  for percentage removal and  $\pm 0.005-0.01$  mg g<sup>-1</sup> for amount adsorbed). The adsorbents selected were very common and eco-friendly. The work mainly helps in bringing bio sorbents into use to handle the heavy metals.

## Results and Discussion

The characteristics of PCB like bulk density, loss on ignition, pH, and silica as SiO<sub>2</sub> were discussed in the Table 1.

**Table -1** Characteristics of PCB

Parameter	Value
Bulk density	1.3207
Loss on ignition	2.70
pH	7.67
Silica as SiO <sub>2</sub>	61.30
Calcium as Ca	0.24
Sodium as Na	0.05

### Effect of Initial Metal Ion Concentration and Equilibrium Time

Equilibrium experiments were carried out by agitating 50ml of different concentrations of chromium(VI) solutions (10-30 mg L<sup>-1</sup>) adjusted to pH 2.0 with 200 mg of adsorbent. After equilibrating for different time periods, the solutions were centrifuged and analyzed for chromium (VI) content. Cr(VI) adsorption as a function of time and different concentrations were shown in (Table 2). It was evident that the equilibrium time was independent of initial concentration. The rate of uptake was rapid in the beginning and became slow in the later stages of the adsorption process.

**Table 2** Adsorption of Cr (VI) and % of removal for different agitation times.

Agitation time, min	Concentration of Chromium (VI) in mg L <sup>-1</sup>								
	10 mg L <sup>-1</sup>			20 mg L <sup>-1</sup>			30 mg L <sup>-1</sup>		
	q, mg L <sup>-1</sup>	q <sub>e</sub> -q	ζ, %	q, mg L <sup>-1</sup>	q <sub>e</sub> -q	ζ, %	q, mg L <sup>-1</sup>	q <sub>e</sub> -q	ζ, %
10	0.94	1.09	37.76	1.34	2.41	26.81	1.54	3.62	20.60
20	1.47	0.56	56.98	2.28	1.47	45.78	3.02	2.14	40.33
30	1.72	0.31	68.80	2.93	0.82	58.65	3.75	1.41	50.04
40	1.86	0.17	74.40	3.28	0.47	65.79	4.41	0.75	58.92
50	1.96	0.07	78.66	3.59	0.16	71.87	4.92	0.24	65.71
60	2.03	-	81.37	3.75	-	75.07	5.16	-	68.80
70	2.03	-	81.37	3.75	-	75.07	5.16	-	68.80
80	2.03	-	81.37	3.75	-	75.07	5.16	-	68.80

**Table 3.** Adsorption of chromium (VI) on different particle sizes (mm) of the adsorbent

Agitation time, min	Particle size in mm								
	0.6 mm			0.8 mm			1.7 mm		
	q, mg L <sup>-1</sup>	q <sub>e</sub> -q	ζ, %	q, mg L <sup>-1</sup>	q <sub>e</sub> -q	ζ, %	q, mg L <sup>-1</sup>	q <sub>e</sub> -q	ζ, %
10	1.33	1.68	40.18	1.13	1.53	34.20	0.94	1.40	28.40
20	2.09	0.92	62.75	1.75	0.91	52.50	1.47	0.87	44.22
30	2.48	0.53	74.69	2.12	0.54	63.85	1.82	0.52	54.74
40	2.77	0.24	83.11	2.43	0.23	72.95	2.08	0.26	62.50
50	2.94	0.07	78.02	2.60	0.06	78.02	2.21	0.13	66.46
60	3.01	-	90.58	2.66	-	80.05	2.34	-	70.13
70	3.01	-	90.58	2.66	-	80.05	2.34	-	70.13
80	3.01	-	90.58	2.66	-	80.05	2.34	-	70.13

The adsorbate metal ions preferentially, occupied many of the active sites in a random manner resulting in rapid uptake of Cr(VI) ions. As the time passed, the active sites were blocked and hence the rate decreased. For maximum removal of chromium(VI) by the adsorbent, the solutions should be equilibrated for 60 min irrespective of the initial concentration. The curves observed in (Figure 1) were single, smooth and continuous indicating the formation of monolayer coverage of the adsorbate on the surface of the adsorbent.

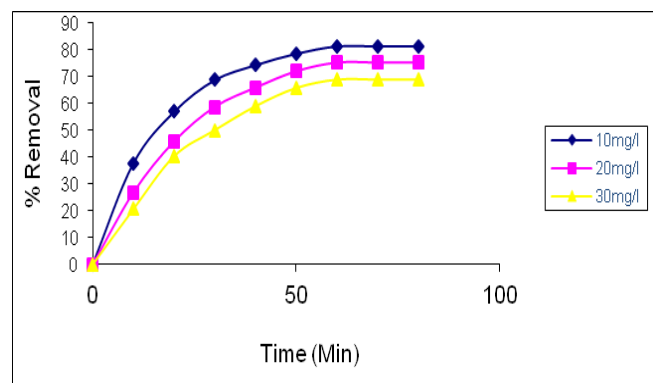


Figure 1 The relationship between time of agitation and % removal

Similar trend has been reported for bituminous coal and photo film waste by Nagesh et al<sup>5</sup> and Selvaraj et al.<sup>6</sup> The amounts of Cr(VI) adsorbed were found to be 2.03, 3.75 and 5.16 mg g<sup>-1</sup> for chromium (VI) at the concentrations of 10, 20 and 30 mg L<sup>-1</sup>, respectively, by PCB.

#### Effect of Particle Size

To study the effect of particle size, adsorbent particles of sizes 0.6 mm, 0.8 mm and 1.7 mm were used. In each study 150 mg of adsorbent in 50 ml of 10 mg L<sup>-1</sup> of Cr(VI) solution was agitated to equilibrium time of 60 min, the adsorbent was separated and the supernatant solution was analyzed for chromium concentration and the values are noted in (Table 3), the amounts adsorbed for 0.6 mm, 0.8 mm and 1.7 mm particle size were 3.01, 2.66 and 2.34 mg g<sup>-1</sup>, respectively. It is evident from (Fig. 2). That increase in particle size decreased the percent removal. At a fixed adsorbent dosage, the decrease in particle size increases the metal uptake. The increase in the uptake by smaller particles was due to the greater accessibility to pores and to the greater surface area for bulk adsorption per unit mass of the adsorbent.

Similar trend had been observed on removal of Cr(VI) by using *Pitchellobium dulce* benth.<sup>7</sup>

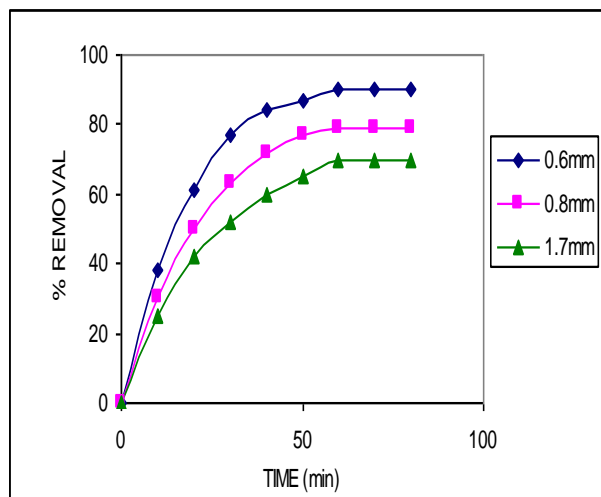


**Figure 2** Relationship between particle size, % removal at different times.

### Adsorption Kinetics

The kinetics of Cr (VI) adsorption followed the first order rate. Eqn. (1) given by Lagergren was:

$$\lg(q_e - q) = \lg q_e - \frac{K_{ad}}{2.303} t \quad (3)$$

where  $q$  and  $q_e$  were the amounts of metal ion adsorbed ( $\text{mg g}^{-1}$ ) at time  $t$  (min) and at equilibrium time, respectively and  $K_{ad}$  was the rate constant of adsorption ( $\text{min}^{-1}$ ). From the Fig. 3 it was evident that, the linear plots of  $\lg(q_e - q)$  vs time at different concentrations show the applicability of the Lagergren equation. Lagergren rate constants using equation (4) were determined. Plots of  $\lg(q_e - q)$  vs  $t$  for different initial metal ion concentrations are shown in Fig. 3 and rate constants calculated for the adsorption of Cr(VI) were given in Table 4.

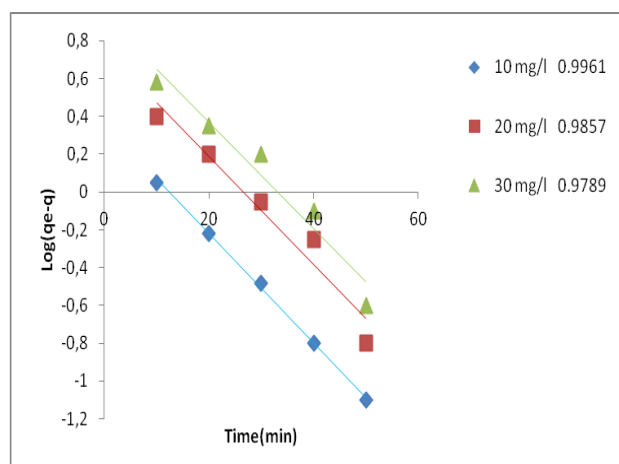


**Figure 3** Relation between log values of initial concentration and different times

The rate constants were more or less constant. The rate constants are comparable with those reported in the literature.<sup>8</sup>

**Table 4** Calculated rate constants for different chromium(VI) concentrations

Cr(VI) ( $\text{mg L}^{-1}$ )	Rate Constant $K_{ad}$ ( $\text{min}^{-1}$ )
10	$6.60 \times 10^{-2}$
20	$6.49 \times 10^{-2}$
30	$6.37 \times 10^{-2}$

### Effect of Particles Size on Lagergren Rate Constant

The effect of particle size on the rate of adsorption was shown in (Fig. 4) and the rate constant  $K_{ad}$  values calculated are given in Table 5. For the adsorption of Cr(VI), increase in particle size from 0.6 mm to 1.7 mm decreased the rate of adsorption from  $6.01 \times 10^{-2}$  to  $4.37 \times 10^{-2} \text{ min}^{-1}$ . The higher rate of metal uptake by smaller particles was due to greater accessibility to pores and greater surface area for bulk adsorption per unit weight of the adsorbent<sup>9</sup> have stated that the breaking up of larger particles to form smaller ones opens some tiny sealed channels that will be available for adsorption and therefore the rate of uptake by smaller particles was higher than that larger particle.

**Table 5** Lagergren rate constants calculated for different particle sizes (mm)

Particle size (mm)	Rate Constant $K_{ad}$ ( $\text{min}^{-1}$ )
0.6	$6.01 \times 10^{-2}$
0.8	$5.21 \times 10^{-2}$
1.7	$4.37 \times 10^{-2}$

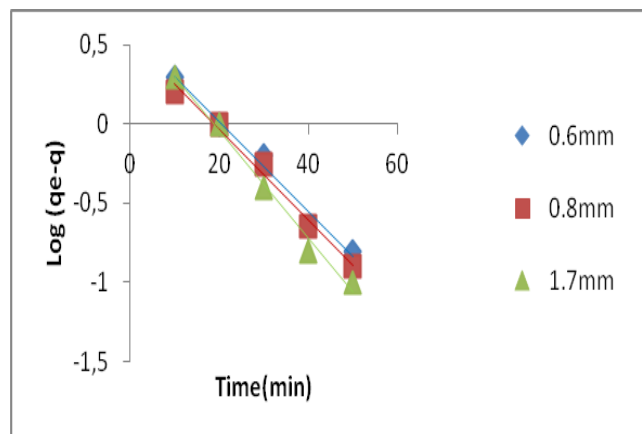


**Figure 4.** Relationship between different particle size and time of adsorption.

### Conclusion

In this study the batch removal of toxic hexavalent chromium ions from aqueous solutions using powder calcined brick was investigated.

It is evident that decrease in particle size increases the percent removal hexavalent Cr (VI) ions. The 81.37% removal of chromium (VI) was observed at 10mg/50 ml of adsorbent dose. The higher kinetic rate of metal uptake by smaller particles was due to greater accessibility to pores and greater surface area for bulk adsorption per unit weight of the adsorbent. The chromium(VI) uptake by the powder of calcined brick followed pseudo first order rate model. Hexavalent chromium metal removal with the above adsorbent appears to be technically feasible, user-friendly, eco-friendly, economical process and with high efficacy.

### Acknowledgement

The authors would like to thank to Prof.Z. Vishnuvarthan, BOS Chairman, Department of Environmental Sciences, Acharya Nagarjuna University, India., for his co-operation and encouragement. Our special thanks also reserved for our family members and friends who stand always by our side in all our endeavors.

### References

- <sup>1</sup>Wu, P. and Yu-shan, Zhou, *J. Hazard Mater.*, **2009**, 168(2-3), 674.
- <sup>2</sup>Weng, C.H., Huang, C. P. Allen H. C. and Sanders, P. F., *J. Environ. Eng.*, **2000**, 127, 1124.
- <sup>3</sup>Navarro, R. R., Fujii, K. S. N. and Matsumuta, M., *Water Res.*, **1996**, 30, 2488.
- <sup>4</sup>Bandyopadhyay, A. and Biswas, M. N., *Indian J. Environ. Protect.*, **1998**, 18(9), 662.
- <sup>5</sup>Nagesh, N. and Krishnaiah, A., *Indian J. Environ. Protect.*, 1989, 9(4): 301 -303.
- <sup>6</sup>Selvaraj, K., Chandramohan V. and Pattabhi, S., *Indian J. Environ. Protect.*, **1998**, 18(9), 641.
- <sup>7</sup>Nagarajan, P., Elizabeth V. D. and Isaiah, S., *Indian J. Environ. Protect.*, **2006**, 26(1), 30.
- <sup>8</sup>Kannan, N. and Vanangamudi, A., *Indian J. Environ. Protect. II*, **1991**, 4, 241.
- <sup>9</sup>Weber, W. J. Jr., and Morris, J., *Sanitary Eng. Div. ASCE.*, **1963**, 89(SA2), 31.

Received: 22. 09. 2012.  
Accepted: 09.10. 2012.



## COMPARATIVE STUDY OF THE ESSENTIAL OILS OF *MONODORA MYRISTICA* FROM NIGERIA

I. A. Owokotomo<sup>[a]\*</sup> and O. Ekundayo<sup>[b]</sup>

**Keywords:** Essential oil; *Monodora myristica*; Hydrodistillation; Nigeria

The essential oils from seeds and stem-bark of *Monodora myristica* (Annonaceae) growing wild in south western Nigeria and used as spice in many parts of Nigeria were extracted by hydrodistillation and analysed by GC- MS. The percentage yields of oils were 2.16% v/w and 0.25% v/w, respectively. The essential oil of seeds contained germacrene D-4-ol (25.48%), tricyclo[5.2.1(1,5)dec-2-ene (13.35%),  $\delta$ -cadinene (11.09%) and linalool (15.10%) as major constituents while the dominant constituents of the stems-bark oil were  $\gamma$ -cadinene (31.31%),  $\alpha$ -elemene (17.98%),  $\alpha$ -cubebene (6.70%) and  $\gamma$ -muurolene (5.94%). The major constituents of the seeds oil of *Monodora myristica* from Nigeria were compared based on literature.

\* Corresponding Authors

E-Mail: [kunleowokotomo@yahoo.com](mailto:kunleowokotomo@yahoo.com)

[a] Department of Chemistry, Federal University of Technology, Akure, Nigeria.

[b] Department of chemistry, University of Ibadan, Ibadan Nigeria

### Introduction

*Monodora myristica* (Annonaceae) commonly known as 'Ariwo' in South Western Nigeria is a tropical tree that grows wild in many African countries including Nigeria.<sup>1,2</sup> Nutritional value of *M. myristica* centres on its usefulness as a seasoning because of its aromatic flavor. The kernel obtained from the seeds is a popular condiment used as spicing agent in both African and Continental cuisines in Nigeria.<sup>3</sup> The seeds are aromatic and used as stimulating addition to snuff and medicine.<sup>4</sup>

There are several reports of its medicinal use; the bark is used in the treatments of stomach-aches, febrile pains, eye diseases and hemorrhoids.<sup>5</sup> In Central African Republic, the seeds are used as condiment and drug in the treatment of headache and hypertension.<sup>6</sup> The antisickling effect of *M. myristica* has also been demonstrated.<sup>4</sup> Earlier determination of the chemical constituents of the seeds reveals the presence of Fiberro-latic oils, resins, terpene, lactose, arocin, saponins, flavonoids and tannins.<sup>7</sup>

*M.myristica* seeds seem to be the major research focus around the globe. Literature report on the essential oils from other parts of the plant is scant. Also significant variation exists in the composition of the seeds essential oils of this plant published in literature, especially from Nigeria. In view of these, we investigate the essential oil compositions of the seeds and stem-bark of *Monodora myristica* grown in Nigeria and compared the seeds' essential oils based on literature.

### Experimental

#### Plant materials

The seeds and stems-bark were collected at a farm at the bank of River Igbeta in Iwaro-Oka, Ondo state, South West Nigeria. The identification was done at the Forest Research Institute of Nigeria, Ibadan. The seeds and the

stem-bark (cut into beans) were air dried and then pulverised using a fast rotating blender. The samples were then separately subjected to hydro distillation using an all glass Clevenger- type apparatus<sup>8</sup> for 3 hours. The essential oils collected were kept in the refrigerator at 0°C before GC-MS analysis without any further treatment.

#### Gas chromatography/mass spectrometry analysis

The essential oils were analysed using GC-MS Agilent 6890N GC Coupled with MS-5973-634071Series. The capillary column type was DB-1MS [30.0 m (length) X320.00 $\mu$ m (diameter) X1.00 $\mu$ m (film thickness)]. The carrier gas was Helium at constant flow rate of 1.0ml/min and average velocity of 37cm/s; the pressure was 0.78psi. The initial column temperature was set at 100°C (hold for 2min) to the final temperature of 250°C at the rate of 5°C/min, Volume injected was 1.0 $\mu$ L and split ratio was 50:1. The total chromatogram was auto-integrated by Shem-Station and the constituents were identified by comparison with published mass spectral database (NIST02.L) and data from literature.

### Results and Discussion

#### Percentage yield

The percentage yield of essential oil of seeds and stem-bark were 2.16% and 0.25% v/w respectively.

#### GC-MS analysis

A total of forty-two compounds were identified in the essential oils of the seed and stem-bark of *Monodora myristica*. The seed oil contained twenty-two compounds while twenty compounds could be identified in the stem-bark oil (Table 1).

In the seed oil, germacrene-D-4-ol (25.48%), tricyclo[5.2.1(1,5)]dec-2-ene (13.35%),  $\delta$ -cadinene (11.09%) and linalool (15.10%) were the major constituents while the dominant constituents of the stem-bark oil were  $\gamma$ -cadinene (31.31%),  $\alpha$ -elemene (17.98%),  $\alpha$ -cubebene (6.70%) and  $\gamma$ -muurolene (5.94%). Caryophyllene and  $\gamma$ -muurolene were the only two constituents common to both the seeds and the stem-bark oils of *M.myristica*. tricyclo[5.2.1(1,5) dec-2-ene found in the seeds oil had not been previously reported.

**Table 1.** Chemical composition of the essential oils of seed and stem-bark of *Monodora myristica*

Chemical compounds	Retention times, <u>min</u>	Percentage composition (%)	
		Seeds	Stem-bark
$\gamma$ -terpinene	2.16	1.31	-
linalool	2.37	15.10	-
trans-p-menth-2-en-1-ol	2.49	1.23	-
cis-p-menth-2-en-1-ol	2.60	0.93	-
1,2,3,4-tetramethylcyclobutene	2.78	1.37	-
1,3-dimethyl-1-cyclohexene	2.81	0.92	-
$\alpha$ -terpineol	3.04	3.35	-
tricyclo[5.2.1(1,5)]dec-2-ene	3.21	13.35	-
hydroxymethyl furfuraldehyde	3.50	1.81	-
p-thymol	4.27	1.39	-
p-fluoroanisole	4.47	1.64	-
$\alpha$ -cubebene	5.80	-	6.70
$\alpha$ -bergamotene	5.99	-	1.31
caryophyllene	6.42	1.17	5.42
$\alpha$ -farnesene	6.84	-	1.87
$\alpha$ -guainene	7.01	0.77	-
$\beta$ -guainene	7.05	-	0.92
$\gamma$ -cadinene	7.16	0.80	-
$\gamma$ -muurolene	7.46	1.35	5.94
$\beta$ -pachoulene	7.80	2.10	-
1,2,4a,5,6,8a-hexahydro-4,7-dimethyl-1-(1-methylethyl)naphthalene	7.95	2.26	-
$\alpha$ -elemene	7.97	-	17.98
2-isopropyl-5-methyl-9-methylenebicyclo[4.4.0]dec-1-ene	8.22	6.73	-
$\delta$ -cadinene	8.46	11.09	-
$\gamma$ -cadinene	8.58	-	31.31
acoradiene	8.94	-	4.35
dehydroarionine (TDN)	9.06	-	0.96
cis-nerolidol	9.46	-	7.62
germacrene-D-4-ol	9.47	25.48	-
$\beta$ -germacrene	9.66	-	0.96
3-(4-methoxyphenylamino)pyrrolidine-2,5-dione	9.79	-	0.81
guaial	9.91	-	1.79
2, 2, 4, 8-tetramethyltricyclo[5.3.1.0(4, 11)]undec-8-ene	10.09	-	1.90
cadinadiene	10.44	-	3.00
copaene	10.72	-	2.71
$\alpha$ -cadinol	10.78	1.74	-
cadala-1(10), 3, 8-triene	11.02	-	0.93
$\alpha$ -bisabolol	11.53	-	1.16
4-(3-methyl-2-butenyl)-1H-indole	13.53	-	1.06
4-chloro-N, N-diethylbenzenamine	16.03	1.62	-

The presence of p-thymol would account for the antimicrobial activity<sup>9</sup> of the *M. myristica* seed oil while the presence of hydromethyl furfuraldehyde (HMF) may be an indicator to toxicity.<sup>10</sup> Literature reports on the chemical constituents of the seed essential oils of *M. myristica* in Nigeria present great variations (Table 2). C.C. Igwe et al. reported<sup>11</sup>  $\alpha$ -phellandrene epoxide (3.02%), carvacrol (2.09%) and  $\delta$ -cadinene (2.21%) as the major constituents of a Nigerian sample of *M. myristica* seed oil, Owolabi et al. reported<sup>12</sup> geranial(40.1%), neral (29.74%) and myrcene (11.3%) in yet another sample from Nigeria. While Onyenekwe et al. generated<sup>13</sup>  $\alpha$ -phellandrene (50.4%),  $\alpha$ -pinene (5.5%), myrcene (4.35%) and germacrene-D-4-ol (9.0%).

The oils of the seeds of *M. myristica* obtained now was similar to the oils of Owolabi's<sup>12</sup> and Onyenekwe's<sup>13</sup> oils, only the presence of  $\delta$ -cadinene (11.09%) and germacrene-D-4-ol (25.48%), respectively were the differences. The presence of myrcene also showed a little similarity between Owolabi's<sup>12</sup> and Onyenekwe's oils.<sup>13</sup> Igwe' oil<sup>11</sup> was completely different from the remaining three oils from Nigeria.

The reasons for this variation may possibly be the origin of the fruits, which were not certain in many cases; Owolabi et al (2009) purchased the seeds used for their analysis at Agege market in Lagos, Nigeria and presumed it to have originated from south west Nigeria.

**Table 2.** Comparison of the percentage (%) composition of the major components of the seeds essential oils of *Monodora myristica* variously reported from Nigeria.

Compounds	Lagos	Agege Lagos	Kaduna	Iwaro-Oka
$\alpha$ -phellandrene epoxide	3.02	-	-	-
$\alpha$ -phellandrene	-	-	50.4	-
carvacrol	2.09	-	-	-
$\delta$ -cadinene	2.21	-	-	11.09
geranial	-	40.1	-	-
neral	-	29.7	-	-
myrcene	-	11.3	4.35	-
germacrene-D-4-ol	-	-	9.0	25.48
$\alpha$ -pinene	-	-	5.5	-
linalool	-	-	-	15.10
tricylo[5.2.1.0(1,5)]dec-2-ene	-	-	-	13.35

Also the kind of treatments the fruits underwent after the harvest may be another important reason. In explaining this type of variation in the chemical constituents of *Xylopiya aethiopica* from Benin, Ayedoun et al.<sup>14</sup> explained that the  $\alpha$ -pinene and the sabinene could vary respectively from 4 to 16% and 3 to 36% according to whether the fruits were boiled or smoked before the drying.

In conclusion, the constituents of the seeds and stem-bark essential oils of *Monodora myristica* in this study were quite different chemically and the presence of hydromethyl furfuraldehyde in the seed oil raised some health concerns as this substance is toxic. The major composition of oils of *Monodora myristica* as reported from Nigeria were so different that one could not be sure whether this large differences were due to environmental, genetic or some procedural differences. Thus further studies would be required to determine these differences.

## References

- Fournier, G., Leboeuf, M., Cave, A. *J. Essential Oil Res.*, **1999**, *11*, 131.
- Okafor, J. C., *Forest Ecol. Manage.*, **1987**, *1*, 235.
- Ekeanyanwu, C. R., Ogu, L. G. and Nwachukwu U. P., *Agricult. J.*, **2010**, *5*(5), 303.
- Uwakwe, A. A. and Nwaoguikpe, R. N., *J. Med. Plant Res.*, **2008**, *2*(6), 110.
- Weiss, E. A., *Spice crops*. Oxon; CABI Publishing. **2002**, p. 102.
- Koudou, J., Etou Ossibi, A. W., Akikokou, K., Abenna, A. A., Gbeassor, M. and Bessiere, J. M., *J. Biol. Sci.*, **2007**, *7*, 937.
- Iwu, M. N. *Handbook of African medicinal plants*, CRC Press, Bole Ralvon and Arbour, Tokyo. **1993**, p. 244.
- British Pharmacopoeia* **1986**, vol.2., 109 HMSO. London.
- Ekundayo, O. *Planta Medica*, 1986, No.3, 200.
- Archer, M. C., Bruce, W. R., Chan, C. C., Medline, A., Stamp, D. and Zhang, X. M., *Proc. Am. Assoc. Cancer Res.*, **1992**, *33*, 130.
- Igwe, C. C., Yayi, E., Moudachirou, M. *Nigerian Food J.*, **2005**, *23*, 21.
- Owolabi, M. S., Oladimeji, M. O., Lajide, L., Singh, G., Mariwuthu, P., Isidorov, V. A., *EJEAF Chem.*, **2009**, *8*(9), 828.
- Onyenekwe, P. C., Ogbadu, G., Deslaurier, H., Gagnon, M. and Collin, G. J., *J. Sci. Food Agric.*, **1993**, *61*, 379.
- Ayedoun, A. M., Adeoti, B. S., Sossou, P. V., Leclerq, P. A., *Flavour and Fragrance*, **1996**, *J11*(4), 245.

Received: 17. Sept. 2012.

Accepted: 09. Oct. 2012.



# AN OVERVIEW OF WAX PRODUCTION, REQUIREMENT AND SUPPLY IN THE WORLD MARKET

Huang Wei<sup>[a]</sup>

**Keywords:** overview; wax production; requirement, world market

The productivity and demand of wax in the world market has been reviewed. The production and consumption of wax, candle and ranking of manufactures in the world market have also been discussed. The production capacity and importance of quantity of Chinese wax have also been a matter of evaluation. The complete development of wax products has resulted in good economic and social benefits around the world.

\* Corresponding Author

Fax: 86-24-56860869

E-Mail: huangwei20121006@hotmail.com

[a] Liaoning Shihua University, Fushun, Liaoning, P.R. China.

## INTRODUCTION

In an oil refinery, wax is one of the important chemical materials. It is white to pale-yellow in colour, gelatinous, crystalline and water-insoluble substance. Its main content consists n-paraffin. Its carbon number, molecular weight, distillation range and density are 16-32, 300-540, 350 °C - 500°C and 0.880-0.915, respectively.<sup>1</sup> Wax plays an important role in the global industrial processes such as lighting, packaging, farming, chemicals, rubber, medicine and in homecare products, etc. *China* is number 1 in production and consumption of wax in the world. The production and consumption of wax in *China* has reached to a tune of 16 and 7.81 million tons respectively in 2011.<sup>2</sup>

In the present paper, the production, consumption and requirement of wax and candles and the manufactures ranking in the world market have been reviewed, with a fact of comparison between the production capacity and import quality of the *Chinese* wax.

## DISCUSSION

### The output and consumption of wax in the world

Fan Xiaoya<sup>3</sup> introduced it as one of the suppliers to the output and requirement of wax in the countries such as *America*, *Canada*, *China*, *West European* area, other *Asian* countries (excluding *China*), *South America* and some other parts of the world. Table 1 shows the use of wax and its products such as candle, packaging, and synthetic wood, hot-melt adhesive, rubber, antirust additive, soap wax, man-made wood, makeup and other such materials. The total consumption of wax at global level has reached up to 3025 kt. The production of candles has also reached 1470 kt, which was almost half of the total wax production in the world. Candles are very popular for their use in lightening and decoration. However, the output and percentage of makeup materials has been raised to 38 kt and 1.3%, respectively. Table 2 shows production and consumption of wax around the world. *USA* and *Canada* top the list in production and consumption the world that are 930 kt and 940 kt, respectively. The export quality production of wax in *China* has now reached up to 300 kt per year. The excess amount of wax around the world was 95 kt per year.

**Table 1.** Consumption of wax around the world (kt)

Products	America and Canada	China	West Europe	Asian other areas	South America	Other areas	Total	Percentage, %
Candle	130	450	290	210	180	210	1470	48.6
Packaging	410	22	75	64	30	35	636	21.0
Synthetic wood	110	15	70	17	30	15	257	8.5
Hot-melt adhesive	54	8	36	12	2	2	114	3.7
Rubber	36	8	30	120	6	140	102	3.4
Antirust additive	45	6	35	14	1	1	102	3.4
Soap wax		70					70	2.3
Man-made wood	54		3				57	1.9
Makeup	27	100	6	1	1	2	38	1.3
Others	74	20	350	20	10	20	179	5.9
Total	940	600	580	350	260	295	3025	

**Table 2.** Production and consumption of wax in the world (kt)

Countries	Production	Consumption	Supply and Demand
USA/Canada	930	940	Import 10
China	900	600	Export 300
West Europe areas	640	580	Export 60
Asian other areas	190	350	Import 160
South America	180	260	Import 80
World other areas	280	295	Import 15
Total	3120	3025	Excess 95

### The consumption and requirement and manufactures ranking of the wax and candles around the world <sup>3</sup>

Table 3 shows the manufactures ranking of wax productivity around in the world. 24 manufactures are recorded till the end of the year 2011.

Total wax products amount has reached 62.93 million tons per year around the world. The wax output of CNPC and Sinopec in *China* was No.1 in the world. However, the wax output of Repsol and Cepsa Company in *Spain* only had 0.66 million tons.

Table 4 presents the consumption and requirement of wax and candle in 2011. *China* was one of the biggest wax production countries. However, the wax production of *Latin America* only had 2.60 million tons per year.

On the other hand *Asian* countries (excluding *China*) and *North America* have huge wax consumption market. They have a demand of about 12 million tons of wax production for their national markets. It has also been noticed that the consumption of candle in *China* was fourteen times of *North American* and *European* markets.

Table 5 shows production and import of *Chinese* wax. There were more distribution of waxes in Northeast of *China* such as *Yanshan, Dalian, Fushun, Jinxi* and *Daqing*. They were about half of the production of *Chinese* wax done by these areas collectively. It has also been noticed that the one fourth of the total *Chinese* wax production is done by those plants which are situated near seashore area. Food grade quality and completely refined wax were about 5% and 50% of *Chinese* total wax production, respectively.<sup>4</sup>

**Table 3.** Ranking of manufactures of wax products in the world (million tons)

Name of the Company	Countries and areas	Production
CNPC and Sinopec	China	16.33
ExxonMobil Corp.	USA, Canada and Europe	10.62
Shell Oil	Europe, Singapore and Malaysia	5.87
Sasol Wax	Europe and South Africa	5.45
Lukoil	Russia	3.45
Venezuela National Oil Company	Venezuela	2.12
IGI Company	USA and Canada	1.09
Petrobras	Brazil	1.60
H&R Chemisce	Germany	1.45
Flying J/BigWest Oil	USA	1.36
Calumet Lubricants Co.	USA	1.27
Naftowax	Poland	1.27
TOTAL	France	1.24
AGIP Petroli	Italy	1.24
Citgo Lubes & Waxes	USA	1.18
Petro-Canada Lubricants	Canada	1.20
Marathon Oil Corp.	USA	1.06
Nippon Siero Co.	Japan	0.85
BP,CORP.	England	0.82
Turkish Petroleum Company	Turkey	0.76
Sonneborn Products Company	USA	0.69
Ergon Regining Company	USA	0.69
Cepsa Company	Spain	0.66
Repsol Company	Spain	0.66
Grand Total (production)		62.93

**Table 4.** The consumption and requirement of wax and candles in the year 2011 (million tons)

Areas	Output	Consumption	Consumption of candle
North America	9.98	14.77	4.54
Europe	8.98	9.52	4.11
Latin America	2.60	5.32	2.66
Africa and the Middle East	-	-	3.05
Asia (including China)	20.5	19.81	4.60
China	16	7.81	59.90

**Table 5.** Production and import of Chinese wax (million tons)

Unit	Total output	Fully refined wax	Semi-refined wax	Food grade wax	Crude quality wax	Soap wax	Others	Import yield	Incremental yield
Yanshan	6.2367	0.2635	5.9672	0.0060				0.8100	2
Dalian	16.9049	3.6955	2.6429	5.0866	4.1347	1.3452		5.6456	3
Fushun	22.1638	5.4645	10.9573	0.2010	0.3275	5.2135		5.1944	15
Jinxi	3.2186		1.8001			1.4185		0.9557	
Daqing	13.0773	0.0140	12.6222	0.1779	0.2220	0.0552		8.9290	2
Gaojiao	10.8195	1.4019	6.4534		1.5655		1.3987		3
Jinan	1.0202				1.0202				
Luoyang	0.1541		0.1541						
Jingmen	7.5395		2.9824		0.7686		0.0324	1.4354	2
Maoming	8.1736		2.1812	0.0422		0.6720		4.3247	2
Lanzhou	2.8857		0.6064		0.7943	1.4850			10.5
Jiangnan	1.0429		0.9409		0.1020				
Qingdao	0.0007	0.0007							
Jilin	0.0829	0.0829							
Yumen	0.0643		0.0643						
Nangchong	0.4627		0.3594		0.1843				
Total	93.8478	10.9230	47.7318	5.5137	9.1191	10.1894	1.4311	27.2948	39.5

## CONCLUSION

Wax is used as high value product for energy reserve in the world. It not only provides various good products for general public, but increases petrochemical plant revenue also. It is an urgent need for *Chinese* scientists to expedite the technical innovation and advancements in good way so that one can improve the international competition ability of *Chinese* wax industries to satisfy market's requirement enterprises and to utilize wax sources in a reasonable.

## REFERENCES

- <sup>1</sup> Chang, Y. H. *Chem. Prod. Technol.*, **2002**, 9(6), 6.
- <sup>2</sup> Li, Y., Yang, G. M. and Wang M. *Shanghai Chem. Ind.*, **2007**, 32(1), 42.
- <sup>3</sup> Fan, X. Y. *Petrochemical Industry Trends*, **1999**, 7(2), 33.
- <sup>4</sup> Zhang, X. L. *Eur. Chem. Bull.*, **2012**, 1(6), 210.

Received: 07. 10. 2012.

Accepted: 11. 10. 2012.



# EXTRACTION OF Ni(II) IONS INTO CHCl<sub>3</sub> SOLUTION OF *N,N'*-ETHYLENEBIS(4-BUTANOYL-2,4-DIHYDRO-5-METHYL-2-PHENYL-3H-PYRAZOL-3-ONE IMINE) SCHIFF BASE

J. Godwin<sup>[a]</sup>, F. C. Nwadike<sup>[b]</sup> and B. A. Uzoukwu<sup>[c]</sup>

**Keywords:** Extraction, Nickel(II), *N,N'*-Ethylenebis(4-butanoyl-2,4-dihydro-5-methyl-2-phenyl-3H-pyrazol-3-one imine), Effect of pH and anions

The extraction of Ni(II) ions in aqueous media was studied using chloroform solution of *N,N'*-ethylenebis(4-butanoyl-2,4-dihydro-5-methyl-2-phenyl-3H-pyrazol-3-oneimine) (H<sub>2</sub>BuEtP) Schiff base as the organic extractant. The synergistic effect of 4-butanoyl-2,4-dihydro-5-methyl-2-phenyl-3H-pyrazol-3-one (HBuP) in these extractions were also investigated. The pH<sub>1/2</sub> of extraction of Ni(II) was significantly lowered from a near neutral pH 7.14 ± 0.10 to an acidic region of 5.51 ± 0.10 when a mixture of the ligands was used. The partition coefficient (log K<sub>DNiI</sub>) 1.89 ± 0.05 (H<sub>2</sub>BuEtP) was same as (log K<sub>DNi2</sub>) 1.89 ± 0.02 (H<sub>2</sub>BuEtP-HBuP) while the extraction constant (log K<sub>exNiI</sub>) -12.39 ± 0.64 (H<sub>2</sub>BuEtP) was slightly less than (log K<sub>exNi2</sub>) -10.57 ± 0.10 (H<sub>2</sub>BuEtP-HBuP). Data analysis indicated that Ni(II) distributed slightly better into chloroform solution of H<sub>2</sub>BuEtP/HBuP as Ni(HBuEtP)(BuP)<sub>(o)</sub> than into a solution of H<sub>2</sub>BuEtP as Ni(HBuEtP)<sub>2(o)</sub>. Mineral acids show a masking effect in the extractions in both ligand alone and mixed ligands systems while mixed ligands system was shown to be a better extractant system for Ni(II) ions in the presence of anions and auxiliary complexing agents studied. Acetate, fluoride, and phosphate ions gave the best percentage extractions and the extraction of Ni(II) ions with the ligand is more efficient at near neutral to basic pH

Corresponding author

Email [godwinj2012@gmail.com](mailto:godwinj2012@gmail.com)  
Tel.: +2348033401456

- [a] Department of Chemical Sciences, Niger Delta University, Wilberforce Island, PMB 71 Bayelsa State, Nigeria.  
[b] Department of Pure and Industrial Chemistry, University of Port Harcourt, Choba, Port Harcourt, Rivers State, Nigeria, Email: [nwadikefc@yahoo.com](mailto:nwadikefc@yahoo.com)  
[c] Department of Pure and Industrial Chemistry, University of Port Harcourt, Choba, Port Harcourt, Rivers State, Email: [uzoukwupob331@yahoo.co.uk](mailto:uzoukwupob331@yahoo.co.uk)

## Introduction

*Schiff bases* are compounds that contain the carbon-nitrogen double bond traditionally connected to an aryl or alkyl group. Earlier studies on isolation and characterization of metal complexes of *schiff bases* have shown that they are capable of forming stable metal complexes with Cu(II) and Ni(II) and unstable metal complexes with Mo(VI), Co(II) and Cd(II).<sup>1,2</sup> Derivatives of 1-Phenyl-3-methyl-4-acylpyrazolone-5 are known for their complexation reactions with transition metals forming metal complexes with interesting coordination chemistry.<sup>3,4,5,6</sup> Most of the current systems used for extracting metals work best mostly at acidic pH. However, natural waters are at near neutral to basic pH, and much of the currently stored wastes are at very caustic conditions. Thus, there is high demand for ligands that can extract over a wide range of pH.

In continuation of our earlier work on the synthesis, characterization<sup>7</sup> of 1-phenyl-3-methyl-4-acylpyrazolone-5 derivatives and extraction of metal ions with *N,N'*-ethylenebis(4-butanoyl-2,4-dihydro-5-methyl-2-phenyl-3H-pyrazol-3-oneimine) *Schiff base*, which has been successfully applied in the extraction of Lead(II)<sup>8</sup> and U(VI) ions<sup>9</sup>, we report the application of the present Schiff base derivative of 4-butanoylpyrazolone as a potential extractant for Nickel(II) ions. The synthesis provided an opportunity

for a N=C-C-OH bonding moiety and extended the scope of coordination to involve tetradentate ligands from the initial bidentate 4-acylpyrazolone.

In this study the solvent extraction of nickel(II) ions from aqueous media using *N,N'*-ethylenebis(4-butanoyl-2,4-dihydro-5-methyl-2-phenyl-3H-pyrazol-3-oneimine) was investigated. Extraction of metal ions with the *Schiff base N,N'*-ethylenebis(4-butanoyl-2,4-dihydro-5-methyl-2-phenyl-3H-pyrazol-3-oneimine) has attracted little attention in the literature. Thus, the synergistic effect of 4-butanoyl-2,4-dihydro-5-methyl-2-phenyl-3H-pyrazol-3-one with O=C-C=C-OH moiety on the distribution behaviour of Ni(II) into a solution of predominantly N=C-C-OH bonding species and the effect of pH, acids, anions and auxiliary complexing agents on the extraction of Ni(II) from aqueous solutions was investigated. The aim of the study was to evaluate the potentials of the *Schiff base N,N'*-ethylenebis(4-butanoyl-2,4-dihydro-5-methyl-2-phenyl-3H-pyrazol-3-oneimine) in the recovery of Ni(II) ions in aqueous media.

## Materials and Methods

### Reagents and Apparatus

*N,N'*-Ethylenebis(4-butanoyl-2,4-dihydro-5-methyl-2-phenyl-3H-pyrazol-3-oneimine) (H<sub>2</sub>BuEtP) was synthesized by methods reported earlier.<sup>7</sup> The ligand's purity after recrystallization from aqueous ethanol was established by elemental analysis for C, H and N; analysis of IR and NMR spectral data at the Institute for Inorganic Chemistry Technology, University of Dresden, Germany.

Stock solutions of 0.05 M H<sub>2</sub>BuEtP were prepared by dissolving appropriate amount of the ligand in CHCl<sub>3</sub>. Stock solutions of 0.05 M 4-butanoyl-2,4-dihydro-5-methyl-2-phenyl-3H-pyrazol-3-one (HBuP) were also prepared by

dissolving appropriate amount of the ligand in CHCl<sub>3</sub>. Stock solutions of 1.704 x 10<sup>-2</sup> M (1,000 mg/L) of Ni(II) were prepared by dissolving appropriate amount of ammonium nickel(II) tetraoxosulphate(VI) hydrate (2:1:2:6), (NiSO<sub>4</sub>·(NH<sub>4</sub>)<sub>2</sub>SO<sub>4</sub>·6H<sub>2</sub>O) in 0.1 mL of 10 M HNO<sub>3</sub> and making up to mark in a 50 ml volumetric flask with deionized water. Buffer solutions were prepared with 0.1M HCl/0.1 M NaCl (pH 1.0-2.9), 0.1 M acetic acid/0.1 M NaCl (pH 3.0-3.5), 0.1 M acetic acid/0.1 M Na-acetate (pH 3.6-5.6), and 0.1 M KH<sub>2</sub>PO<sub>4</sub>/0.1 M NaOH (pH 5.7-10.0). pH of the buffered solutions were determined with a Labtech Digital pH meter. Solutions of 0.001-3.0M mineral acid, 0.001 - 1.0M anions or 0.0005M - 0.5M auxiliary complexing agent concentrations were prepared by diluting appropriate volumes of stock solutions of mineral acids or sodium salts of anions or auxiliary complexing agent. All experiments were performed at ionic strength of 0.1 M (NaClO<sub>4</sub>).

### Extraction Procedure

2 mL aliquot of a buffer solution containing 8.52×10<sup>-4</sup> M (50 mg/L) of Ni(II) ions and the desired pH of solution was prepared in a 10 ml extraction container. For extraction studies involving mineral acid or complexing agents, 2 ml aliquot of solution containing 8.52×10<sup>-4</sup> M of Ni(II) ions and the desired mineral acid or complexing agent concentration was prepared in a 10 ml extraction container. An equal volume (2 mL) of chloroform solution of 0.05 M concentration of H<sub>2</sub>BuEtP or 0.05M H<sub>2</sub>BuEtP : 0.05 M HBuP (9:1 ratio by volume) was added and the mixture shaken mechanically for 30 minutes at room temperature of about 30 °C. A shaking time of 30 minutes was found suitable enough for attaining the equilibration. The phases were allowed to settle and separated. Concentration of Ni(II) ion in aqueous phase was determined with a Buck Scientific Atomic Absorption Spectrophotometer (AAS) 205 at wavelength of 232.0nm. Ni(II) ion concentration extracted into the organic phase was determined by the difference between the concentration of Ni(II) ion in aqueous phase before and after the extraction. Distribution ratio *D* was calculated as the ratio of metal ion concentration in the organic phase (*C<sub>o</sub>*) to that in the aqueous phase (*C*). Thus  $D = C_o/C$ .

## Results and Discussion

### Effect of buffer solutions

Extraction of Ni(II) from aqueous phase into an organic phase '(o)' containing the ligand H<sub>2</sub>BuEtP can be represented by equation



where H<sub>2</sub>BuEtP is a tetradentate ligand. It shows that the reaction should take place in the metal:ligand mole ratio of 1:1. Thus the extraction constant *K<sub>ex</sub>* can be represented by,

$$K_{ex} = \frac{[\text{Ni}(\text{BuEtP})_{(o)}][\text{H}^+]^2}{[\text{Ni}^{2+}][\text{H}_2\text{BuEtP}_{(o)}]} \quad (2)$$

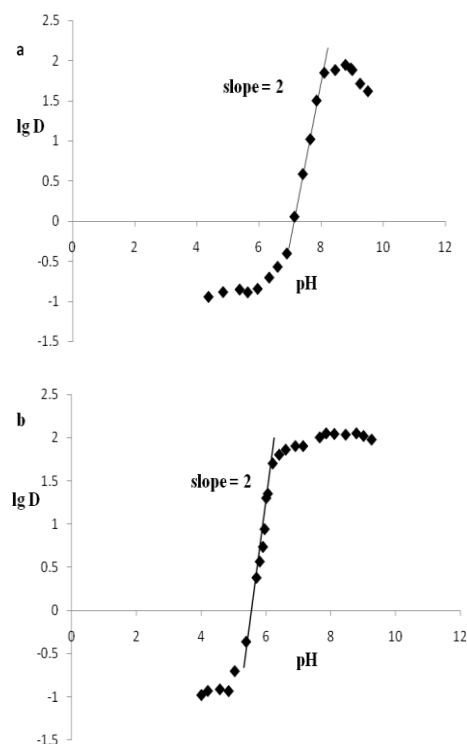


**Figure 1.** Plot of extraction of 8.52 x 10<sup>-4</sup> M Ni(II) from buffer solutions into (a) chloroform solution of 0.05 M H<sub>2</sub>BuEtP and (b) chloroform solution of 0.05 M H<sub>2</sub>BuEtP-0.05 M HBuP in the 9:1 ratio by volume

The distribution ratio  $D = [\text{Ni}(\text{BuEtP})_{(o)}]/[\text{Ni}^{2+}]$ . Substitution into equation (2) gives,

$$\lg D = \lg K_{ex} + \lg[\text{H}_2\text{BuEtP}] + 2\text{pH} \quad (3)$$

Extraction plots presented in Figure 1 show the effect of pH of solution on the distribution nature of Ni(II) into chloroform solutions of H<sub>2</sub>BuEtP and H<sub>2</sub>BuEtP-HBuP respectively. A slope of 2 was recorded in each of the graphs indicating that 2 moles of hydrogen ion was displaced during extraction in each of the different extraction systems. Slope analysis of extraction results presented in Figures 2a and 5a shows that one mole of the metal interacted with two moles of H<sub>2</sub>BuEtP. The probable reaction during the extraction process may therefore be represented as shown.



$$K_{Niex1} = \frac{[\text{Ni}(\text{HBuEtP})_{2(o)}][\text{H}^+]^2}{[\text{Ni}^{2+}][\text{H}_2\text{BuEtP}_{(o)}]^2} \quad (5)$$

The distribution ratio  $D = [\text{Ni}(\text{HBuEtP})_{2(o)}]/[\text{Ni}^{2+}]$ . Substitution into equation (5) gives,

$$\lg D_{\text{Ni1}} = \lg K_{\text{Niex1}} + 2\log[\text{H}_2\text{BuEtP}] + 2\text{pH} \quad (6)$$

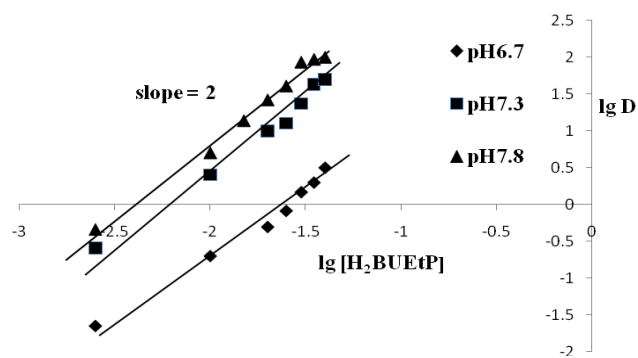


**Figure 2.** kgD-lg [H<sub>2</sub>BuEtP] plot of extraction of  $8.52 \times 10^{-4}$  M of Ni(II) from buffer solutions at constant pH of 6.7, 7.3, and 7.8 in the absence of synergist

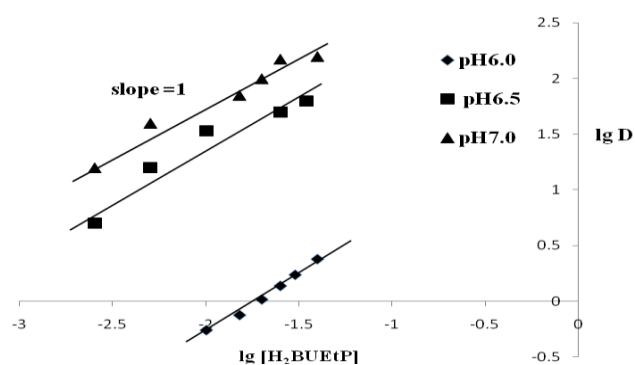


**Figure 3.** kgD-lg[H<sub>2</sub>BuEtP] plot of extraction of  $8.52 \times 10^{-4}$  M of Ni(II) from buffer solutions into chloroform solutions of ligands with [HBuP] kept constant ( $5 \times 10^{-3}$  M)

In this study, it was observed that the extraction of Ni(II) ion increased with an increase in pH and reached a maximum at pH of 8.78 after that further increase in pH resulted in a decrease in the percentage extraction of Ni<sup>2+</sup>. Quantitative percentage extraction of 98.87% was obtained at pH of 8.78. The partition coefficient  $K_{NiD1}$  is given by  $K_{NiD1} = [Ni(HBuEtP)_{2(o)}]/[Ni(HBuEtP)_2]$  for which a value of  $1.89 \pm 0.05$  was determined for  $\log K_{NiD1}$  from the graph. The  $pH_{1/2}$  was also found to be  $7.14 \pm 0.01$ . Data of all the extraction processes are recorded in Table 1.

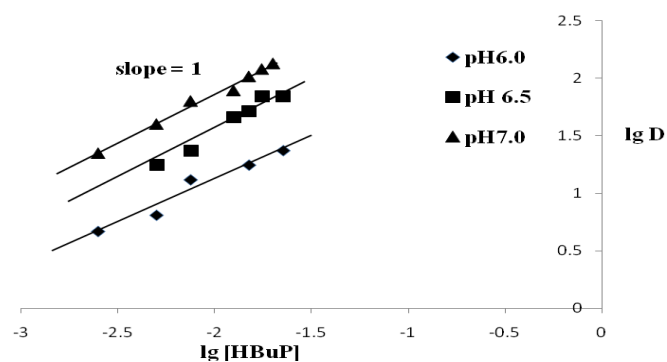


**Figure 4.** lgD-lg[HBuP] plot of extraction of  $8.52 \times 10^{-4}$  M of Ni(II) from buffer solutions into chloroform solution of ligands with [H<sub>2</sub>BuEtP] was kept constant ( $2.5 \times 10^{-2}$  M)

#### Effect of addition of HBuP on the distribution of Ni(II)

Quantitative percentage extraction of 99.11% at pH of 7.85 was obtained and there was a shift of  $pH_{1/2}$  to  $5.51 \pm 0.10$ , a

more acidic region indicating that extraction of Ni<sup>2+</sup> ions at lower pH values was more effective in chloroform solutions containing HBuP as a synergist. Uzoukwu et al<sup>10</sup> obtained a similar result from their studies on the effect of chloride ion (Cl<sup>-</sup>) concentration on Cu(II) and Ni(II) ions using 1-phenyl-3-methyl-4-trichloroacetylpyrazol-5-one. The partition coefficient  $K_{NiD2}$  is given by the equation of  $K_{NiD2} = [Ni(HBuEtP)(BuP)_{(o)}]/[Ni(HBuEtP)(BuP)]$ , for which a value of  $1.89 \pm 0.02$  that was statistically same with  $\lg K_{NiD1}$  was determined from the graph in Fig. 1b.

Plots of log D against pH in the mixed ligands system in figure 1b gave a slope of 2 indicating that 2 moles of hydrogen were displaced during the extraction process. Interaction between Ni(II) and H<sub>2</sub>BuEtP in the presence of HBuP at constant pH 6.0, 6.5 and 7.0 in fig 3 and fig 4 all gave a slope of 1 confirming 1 mole of both ligands were involved in the interactions. Combining these results with metal variation plots in the presence of synergist in figure 5b, the probable reaction during the extraction process can therefore be represented as;



$$K_{Niex2} = \frac{[Ni(HBuEtP)_{(o)}][H^+]^2}{[Ni^{2+}][H_2BuEtP_{(o)}]} \quad (8)$$

where [HBuP] is constant and incorporated in  $K_{Niex2}$ . The distribution ratio  $D_{Ni2} = [Ni(HBuEtP)_{(o)}]/[Ni^{2+}]$ , on substitution into Eqn. (8) gives,

$$\lg D_{Ni2} = \lg K_{Niex2} + \lg [H_2BuEtP] + 2pH \quad (9)$$

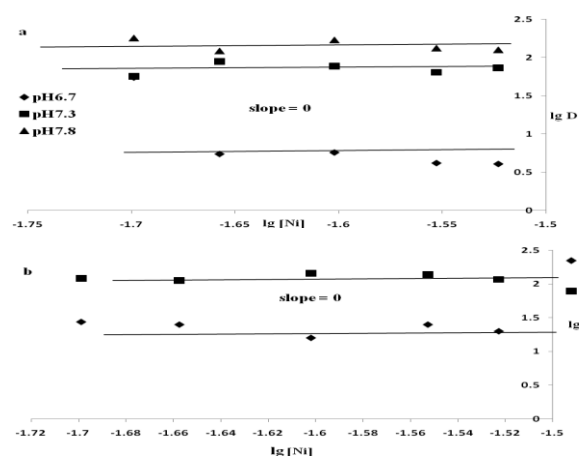


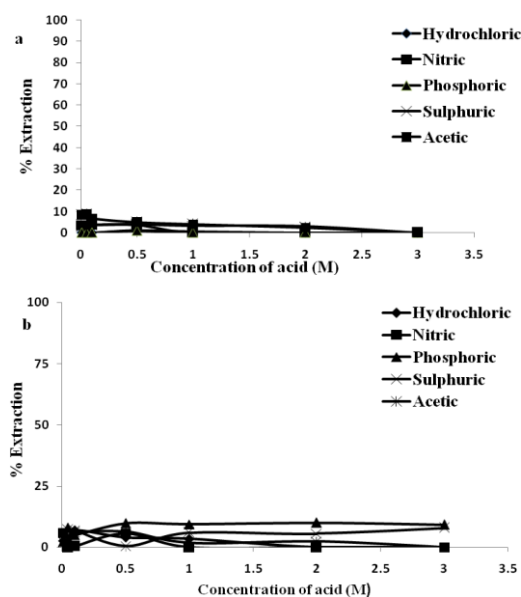
**Figure 5.** lg D-log [Ni(II)] plot of extraction of Ni(II) from buffer solutions into chloroform solutions of ligand 0.05 M H<sub>2</sub>BuEtP (a) mixture of 0.05 M H<sub>2</sub>BuEtP and 0.05 M HBuP in a 9:1 ratio

**Table 1.** Extraction data of the influence of pH of aqueous phase on the extraction of  $8.52 \times 10^{-4}$  M of Ni(II) into organic solutions of 0.05 M H<sub>2</sub>BuEtP and mixture of 0.05 M H<sub>2</sub>BuEtP-0.05 M HBuP (9:1) ratio at room temperature of 30 °C (ionic strength of 0.1 M NaClO<sub>4</sub>)

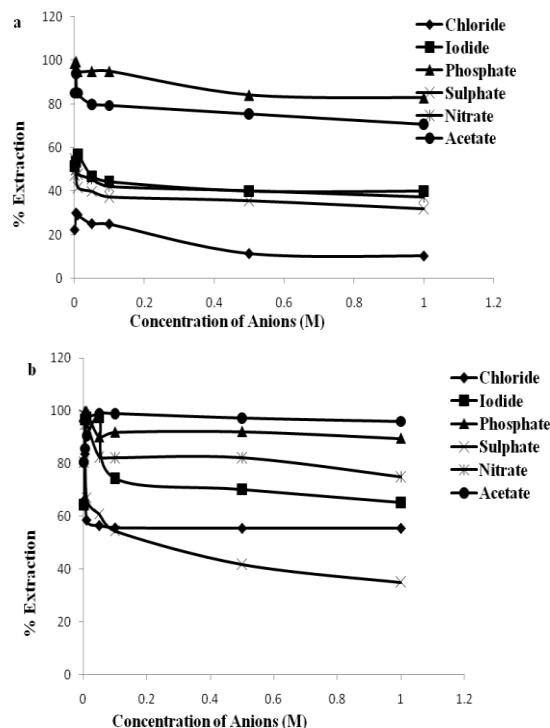
Organic Phase	lg K <sub>ex</sub>	pH <sub>½</sub>	lg K <sub>D</sub>	Species extracted
0.05 M H <sub>2</sub> BuEtP	-12.39 ± 0.64	7.14 ± 0.10	1.89 ± 0.05	Ni(HBuEtP) <sub>2(o)</sub>
0.05 M H <sub>2</sub> BuEtP-0.05 M HBuP (9:1) mixture	-10.57 ± 0.52	5.51 ± 0.10	1.89 ± 0.02	Ni(HBuEtP)(BuP) <sub>(o)</sub>

### Effect of mineral acids, anions and auxiliary complexing agents on the distribution of Ni(II)

Results presented in fig 6 show that extraction of nickel is masked in the presence of mineral acids as percentage extraction was less than 10% even in the presence of the HBuP at all concentrations of the various mineral acids used in this study as was observed in the extraction of Pb(II) with most mineral acids with same ligand system.<sup>8</sup> This can be attributed to the formation of unextractable hydrophilic ion pair nickel anionic species in acidic media even in the presence of H<sub>2</sub>SO<sub>4</sub> which could be responsible for poor percentage extractions in the acidic regions in plots of extraction of Ni(II) ions in buffered media shown in Fig 1.

**Figure 6.** Plot of % extraction of  $8.52 \times 10^{-4}$  M Ni(II) from mineral acid solutions into (a) 0.05 M H<sub>2</sub>BuEtP solution (b) 0.05 M H<sub>2</sub>BuEtP-0.05 M HBuP (9:1) solution

The effect of anions on the distribution of Ni(II) ions in Fig. 7 indicate that chloride ion show the least enhancing effect (with an highest % extraction of 30) in the extraction of Nickel with the ligand H<sub>2</sub>BuEtP while phosphate ion gave the highest percentage extraction (99.43%) of Ni(II). In most cases, at anion concentrations above 0.01M the percentage extraction starts to decrease. This trend was also observed in the mixed ligands organic phase. The results in fig 7b clearly show that a mixture of H<sub>2</sub>BuEtP- HBuP/CHCl<sub>3</sub> was a better extractant than H<sub>2</sub>BuEtP/CHCl<sub>3</sub> for Ni(II) ions, as the following increases in percentage extraction was

**Figure 7.** Plot of % extraction of  $8.52 \times 10^{-4}$  M Ni(II) from solutions of anions into (a) 0.05 M H<sub>2</sub>BuEtP solution (b) 0.05 M H<sub>2</sub>BuEtP-0.05 M HBuP (9:1) solution

observed; Cl<sup>-</sup> (29.18% to 58.71%), I<sup>-</sup> (56.8% to 97.5%), PO<sub>4</sub><sup>2-</sup> (95% to 99.9%), SO<sub>4</sub><sup>2-</sup> (41.83% to 67.05%), NO<sub>3</sub><sup>-</sup> (47.68% to 95.2%) and CH<sub>3</sub>COO<sup>-</sup> (85% to 90.59%) at 0.01M concentration of ions. Most of the results on the effect of these anions follow trends observed in the distribution of Pb(II) using the same ligand system.<sup>8</sup>

From the results presented in Fig 7, the influence of auxiliary complexing agents on the extraction of Ni(II) ions was not appreciable as all percentage of extraction was less than 50% at all concentrations of complexing agents used for the study except for F<sup>-</sup> ion at 0.5M when H<sub>2</sub>BuEtP only was used. There was an increase in % extraction when a mixed ligand H<sub>2</sub>BuEtP/HBuP organic phase was used as > 50% extraction of Ni(II) was obtained in all complexing agents except EDTA. The % extraction decreases at concentrations above 0.005M of complexing agents in both type of ligand system, except for fluoride and tartrate ions. For fluoride ion, the % extraction increases steadily from 44.1% at 0.0005M to 99.6% at 0.5M whilst, for tartrate, from 52.5% at 0.0005M to 70.3% at 0.1M.

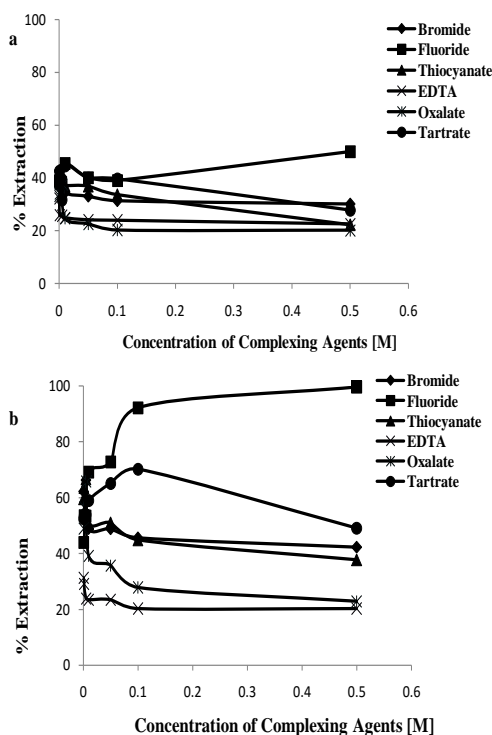


**Figure 8:** Plot of % extraction of  $8.52 \times 10^{-4}$  M Ni(II) from solutions of auxiliary complexing agents into (a) 0.05 M H<sub>2</sub>BuEtP solution (b) 0.05 M H<sub>2</sub>BuEtP-0.05 M HBU P (9:1) solution

H<sub>2</sub>BuEtP solution (b) 0.05 M H<sub>2</sub>BuEtP-0.05 M HBU P (9:1) solution

## Conclusion

The study on the distribution of Ni(II) in buffered medium with chloroform solution of H<sub>2</sub>BuEtP alone and H<sub>2</sub>BuEtP/HBU P mixture show that the  $pH_{1/2}$  shifted from  $7.14 \pm 0.10$  in H<sub>2</sub>BuEtP alone to an acidic region of  $5.51 \pm 0.10$  in a mixture of the ligands system. The partition coefficients were; H<sub>2</sub>BuEtP alone  $K_{NiD1} 1.89 \pm 0.05$  and H<sub>2</sub>BuEtP/HBU P mixture  $K_{NiD2} 1.89 \pm 0.02$ , indicating that in buffered media there was no noticeable difference in the distribution of Ni(II) ions into H<sub>2</sub>BuEtP alone as Ni(HBU EtP)<sub>2(o)</sub> and into H<sub>2</sub>BuEtP/HBU P mixture as Ni(HBU EtP)(BU P)<sub>(o)</sub>. The extraction constant  $\log K_{exNi1} -12.39 \pm 0.64 < \log K_{exNi2} -10.57 \pm 0.52$  indicates that H<sub>2</sub>BuEtP/HBU P mixture was slightly a better extractant in buffered media than H<sub>2</sub>BuEtP alone.

All mineral acids used for the study show less than 10% extraction of Ni(II) in both H<sub>2</sub>BuEtP alone and mixture of ligands H<sub>2</sub>BuEtP/HBU P organic phases as against the above 50% in almost all the anions except chloride ion in H<sub>2</sub>BuEtP alone. Combining this observation with % extraction of Ni(II) ions with the ligand in buffered media,

we conclude that extraction of Ni(II) ions with the ligand alone or its mixture with HBU P is better in alkaline medium.

From results of the effect of anions and auxiliary complexing agents on the extraction of Ni(II) ions, we may confirm that the mixture of ligands H<sub>2</sub>BuEtP/HBU P was a better extractant for Ni(II) ion than H<sub>2</sub>BuEtP alone collaborating the calculated physicochemical parameter values from distribution of Ni(II) ions in buffered media.

Though extraction of Ni(II) ions can be obtained in acidic pH between 4 – 6 with a mixture of the ligands, the optimal conditions for the extraction of Ni(II) ions was in the mixture of ligands H<sub>2</sub>BuEtP/HBU P organic phase in the presence of phosphate ion at  $\leq 0.01$ M, acetate ion at  $\leq 0.1$ M and fluoride ion at  $\leq 0.5$ M in near neutral to alkaline condition were  $\geq 99\%$  extraction of Ni(II) ions was obtained.

## Acknowledgement

The authors wish to thank the University of Port Harcourt, Alexander von Humboldt Stiftung, Germany and Prof. Karsten Gloe for research assistance to BAU.

## References

- <sup>1</sup>Uzoukwu, B. A.; Gloe, K.; Duddeck, H. *Synth. React. Inorg. Met.*, **1998**, *2*(5), 819.
- <sup>2</sup>Amarasekara, A. S.; Owereh, O. S.; Lyssenko, K. A.; Timofeeva, T. V. *J. Struct. Chem.*, **2009**, *50*(6), 1159.
- <sup>3</sup>Maurya, R. C., Mishra, D. D., and Trivedi, P. K. *Synth. React. Inorg. Met.*, **1994**, *24*, 17.
- <sup>4</sup>Uzoukwu, B. A.; Gloe, K.; Menzel, M., Rademacher, O. Z. *Anorg. Allg. Chem.*, **2001**, *627*, 103.
- <sup>5</sup>Xiao-yuan, C.; Shu-zhong, Z.; Qing-jin M. *Transit. Met. Chem.*, **1996**, *21*, 345.
- <sup>6</sup>Uzoukwu, B. A.; Al-Juaid, S.S.; Hitchcock, P. B.; Smith, J. D. *Polyhedron*, **1993**, *12*(22), 2719.
- <sup>7</sup>Uzoukwu, B. A.; Gloe, K.; Duddeck, H. *Indian J. Chem. A.*, **1998**, *37B*, 1180.
- <sup>8</sup>Godwin, J and Uzoukwu, B. A. *IOSR-JAC*, **2012**, *1*(3,) 14
- <sup>9</sup>Godwin, J and Uzoukwu, B. A. *Int. J. Chem. (Toronto, ON, Can.)*, **2012**, *4*(4), 105
- <sup>10</sup>Uzoukwu, B. A., and Mbonu J. I. *Solvent. Extr. Ion Exch.* **2005**, *23*, 750

Received: 01.10.2012.

Accepted: 15.10.2012.



# APPLICATION OF MULTIVARIATE REGRESSION MODELS IN CHROMATOGRAPHY. NEW ADVANCES.

Tibor Cserhádi<sup>[a]</sup> and Mária Szógyi<sup>[a]</sup>

**Keywords:** multivariate regression; retention behavior, retention-structure relationships

The aims of the review are the collection, concise description and evaluation of the multivariate mathematical-statistical methodologies used for the elucidation of the similarities and dissimilarities among retention parameters measured under various chromatographic conditions and the determination of the relationship between the physicochemical parameters and chromatographic retention behaviour of solutes.

\* Corresponding Authors

Fax: +36-1-3257554

E-Mail: szogyim@t-online.hu

[a] Research Centre for Natural Sciences, Hungarian Academy of Sciences, H-1025, Budapest, Pusztaszeri u. 59-67, Hungary

## Introduction

Chromatographic technologies have been developed and successfully applied for the analysis of a considerable number of organic and inorganic compounds of different molecular mass even present in complicated accompanying matrices at the trace level.

The rapid development of the capacity of personal computers and the corresponding softwares allowed the reliable evaluation of chromatographic retention data measured under different conditions (application of a wide variety of stationary and mobile phases), etc. The extraction of maximal information of large data sets is practically impossible by the application of the traditional linear regression model. Multivariate regression technologies overcome this difficulty making possible the simultaneous evaluation of a considerable number of variables and observations.

## Theoretical studies

The number of papers dealing with the development and application of various MLR techniques is rapidly growing. These methods improve the separation capacity and information content of the chromatographic separation process. Thus, multivariate statistical methods and pattern recognition methods were developed for the detection of differential protein expression from pre-processed LC-MS data.<sup>1</sup>

The modification of the three-way PARAFAC model has also been recently reported.<sup>2</sup>

## Health care

The relationship between the carotid and femoral plaque burden and the  $\alpha$ -linolenic acid (ALA) proportion of serum phospholipids in subject with primary dyslipidemia has been investigated in detail. The investigations were carried out by using gas chromatographic (GC) technique for the assessment of fatty acid composition of serum phosphatidylcholine and various methods for the study of plaque outcomes (frequency, number, maximum height and sum of plaque height). The results were evaluated by multivariate regression analysis. Before analysis the data were adjusting for age, gender, lipid genotype, smoking, hypertension, diabetes mellitus, BMI, APOE4 genotype, prior station treatment. Calculations indicated that the concentration of ALA in serum phosphatidylcholine and plaque formation in carotid and femoral arteries is negatively correlated. The consumption of ALA enriched foods is proposed.<sup>3</sup>

The level of p-cresylsulfate and indoxyl sulfate was determined at different stages of chronic kidney disease (CKD) using ultra performance liquid chromatography and the relationship between the concentration of toxic compounds and biological parameters was elucidated by multivariate regression analysis. It was established that the amount of p-cresylsulfate and indoxyl sulfate was highly correlated in the samples. It was further found that the concentration of p-cresylsulfate and indoxyl sulfate increased linearly with the decline of renal function.<sup>4</sup>

The compounds 4-(methylnitrosamino)-1-(3-pyridyl)-1-butanone (NNK) and its metabolite 4-(methylnitrosamino)-1-3-pyridyl-1-butanol (NNAL) were analysed using liquid chromatography-tandem mass spectrometry. The investigators were motivated by the fact that both NNK and NNAL are considered as biomarkers for cigarette smoking. The objective of the investigation was the elucidation of the impact of NNK and NNAL on the urothelial carcinoma (UC) risk. The relationship between chromatographic and biological parameters was assessed by multivariate logistic

regression. It was concluded from the data that the amount of NNK and NNAL in urine be used for the detection of urothelial risk.<sup>5</sup>

Gas chromatography combined with mass spectrometry (GC-MS) has been used for the elucidation of socioeconomic factors on exposure to persistent organic pollutants such as organochlorine pesticides (OCPs). The relationship between the GC-MS results and the maternal social class was elucidated by multivariate regression analysis. Calculation revealed that the amount of OCPs in placenta markedly depended on the maternal social class.<sup>6</sup>

The prenatal exposure to OCPs has been investigated in detail. Gas chromatographic technique was applied for the analysis of OCPs, and the level of thyroid-stimulating hormone (TSH) was measured in 220 placentas. Multivariate regression analysis was employed for the elucidation of the relationship between pesticide exposure and neonatal TSH levels. The calculations indicated that endrin, encosulfan-sulfate, hexachlorobenzene, and p,p'-DDE exerted a marked influence of the TSH level, while the other pesticides showed no activity.<sup>7</sup>

Simple linear and stepwise multiple linear regressions were employed for the determination of the correlations between urinary catechol levels and some physicochemical parameters. The concentrations of noradrenaline, adrenaline and dopamine were assessed by high performance liquid chromatography (HPLC). Regression models were applied for the elucidation of the relationships between catecholamine levels and age, gender, BMI z-score, systolic BP z-score, diastolic BP z-score, and apnea hypopnea index (AHI). Significant relationships were found between noradrenaline and AHI ( $r=0.32$ ) and age ( $r=-0.20$ ,  $p<0.05$  for both), between adrenaline and AHI ( $r=0.27$ ) and age ( $r=-0.25$ ,  $p<0.05$  for both). Systolic BP z-score and diastolic z-score correlated with adrenaline ( $r=0.22$  and  $r=0.20$ , respectively,  $p<0.05$  for both). Multivariate methods established that AHI was a significant independent predictor of noradrenaline, similarly only AHI and age were significant predictors of adrenaline.<sup>8</sup>

Multivariate logistic regression analysis was applied for predicting prostate cancer (CaP). The parameters included in the calculations were results of Western blot, liquid chromatography mass spectrometry, expression patterns of PCA3, and TMPRSS2. Calculations indicated that the combination of single biomarkers such as prostate-specific antigen, gene-based, protein-based and metabolite-based markers can be employed for the earlier detection of CaP.<sup>9</sup>

Multivariate logistic regression has also found application in the early detection of hepatocellular carcinoma (HCC) one of the most common malignancies in the world. Samples were analysed by two-dimensional gel electrophoresis and HPLC. Control patients, patients with liver cirrhosis and HCC were included in the experiments. It was established that the application of multivariate logistic regression for the evaluation of various biochemical and biophysical data sets increase considerably the efficacy of the detection of CaP.<sup>10</sup>

The presence of acrylamide metabolised in workers exposed to acrylamide (AA) was measured using liquid chromatography-electron ionization/tandem mass

spectrometry (LC-ESI-MS/MS). The metabolites included in the investigations were N-acetyl-S-(2-carbamoyl-ethyl)-cystein (AAMA), N-acetyl-S-(1-carbamoyl-2-hydroxyethyl)-cystein (GAMA2) and N-acetyl-S-(carbamoyl-2-hydroxyethyl)-cystein (GAMA3). The enzymes involved in the detoxification process were cytochrom P450 2E1 (CYP2E1), microsomal epoxide hydrolase (mEH) in exon 3 and exon 4, glutathione transferase  $\theta$  (GSTT1) and  $\mu$  (GSTN1). It was concluded from the data that GSTM1 genotypes modify considerably the excretion of urinary AAMA.<sup>11</sup>

The correlation between the concentration of asymmetric dimethylarginine (ADMA) in plasma has been investigated by using HPLC combined with multivariate analysis. The measurements and calculation indicated that the concentration of ADMA was significantly higher in patients with significant coronary artery disease (CAD). Furthermore, calculations revealed that plasma ADMA level is a significant independent risk factor.<sup>12</sup>

Helix pomatia agglutinin binding glycoproteins (HPA) were isolated from specimens of various thyroid tumors and analysed by affinity chromatography, SDS-PAGE and western blotting. The data were analysed by Cox regression analysis. The investigations were motivated by the possible effect of HPA on cellular glycosidation and found considerable differences between the profile of HPA-binding glycoproteins of specimens of various thyroid tumors.<sup>13</sup>

The influence of the concentration of N-acetylaspartate NAA on the amyotrophic lateral sclerosis (ALS) has been studied by using liquid chromatography mass spectrometry and multivariate logistic regression analysis. Regression analysis proved the strong relationship between the serum NAA level and the presence of ALS. The results suggest that serum NAA may be a useful biomarker.<sup>14</sup>

A GC-MS method was employed for the determination of the metabolic profile of Type 2 diabetes mellitus using multivariate resolution method and Monte Carlo PLS—DA. Metabolites suitable as biomarkers were lactate, alanine,  $\alpha$ -hydroxybutyric acid, phosphate seine, pyroglutamic acid, palmitic acid, stearic acid, palmitic acid, 1-monopalmitin and cholesterol.<sup>15</sup>

## Pharmaceuticals

Multivariate regression methods have been frequently used for the evaluation of the chromatographic analysis of pharmaceuticals. Thus, the simultaneous detection and quantitation of paracetamol (PAR) pseudoephedrin hydrochloride (PSE), and dextromethorphan hydrobromide (DEX) in tablets was reported. As the spectrograms of the analytes were considerably overlapping the data were evaluated by PCA and principal component regression (PCR). The calculations proved that the multivariate methods make possible the correct separation of analytes. The recoveries were between 0.961–100.2% and 97.1–100.4%, the relative error of prediction was 0.5–6.7 and 0.8–7.0% for PLS and PCR, respectively. The results obtained by HPLC and the multivariate methods were not significantly different. It was established that the method

applies a simple mobile phase and shorter analysis time, does not require internal standard and gradient elution.<sup>16</sup>

A HPLC technology was applied for the simultaneous determination of clavulanic acid (CA) and amoxicillin (AMO). Analytes were detected using Fourier transform technique coupled with ATR/FTIR. The data were analysed by using various calibration model such as PLS, interval PLS (iPLS), synergy PLS (siPLS), and backward PLS (biPLS). Multiplicative scatter correction and mean centering produced the best models. Relative standard error of prediction were 3.8 and 5.1 % for CA and AMO %, respectively. It was stated that the method can be applied for the simultaneous analysis of CA and AMO in commercial pharmaceutical products.<sup>17</sup>

HPLC-DAD coupled with partial least squares multivariate calibration was applied for the simultaneous determination of potassium guaiacol sulfonate (PG), guaifenesin (GU), diphenhydramine HCl (DP) and carbetapentane citrate (CP) in syrups. It was stated that the new HPLC-DAD method applies a simple mobile phase and shorter separation time. It was further established that the method does not require internal standard and gradient elution.<sup>18</sup>

Chromatographic profiling and multivariate analysis was applied for the screening and quantifying the contributions from individual components of traditional Chinese medicine. It was established that the method is suitable for the assigning bioactivity to individual components in extracts from natural products.<sup>19</sup>

A chromatographic and spectroscopic data fusion analysis was developed for the study of photodegradation processes. Results of HPLC-DAD-MS and UV-Vis were evaluated by hybrid hard- and soft modelling multivariate curve resolution. The photodegradation of ketoprofen was investigated with this method. Four degradation products were identified: (3-(1-hydroperoxyethyl)benzophenone, 3-acetylbenzophenone, 3-(1-hydroxyethyl)benzophenone and 3-ethylbenzophenone). The method was proposed for the study of photodegradation processes.<sup>20</sup>

## Food and food products

Quantitative structure-retention relationship methods were employed for the study of the correlations between molecular structure and retention behavior of essential oils. The calculations included genetic algorithm and multiple linear regression (GA-MLR), partial least square (GA-PLS), kernel PLS (GA-KPLS) and Levenberg-Marquardt artificial neural network (L-MANN). The correlation coefficients between the measured and calculated characteristic were in each case significant: GA-MLR 0.886; GA-PLS 0.912; GA-KPLS 0.937; and L-MANN 0.964.<sup>21</sup>

Similar calculations were carried out on a matrix of retention indices of essential oils. It was established that GA-KPLS can be applied as an alternative modeling tool for Quantitative Structure Retention (QSRR) studies<sup>22</sup>

The GC retention indices of 100 components of essential oils were measured on three GC columns of different polarity. QSRR models such as ridge regression, PLS, Kernel orthogonal projection to latent structure (KOPLS) were

developed for the elucidation of the relationship between calculated molecular parameters and retention parameters. It was found that linear model using only one variable (solvation energy) explains 95 – 94 % of variance. The application of PLS and ridge regression resulted in elevated predictive power.<sup>23</sup>

Various analytical technologies were employed for the following of the ageing of Madeira wines. The methods included were UV-vis, GC-MS, and HPLC-DAD. The volatile and phenolic composition of the samples were separately determined. Multivariate prediction models were used by applying PLS regression to each chemical data set. The calculations indicated that the complicated GC-MS and HPLC-DAD methods are leading to more precise results, however, UV-vis can also be applied for the prediction of the age of Madeira wines.<sup>24</sup>

Stir bar sorptive extraction method (SBSE) coupled to GC/MS was employed for the separation and quantitative determination of the composition of the aroma profile of Sherry brandies. Analysis of variance indicated that some volatile compounds show considerable differences. Principal component analysis (PCA) established that only one sherry differed markedly from the others. Partial least squares discriminant analysis (PLS-DA) proved the capacity of the method to discriminate among samples. The results of linear discriminant analysis were highly similar.<sup>25</sup>

Quantitative structure-property relationships technologies (QSPR) were developed for the prediction of the lipophilicity of food preservatives employing MLR and genetic algorithm (GA) methodologies. Parameters included in the calculations were theoretical molecular descriptors and experimental chromatographic data. The molecular descriptors were calculated using the DRAGON package. It was established that molecular descriptors such as information indices, topological, 3D-MORSE and WHIM descriptors are suitable for the prediction of the lipophilicity of food preservatives. It was further established that atomic polarizabilities, atomic Sanderson electronegativities and atomic van der Waals volume of the molecules have the highest predictive power.<sup>26</sup>

HPLC and attenuated total reflectance (ATR) Fourier transform infrared (FT-IR) spectroscopy followed with multivariate analysis were applied for the separation and quantitative determination of quercetin-3,4'-O-diglucoside (3,4'-Qdg) and quercetin-4'-O-glucoside (4'-Qmg) in onion. It was established that the results obtained by HPLC and ATR FT-IR were well correlated ( $R < 0.95$ ). Cross-validated (leave-one-out) partial least-squares regression (PLSR). It was further established that this calculation method can be successfully used for the prediction of the concentration of analytes. The data were also evaluated by PCA, discriminant function analysis and soft independent modeling of class analogue method. It was concluded from the data that the ATR FT-IR procedure requires less sample preparation than the traditional HPLC analysis.<sup>27</sup>

The relationship between methane production of cattle and the fatty acid (FA) production was elucidated by using GC. The data were evaluated by using univariate mixed model regression technique. The calculations suggested that milk FA profiles can be employed for the prediction of methane production in dairy cattle.<sup>28</sup>

GC has also found application in the study of the composition of volatile compounds influencing the sensory and fruit attributes of kiwi fruit. The chromatographic retention data were evaluated by multivariate mathematical-statistical methods (PCA and MLR). It was stated that the method is suitable for the identification of compounds with marked sensory activity.<sup>29</sup>

The biological activity of various green tea cultivars was investigated by combining HPLC measurements with the evaluation of the data with PCA and orthogonal partial least-squares-discriminant analysis (OPLS-DA). It was established that metabolic profiling can be successfully employed for nutraceutical evaluation of tea cultivars.<sup>30</sup>

GC-MS followed with PCA and PLS was employed for the elucidation of the relationships between Godello white wine sensory properties and its aromatic fingerprinting. Calculations indicated that ethyl ethers and acetates accounted 55.1 % of the odour activity values (fruity); spicy (fatty acids, 35.3 %) and floral aroma (terpenes, 3.1 %). It was found that the main aroma components were fruity and floral aromas (floral, apple and citrus).<sup>31</sup>

## Environmental studies

The complex composition of environmental samples made necessary the application of various multivariate methods for the evaluation of complicated chromatographic retention profiles. Thus, various analytical methods were employed for the study of biological wastewater treatment plants (WWTP). The considerable number of measured parameters were evaluated by various multivariate mathematical statistical methods such as PCA, and multivariate regression analyses. Size exclusion chromatography was employed for the determination of extra-cellular polymeric substances (EPS), the internal structure was observed by confocal laser scanning microscopy. The main characteristics of the paper mills were the EPS production, the presence of nitrification process and the presence of H<sub>3</sub>PO<sub>4</sub>.<sup>32</sup>

Computational molecular descriptors were employed for the prediction of the chromatographic lipophilicity of some pesticides and polycyclic aromatic hydrocarbons (PAH). Measurements of lipophilicity were carried out by HPLC using various stationary phases (C18, C8, CN, and Phenyl) and methanol and acetonitrile organic modifiers. The results were evaluated by the traditional multivariate analysis and genetic algorithm. The calculations revealed that quantitative structure property relationship can be employed for the prediction of the lipophilicity of these types of analytes.<sup>33</sup>

Comprehensive two dimensional gas chromatographic method was developed for the determination of the distillation points and relative density of gasoline and similar fuels. These parameters are important for the quality control of gasoline. The new method employs two GC columns with flame ionization detection (FID). The data were evaluated by multivariate analysis. It was established that the root mean square prediction differences (RMSPD) were 0.85%, 0.43%, 1.07%, and 1.71% for 10, 50, and 90% v/v of distillation.<sup>34</sup>

Various multivariate mathematical statistical methods were applied for the prediction of the retention behavior of nitrobenzene derivatives. Quantitative structure-retention relationship calculations (QSSR) included MLR, PLS, and ANN techniques. Multivariate image analysis (MIA) descriptors were evaluated by correlation ranking-principal component regression (CR-PCR) and correlation ranking principal component artificial neural network (CR-PC-ANN). It was established that the separation power of CR-PC-ANN method was the highest the R<sup>2</sup> values varying between 0.989, 0.999, and 0.999.<sup>35</sup>

Gas chromatography coupled with multivariate evaluation technologies was employed for the estimation of the age of weathered volatile organic compounds. The aging process was followed with GC measurements. The evaluation of the chromatograms was carried out by using different multivariate technologies such as non-linear PLS (PolyPLS), partial least squares discriminant analysis (PLSDA) and locally weighted regression (LWR). The prediction capacity of calculation methods was evaluated according to the root mean square error prediction (RMSEP). The results suggested that LWR has the highest predictive power and can be employed for the estimation the age of more complicated light petroleum mixtures such as gasoline.<sup>36</sup>

A two-dimensional GC method was applied for the study of the profile of weathered gasoline samples. The data were evaluated by various mathematical-statistical techniques such as PLS, PolyPLS, LWR, and partial least squares discriminant analysis. Calculations indicated that the best results can be achieved by the application of LWR method.<sup>37</sup>

The retention behaviour of 50 phenol derivatives was studied in a dual-capillary column system containing SE-54 and OV-17 bonded phase. The correlation between structure and retention of analytes was elucidated by using various quantitative structure, retention calculation techniques such as MLR, PLS, and ANN. It was stated that models with low standard errors and high correlation coefficients can be developed for the prediction of the retention behaviour of this class of phenol derivatives. The squared regression coefficients of prediction for the MLR, PLS and ANN models for DB-5 column were 0.9645, 0.9606, and 0.9808, respectively, while on DB-17 column the respective squared regression coefficients were 0.9757, 0.9757, and 0.9875. It was stated that non-linear model can be successfully employed for the description between structural descriptors and the chromatographic retention behavior of this class of analytes.<sup>38</sup>

## Abbreviations

AAMA	N-acetyl-S-(2-carbamoyl-ethyl)-cystein
ADMA	asymmetric dimethylarginine
ALA	$\alpha$ -linoleic acid;
AMO	amoxicillin
ATR	attenuated total reflectance
CAD	coronary artery disease
CA	clavulanic acid
CaP	prostate cancer

CHD	coronary heart disease		
CKD	chronic kidney disease		
CR-PC-ANN	correlation ranking-principal component artificial neural network		
CR-PCR	correlation ranking-principal component regression		
DAD	diode array detector		
FA	milk fatty acid profile		
FID	flame ionization detection		
FT-IR	Fourier transform infrared spectroscopy		
GA	genetic algorithm		
GC	gas chromatography		
GC-MS	gas chromatography mass spectrometry		
HCC	hepatocellular carcinoma		
HPLC	high performance liquid chromatography		
biPLS	backward PLS		
iPLS	interval PLS		
siPLS	synergy PLS		
KOPLS	Kernel orthogonal projection to latent structure		
KPLS	kernel partial least square		
L-MANN	Levenberg-Marquardt artificial neural network		
LWR	locally weighted regression		
MLR	multiple linear regression		
NAA	N-acetylaspartate		
NNK	4-(Methylnitrosamino)-1-(3-pyridyl)-1-butanone		
NNAL	1-(3-pyridyl)-1-butanol (NNAL)		
OCPs	organochlorine pesticides		
OPLS-DA	orthogonal partial least-squares-discriminant analysis		
PCA	principal component analysis		
PCR	principal component regression		
PLS	partial least squares		
PLS-DA	partial least squares		
PLSR	partial least-squares regression		
PolyPLS	nonlinear PLS		
QSPR	quantitative structure-property relationship		
QSRR	quantitative structure retention relationship		
RMSEP	root mean square error of prediction		
RMSPD	root mean square prediction differences		
SBSE	stir bar sorptive extraction method		
TSH	thyroid-stimulating hormone		
TVR	clinically-driven target vessel revascularization		

## References

- <sup>1</sup> Varghese, R. S., Resson, H. W., *Bioinform. Comparative Proteomics*, **2011**, *694*, 139-150.
- <sup>2</sup> Sajjadi, S. M., Abdollahi, H., J., *Chemometrics*, **2011**, *25*, 169-182.

- <sup>3</sup> Sala-Vila, A., Cofan, M., Nunez, I., Gilabert, R., Junyent, M., Ros, E., *Atherosclerosis*, **2011**, *214*, 209-214.
- <sup>4</sup> Lin, C. J., Chen, H. H., Pan, C. F., Chuang, C. C., Wang, T. J., Sun, F. J., Wu, C. J., *J. Clin. Lab. Anal.*, **2011**, *25*, 191-197.
- <sup>5</sup> Chung, C.J., Lee, H. L., Yang, H. Y., Haiu-Yuan, Lin, P. P., Pu, Y. S., Shiue, H. S., Su, C. T., Hsueh, Y. M., *Sci. Total Environ.*, **2011**, *409*, 1638-1642.
- <sup>6</sup> Freire, C., Amaya, E., Fernandez, M.F., Gonzalez-Galarzo, M. C., Ramos, R., Molina-Molina, J. M., Arrebola, J. P., Olea, N. *Chemosphere*, **2011**, *83*, 831-838.
- <sup>7</sup> Freire, C., Lopez-Espinosa, M. J., Fernandez, M., Molina-Molina, J. M., Prada, R. and Olea, M., *Sci. Total Environ.*, **2011**, *409*, 3281-3287.
- <sup>8</sup> O'Driscoll, D. M., Horne, R. S. C., Davey, M. J., Hope, S. A. Anderson, V., Trinder, J., Walker, A. M., Nixon, G. M., *Sleep Medicine*, **2011**, *12*, 483-488.
- <sup>9</sup> Cao, D. L., Ye, D. W., Zhang, H. L., Zhu, Y., Wang, Y. X. Yao, X. D., *Prostate*, **2011**, *71*, 700-710.
- <sup>10</sup> Communale, M. A., Wang, M. J., Rodemich-Betesh, L., Hafner, J., Lamontagne, A., Klein, A., Marrero, J., Bisceglie, A. M., Gish, R., Block, T., and Mehta, A. *Cancer Epidemiol. Biomarkers Prevent.*, **2011**, *20*, 1222-1229.
- <sup>11</sup> Huang, Y. F., Chen, M. L., Liou, S. H., Chen, M. F., Uang, S. S. N., Wu, K. Y., *Toxicol. Lett.*, **2011**, *203*, 118-126.
- <sup>12</sup> Lu, T. M., Chung, M. Y., Lin, M. W., Hsu, C. P., Lin, S. J., *Int. J. Cardiology*, **2011**, *153*, 135-140.
- <sup>13</sup> Parameswaran, R., Sadler, G.; Brooks, S. *World J. Surgery*, **2011**, *35(10)*, 2219-27.
- <sup>14</sup> Simone, I.L., Ruggieri, M., Tortelli, R., Ceci, E., D'Errico, E., Leo, A., Zoccollella, S., Mastrapasqua, M., Capozzo, R., Livrea, P., and Logroscino, G., *Arch. Neurology* **2011**, *68*, 1306-1310.
- <sup>15</sup> Zeng, M. M., Liang, Y. Z., Li, H. D., Wang, B. Chen, X., *Anal. Methods*, **2011**, *3(2)*, 438-445.
- <sup>16</sup> Asci, B., Donmez, Q. A., Bozdogan, A., Sungur, S., *J. Liq. Chromy. Related Technol.*, **2011**, *34*, 1686-1698.
- <sup>17</sup> Muller, A., L., H., Flores, E. M. M., Muller, E., I., Silva, F., E., B., Ferrao, M. F., *J. Brazil. Chem. Soc.*, **2011**, *22*, 1903-1912.
- <sup>18</sup> Donmez, O. A., Asci, B., Bozdogan, A., Sungur, S., *Talanta*, **2011**, *83*, 1601-1605.
- <sup>19</sup> Kvalheim, O. M., Chan, H. Y., Benzie, I. F. F. Szeto, Y. T., Tzang, A. H. C., Mok, D- K. W., Chau, F. T. *Chemometrics Intelligent Lab. Systems*, **2011**, *107(1)*, 98-105.
- <sup>20</sup> Mas, S., Tauler, E., de Juan, A., *J. Chromy A*, **2011**, *1218*, 9260-9268.
- <sup>21</sup> Noorizadeh, H., Farmany A., Noorizadeh, M., *Quim. Nova* **2011**, *34*, 242-249.
- <sup>22</sup> Noorizadeh, H., Farmany A., Noorizadeh, M., *Quim. Nova* **2011**, *34*, 1398-1404.
- <sup>23</sup> Jalali-Heravi, M., Ebrahimi-Najafabadi, H., *J. Separ. Sci.*, **2011**, *34(13)*, 1538-1546.
- <sup>24</sup> Pereira, A. C., Reis, M. S., Saraiva, P. M., Marques, J. C., *Chemometrics Intelligent Lab. Systems*, **2011**, *105*, 43-55.
- <sup>25</sup> Guerrero, E. D., Bastante, M. J. C., Mejias, R. C., Marin, R. N., Barroso, C. G., *J. Agric. Food Chem.*, **2011**, *59*, 2410-2415.
- <sup>26</sup> Casoni, D., Sarbu, C., *Rev. Roum. Chim.*, **2011**, *56*, 381.
- <sup>27</sup> Lu, X. N., Ross, C. F., Powers, J. R., Rasco, B. A., *J. Agric. Food Chem.*, **2011**, *59* (12), 6376-6382.
- <sup>28</sup> Dijkstra, J., van Zijderveld, S. M., Apajalahti, J. A., Bannink, A., Gerrits, W. J. J., Newbold, J. R., Perdok, H. B., Berends, H., *Animal Feed Sci. Technol.* **2011**, *166-167*, 590-595.

- <sup>29</sup> Cheng, C., H., Seal, A. G., MacRae, E. A., Wang, M. Y., *Euphytica* **2011**, *181*, 179-195.
- <sup>30</sup> Yoshinori F., Kana, K., Megumi, I., Reia, K., Daisuke, M., Hiroyuki, W., Mari, M. Y., Atsushi, N., Takeshi, S., Tomomasa, K., Koji, Y., Hirofumi, T., *Plos One*, 2011, *6*(8), e23426. doi:10.1371/journal.pone.0023426
- <sup>31</sup> González-Álvarez, M., González-Barreiro, C., Cancho-Grande, B., Simal-Gándara, J., *Food Chem.*, **2011**, *129*, 890-898.
- <sup>32</sup> Avella, A. C., Gorner, T., Yvon, J., Chappe, P., Guinot-Thomas, P., de Donato, P., *Water Research*, **2011**, *45*, 981-992.
- <sup>33</sup> Casoni, D., Petre, J., David, V., Sarbu, C., *J. Separ. Sci.* **2011**, *34*, 247-254.
- <sup>34</sup> De Godoy, L. A., F., Pedroso, M. P., Ferreira, E. C., Augusto, F., Poppi, R., J., *J. Chromy. A.*, **2011**, *1218*, 1663-1667.
- <sup>35</sup> Garkani-Nejad, Z., Ahmadvand, M., *Chromatographia*, **2011**, *73*, 733-742.
- <sup>36</sup> Zorzetti, B. M., Shaver, J. M., Harynuk, J. J., *Anal. Chim. Acta*, **2011**, *694*, 31-37.
- <sup>37</sup> Zorzetti, B. M., Harynuk, J. J., *Anal. Bioanal. Chem.* **2011**, *401*, 2423-2431.
- <sup>38</sup> Alizadeh, M., Chamsaz, M., Asadpour, S., *Asian J. Chem.*, **2011**, *23*, 2571-2576.

Received: 13.10.2012.  
Accepted: 15.10.2012.



# MICROELEMENTS IN DRUG AND EXTRACTS OF *PLANTAGO LANCEOLATA* L.

Mária Rábai<sup>a,b</sup>, Nóra Veronika Nagy<sup>a</sup>, Zoltán May<sup>a</sup>, Klára Szentmihályi<sup>a</sup>

Presented at 4th International Symposium on Trace Elements in the Food Chain, Friends or Foes, 15-17 November, 2012, Visegrád, Hungary

**Keywords:** plantain, decoctum, infusum, essential elements.

Plantain (*Plantago lanceolata* L.) is a popular medicinal plant for its beneficial effect for respiratory and other antiinflammatory diseases. As the metal ions have significant role in inflammatory processes and antiinflammatory effect, the element content of plantain drug and in extracts has been determined. Element content in drug and different extracts (decoctum and infusum) was measured by inductively plasma optical emission spectrometry (ICP-OES) after nitric acid digestion. Most of the elements in drug had average concentration, except Al, Ba, Ca, S, Sn, Sr and Ti concentration that crossed their average level. Significant difference was found in the concentration of Al, Ba, Ca, Co, Cu, Fe, K, Mg, Mn, Na, S, Sr and V between decoctum and infusum. In most cases concentration of elements was evidently higher in decoctum samples, than in infusum. In conclusion decoctum is a richer source of elements than that of other extracts and generally these teas are relevant sources for several elements (Ca, Co, Cu, K, Mn).

\* Corresponding Authors

Fax: +36-1-438-1139

E-Mail: szentmihalyi.klara@ttk.mta.hu

- [a] Institute of Materials and Environmental Chemistry  
Research Centre for Natural Sciences of the HAS, H-1025 Budapest, POBox 17, Hungary
- [b] Budapest University of Technology and Economics  
Budapest, Hungary

That's why a new law is still under consideration in Hungary, which is influenced by the European Union. According to it, herbs are also qualified as medicines.

In result of this requirement herbs are also be tested and proved their efficiency. Though it may improve the safety of these products to consume them, but most of these products would disappear from the market, because the qualifying requirements need a lot of time and investments to get the good results, due to which the cost would also increase. Determining the plant samples have got a great difference so it is an important and challenging task to solve.<sup>4</sup>

Present article is about testing ribwort plantain (*Plantago lanceolata* L.). It is also well known as Englishman's foot, broad-leaved plantain, Cuckoo's Bread, the leaf of Patrick, Patrick's dock, ripple grass, St. Patrick's leaf, slan-lus, snakebite, snakeweed, waybread, waybroad, (Anglo Saxon) weybroed, white man's foot.<sup>5</sup> This plantain is originated from the Plantaginaceae. It can be found beside acres, pastures and commons. Its small, white flowers are blossomed from April until June. Its mature leaves are used for therapeutical values. Mucous, tannin, favonoids, silica, zinc, potassium salts and irinoids are located in the leaves. Due to the presence of irinoids, akubin agent, this plant is a powerful bactericide, anti-inflammatory and wound-healer herb. Extracts made of it is used for cough and respiratory diseases. It is an excellent antidote against heartburn, respiratory rheum and sore throat.<sup>6</sup>

## INTRODUCTION

At present different herbs and medicinal plant products are widely spread all over the world. They are traditionally tested for centuries, evidently they are the healthiest medicines ever. These days antibiotics are not so popular as they were a few decades ago. Their "Adverse", effects are also visible. Leading a healthy way of life is becoming more and more important, that's why bio foods and natural medical products are preferred by most of the people, especially medium-aged and younger ones.

As these products are not real medicines, earlier they were not needed follow the strict qualifying requirements. Only their origin, expective effect, recipe and the time of warranty can be seen on the package. There is still an enormous problem with regulating herbs. Their double standard principle caused an unbalanced distribution. According to the Hungarian Medicine Codex (Pharmacopoeia Hungarica) and the European Pharmacopoeia there is a limit for organic components, but at the point of inorganic compound it is a bit incomplete.<sup>1,2</sup> There is a strict quality and quantitative limitation just for the toxic heavy metals. On the other hand only the inorganic components are examined in the Hungarian Victual Codex (Codex Alimentarius Hungaricus)<sup>3</sup>, and it is much more strict than the previous formulate. As herbs are classified in both, the medicine and foods, it is to be discussed that which guideline should be followed. Generally the concentration of toxic or non-essential elements was not determined, as they could also be poisonous to human organism.

## EXPERIMENTAL

### Materials

Leaves of the ribwort plantain (*Plantago Lanceolata* L.) were produced by Herbária Patikája. Trade from the producing series of 07533-07534, K-101/111.

### Aqueous extracts

Two different kinds of aqueous extract (teas); decoctum and infusum were examined.

Infusums were made from 1 g ribwort plantain and 20 mL hot distilled water. Four different extracts were made: drug soaked in hot water for 5, 10, 15 and 20 minutes. After the reaction time was over, they were filtered and stewed for 1-2 hours.

Decoctum was made by the same procedure as infusum. The only difference was the amount of drug (2.5 g in 50 mL water), and the 5 minutes boiling instead of soaking.

### Measurement of elements

Element concentration (Al, As, B, Ba, Ca, Cd, Co, Cr, Cu, Fe, K, Mg, Mn, Ni, P, Pb, S, Si, Sn, Sr, Ti, V, Zn) of the samples was determined with an ICP-OES (inductively coupled plasma optical emission spectrometer). Type of instrument: Spectro Genesis ICP-OES (Kleve, Germany). After digestion of the samples (0.5 g from drug, 20 mL of evaporated extracts) with a mixture of nitric acid and hydrogen peroxide (10 + 4 mL) and dilution with deionised water to 20 mL (extracts) or 25 mL (drug), concentration of elements was determined.<sup>7</sup>

### Statistical analysis

Mean values and standard deviations (SD) were calculated from the results obtained. One way analysis of variance (ANOVA) was used for comparing the means of the four groups. To determinate the difference between two groups, the Student *t*-test was used by GraphPAD software version 1.14 (1990). Significance was determined as  $P < 0.05$ .

## RESULTS

The element concentration in ribwort plantain is shown in Table 1. The concentration of As and Pb was under the detection limit, therefore these elements are omitted from the table. In ribwort plantain drug a little bit higher concentration was measured in case of Al, Ba, Ca and S above the average level.<sup>8,9</sup> Strontium concentration was found to be double the amount of the average amount (40 mg/kg).<sup>8</sup> The other elements were at the normal intervallum of concentration (Table 1).<sup>9,10</sup>

The aqueous extracts of ribwort plantain did not contain As, B, Cr, Pb, Sn and Ti concentrations above the detection limit. The concentration of most elements (Tables 2 and 3) are similar to other data found in extracts earlier, while concentration of Ba, Ca, K, Na, Mn seems to be relevant compared to other aqueous extracts.<sup>7,9,10</sup>

Surprisingly the time of the „reaction“ (= time of soaking) wasn't in direct proportion with the element content (Table 2). In most cases the element concentration in infusums are mainly depend on time of soaking and several significant difference was found between infusums calculated by Student *t*-test. A rising tendency can be observed in respect of Ba, Ca, K, Mg, Na, Ni, P, S, Sr and Zr content till 15

minutes of soaking. Then from 15 to 20 minutes the concentration of most elements was decreased except of Co. Significant difference of the element contents can be observed for Ba, Ca, Cu, Fe, K, Mg, Na, Ni, P, Sr and V in the comparison of four extracts by ANOVA ( $P < 0.05$ ). According to these results we can conclude that the time of soaking greatly affect on the element content in infusum.

**Table 1.** Element concentrations (mg/kg,  $\pm$  standard deviation,  $n=3$ ) in ribwort plantain (*Plantago lanceolata* L.)

Elements	Mean $\pm$ standard deviation (mg kg <sup>-1</sup> )
Al	375.2 $\pm$ 62.6
B	40.84 $\pm$ 20.88
Ba	44.71 $\pm$ 2.67
Ca	16154 $\pm$ 150
Cd	0.164 $\pm$ 0.029
Co	0.465 $\pm$ 0.055
Cr	1.50 $\pm$ 0.47
Cu	13.57 $\pm$ 1.82
Fe	278.7 $\pm$ 42.9
Mg	4518 $\pm$ 22
Mn	49.60 $\pm$ 6.00
Na	997.1 $\pm$ 25.1
Ni	0.735 $\pm$ 0.132
P	4634 $\pm$ 21
S	3218 $\pm$ 115
Si	193.9 $\pm$ 73.3
Sn	8.63 $\pm$ 2.70
Sr	96.16 $\pm$ 6.00
Ti	6.06 $\pm$ 0.67
V	0.544 $\pm$ 0.139
Zn	18.28 $\pm$ 1.46

Concentration of Ba, Ca, Co, K, Mg, Sr and V are remarkably raised in decoctum (Table 3) compared to infusum made with soaking for 20 min (Table 2), however Cu, Na and Zn were decreased. Element content of Al, Mn, Ni, P, S and Zn was nearly the same as it was in the 15-20 minutes infusums (Tables 2 and 3). Boiling a sample for 5 minutes is almost the same as soaking it for 15-20 minutes in respect of many elements. In case of other minerals making a decoctum is the way to get a richer solution. (Tables 2 and 3). Most of the element concentration in decoctum significantly different to infusums except of Ba, Cu and P (Table 3).

The dissolution rate of drug into the different extracts can be seen on the Table 4. Generally the 15 minutes infusum solved the elements in the highest amount. Boiling reduces the tripping of the Cu, Na and Zn while helps other elements extracting. The dissolution into the aqueous extracts is relatively high (>50%) for Co, Cu and Na in all cases, while the dissolution of Fe from drug into the teas was found to be very low (1.67-6.35%).

## DISCUSSION

It is demonstrated that ribwort plantain (*Plantago lanceolata* L.) is a valuable medicinal plant in respect of mineral constituents. A generally higher amount of elements were found in decoctum (5 min) than in infusum (5 min). These elements are Co, K, V and some alkaline earth metals, like Mg, Ca, Ba and Sr.

**Table 2.** Element concentrations ( $\text{mgL}^{-1}$ ,  $\pm$  standard deviation,  $n=3$ ) in aqueous ribwort plantain infusum extracts (*Plantago lanceolata* L.)

	Element content in <i>Plantago Lanceolata</i> aqueous extract ( $\text{mg L}^{-1} \pm \text{SD}$ )				ANOVA, calculated for four infusums ( $P<0.05$ )
	Infusum 5 min.	Infusum 10 min.	Infusum 15 min.	Infusum 20 min.	
Al	1.34 $\pm$ 0.29	0.874 $\pm$ -0.022	1.44 $\pm$ 0.36	0.934 $\pm$ 0.070	Not sign.
Ba <sup>b, f</sup>	0.257 $\pm$ 0.030	0.267 $\pm$ -0.050	0.332 $\pm$ 0.030	0.268 $\pm$ 0.200	Sign.
Ca <sup>a, b, d, f</sup>	127.0 $\pm$ 8.6	141.0 $\pm$ 33.1	185.2 $\pm$ 13.4	143.6 $\pm$ 14.2	Sign.
Co	0.008 $\pm$ 0.001	0.008 $\pm$ 0.003	0.0096 $\pm$ 0.0020	0.0096 $\pm$ 0.0020	Not sign.
Cu	0.196 $\pm$ 0.009	0.172 $\pm$ 0.004	0.232 $\pm$ 0.035	0.211 $\pm$ 0.020	Sign..
Fe <sup>b, d, f</sup>	0.293 $\pm$ 0.290	0.116 $\pm$ 0.060	0.443 $\pm$ 0.230	0.210 $\pm$ 0.050	Sign.
K <sup>b, f</sup>	795.6 $\pm$ 41.8	821.1 $\pm$ 210.7	961.7 $\pm$ 41.8	830.3 $\pm$ 25.4	Sign.
Mg <sup>a, b, c, f</sup>	27.23 $\pm$ 0.97	31.61 $\pm$ 7.69	41.76 $\pm$ 3.23	33.95 $\pm$ 3.27	Sign.
Mn <sup>b</sup>	0.658 $\pm$ -0.260	0.558 $\pm$ 0.13	0.715 $\pm$ 0.070	0.586 $\pm$ 0.050	Not sign.
Na <sup>a, b, d, e, f</sup>	15.66 $\pm$ 1.84	15.68 $\pm$ 5.14	19.13 $\pm$ 1.13	15.55 $\pm$ 0.99	Sign.
Ni <sup>c</sup>	0.0023 $\pm$ 0.0008	0.0112 $\pm$ 0.003	0.0155 $\pm$ 0.0060	0.0068 $\pm$ 0.0030	Sign.
P <sup>a, b, c, d, f</sup>	38.65 $\pm$ -4.79	43.44 $\pm$ 9.22	58.33 $\pm$ 2.25	51.12 $\pm$ 3.40	Not sign.
S <sup>a, b, d, f</sup>	25.90 $\pm$ 2.21	28.26 $\pm$ 6.65	39.54 $\pm$ 1.45	29.46 $\pm$ 3.06	Sign.
Sr <sup>a, b, d, f</sup>	0.558 $\pm$ 0.040	0.611 $\pm$ 0.140	0.820 $\pm$ 0.067	0.648 $\pm$ 0.060	Sign.
V <sup>a, d</sup>	0.0068 $\pm$ 0.0020	0.0020 $\pm$ 0.0003	0.0061 $\pm$ 0.002	0.0034 $\pm$ 0.0010	Sign.
Zn <sup>d, e</sup>	0.0363 $\pm$ 0.0300	0.117 $\pm$ 0.0002	0.180 $\pm$ 0.103	0.102 $\pm$ 0.050	Not sign.

<sup>a</sup> significant difference between infusum 5 min and infusum 10 min, <sup>b</sup> significant difference between infusum 5 min and infusum 15 min, <sup>c</sup> significant difference between infusum 5 min and infusum 20 min, <sup>d</sup> significant difference between infusum 10 min and infusum 15 min, <sup>e</sup> significant difference between infusum 10 min and infusum 20 min, <sup>f</sup> significant difference between infusum 15 min and infusum 20 min (Student t-test,  $P<0.05$ )

**Table 3.** Element concentrations ( $\text{mgL}^{-1}$ ,  $\pm$  standard deviation,  $n=3$ ) in aq. ribwort plantain decoctum extracts (*Plantago lanceolata* L.)

	Element content ( $\text{mgL}^{-1} \pm \text{SD}$ )	Significant difference by Student t-test ( $P<0.05$ )			
		between infusum 5 min. and decoctum	between infusum 10 min. and decoctum	between infusum 15 min. and decoctum	between infusum 20 min. and decoctum
Al	1.02 $\pm$ 0.32	Sign.	Sign.	Sign.	Not sign.
Ba	0.423 $\pm$ 0.040	Sign.	Sign.	Not sign.	Sign.
Ca	196.3 $\pm$ 38.7	Sign.	Sign.	Not sign.	Sign.
Co	0.0119 $\pm$ 0.0010	Sign.	Sign.	Not sign.	Not sign.
Cu	0.102 $\pm$ 0.025	Sign.	Sign.	Sign.	Sign.
Fe	0.322 $\pm$ 0.080	Not sign.	Sign.	Sign.	Sign.
K	1093 $\pm$ 23	Sign.	Sign.	Not sign.	Sign.
Mg	47.55 $\pm$ 7.76	Sign.	Sign.	Not sign.	Sign.
Mn	0.682 $\pm$ 0.080	Not sign.	Not sign.	Not sign.	Not sign.
Na	8.3938 $\pm$ 5.56	Sign.	Sign.	Sign.	Sign.
Ni	0.0016 $\pm$ 0.0010	Sign.	Sign.	Sign.	Sign.
P	55.64 $\pm$ 2.56	Sign.	Sign.	Not sign.	Not sign.
S	38.80 $\pm$ 2.58	Sign.	Sign.	Not sign.	Sign.
Sr	0.952 $\pm$ 0.060	Sign.	Sign.	Not sign.	Sign.
V	0.0082 $\pm$ -0.0002	Sign.	Sign.	Sign.	Sign.
Zn	0.0948 $\pm$ 0.0300	Sign.	Sign.	Sign.	Not sign.

**Table 4.** Dissolution rate of drug into extracts (%)

	Infusum 5 min.	Infusum 10 min.	Infusum 15 min.	Infusum 20 min.	Decoctum 5 min.
Al	14.33	9.32	15.37	9.95	10.88
Ba	25.22	26.13	32.49	26.23	41.42
Ca	31.45	34.92	45.85	35.56	48.60
Co	68.85	68.85	82.62	82.62	102.41
Cu	57.89	50.67	68.36	62.11	29.98
Fe	4.21	1.67	6.35	3.01	4.63
Mg	31.38	35.27	46.29	37.74	39.60
Mn	53.92	45.70	58.59	48.02	55.87
Na	62.84	62.89	76.73	62.37	33.67
Ni	12.52	60.97	84.38	37.02	8.71
P	33.36	37.50	50.35	44.13	48.03
S	32.20	35.13	49.15	36.62	48.22
Sr	23.20	25.42	34.12	26.93	39.60
V	50.03	14.71	44.88	25.01	60.33
Zn	40.57	24.03	39.15	34.95	17.66

Consuming extracts made of this medicinal plant as a medicine helps us to get an appreciable part of the essential minerals. A tea is said to be a fine element source if 15 % of the Recommended Dietary Allowances (RDA) is covered by its well-defined amount of consumption.<sup>11</sup> According to this, drinking 1 litre of any kind of extract made of this drug contains and supports 15.9-24.5% of Ca, 27.6-41.4% of Co, 39.0-54.6% of K and 27.5-35.7% of Mn (RDA: 800 mg for Ca, 0.029 mg for Co, 2000 mg for K and 2 mg for Mn per day<sup>11</sup>). Infusums were also found to be good Cu sources with 17.2-32.2% of RDA, while decoctum covers only the 10% of RDA. It is worthy to mention that extracts made of ribwort plantain contain 1/3 of the daily Al intake (Dietary Reference Intakes<sup>12</sup>).

In conclusion ribwort plantain plant is a unique herb, which contains a lot of necessary elements. This plantain is available easily and economically to every one Thanks to the nature for its excellent compositions and its relevance to be a valuable source for several elements. It can also be favourable to use in preventions and symptomatic treatments as well.

## REFERENCES

- <sup>1</sup>*Hungarian Pharmacopoeia* VIII. (Ph.Hg. VII). Medicina Könyvkiadó, **2004**.
- <sup>2</sup>*European Pharmacopoeia* 5. Edition (Ph.Eur. 5.), Council of Europe, **2004**.

<sup>3</sup>*Codex Alimentarius Hungaricus*, **2008**.

<sup>4</sup>[http://www.eletforma.hu/orvosi\\_rendelo/aprilistol\\_eltunhetnek\\_a\\_drogeriak\\_polcairol\\_a\\_gyogynovenyek.html](http://www.eletforma.hu/orvosi_rendelo/aprilistol_eltunhetnek_a_drogeriak_polcairol_a_gyogynovenyek.html)

<sup>5</sup>[http://www.hazipatika.com/gyogynovenytar/landzsas\\_utifu/39](http://www.hazipatika.com/gyogynovenytar/landzsas_utifu/39)

<sup>6</sup><http://www.rowanremedies.com/herbal-medicine-articles/herb-profiles/plantago-lanceolata-plantain/>

<sup>7</sup> Szentmihályi K., Then M., *Acta Aliment.*, **2000**, 29, 43.

<sup>8</sup> Kabata-Pendias, A., Mukherjee, A. B., *Trace Elements from Soil to Human*. Springer Verlag, **2007**.

<sup>9</sup> Szentmihályi, K., Hajdú, M., Then, M., *Medicinal and Aromatic Plant Sci. Biotechnol.* **2008**, 2, 57-62.

<sup>10</sup> Szentmihályi, K., May, Z., Then M., Hajdú, M., Böszörményi, A., Fodor J., Balázs, A., Lemberkovich, É., Marczal, G., Szöke, É., *Eur. Chem Bull.*, **2012**, 1, 14-21.

<sup>11</sup> *Recommended Dietary Allowances (RDA)* 10th ed. National Academy Press, Washington D.C., **1989**.

<sup>12</sup> *Dietary Reference Intakes for vitamin A, vitamin K, arsenic, boron, chromium, copper, iodine, iron, manganese, molybdenum, nickel, silicon, vanadium, and zinc*. Food and Nutritional Board, Institute of medicine. Academic Press, Boston, **2002**.

Received: 19.10.2012.

Accepted: 22.10.2012